NOTICE

The quality of this microform is heavily dependent upon the quality of the original thesis submitted for microfilming. Every effort has been made to ensure the highest quality of reproduction possible.

If pages are missing, contact the university which granted the degree.

Some pages may have indistinct print especially if the original pages were typed with a poor typewriter ribbon or if the university sent us an inferior photocopy.

Previously copyrighted materials (journal articles, published tests, etc.) are not filmed.

Reproduction in full or in part of this microform is governed by the Canadian Copyright Act, R.S.C. 1970, c. C-30.

AVIS

La qualité de cette microforme dépend grandement de la qualité de la thèse soumise au microfilmage. Nous avons tout fait pour assurer une qualité supérieure de reproduction.

S'il manque des pages, veuillez communiquer avec l'université qui a conféré le grade.

La qualité d'impression de certaines pages peut laisser à désirer, surtout si les pages originales ont été dactylographiées à l'aide d'un ruban usé ou si l'université nous a fait parvenir une photocopie de qualité inférieure.

Les documents qui font déjà l'objet d'un droit d'auteur (articles de revue, tests publiés, etc.) ne sont pas microfilmés.

La reproduction, même partielle, de cette microforme est soumise à la Loi canadienne sur le droit d'auteur, SRC 1970, c. C-30.

Canada

THE UNIVERSITY OF ALBERTA

COMPRESSIVE BEHAVIOR OF GUSSET PLATE CONNECTIONS

by

© SHOU-ZON HU

A THESIS

SUBMITTED TO THE FACULTY OF GRADUATE STUDIES AND RESEARCH

IN PARTIAL FULFILMENT OF THE REQUIREMENTS FOR THE DEGREE

OF MASTER OF SCIENCE

DEPARTMENT OF CIVIL ENGINEERING

EDMONTON, ALBERTA

Fall 1987

ISBN 0-315-40947-9

THE UNIVERSITY OF ALBERTA

RELEASE FORM

NAME OF AUTHOR SHOU-ZON HU

TITLE OF THESIS *COMPRESSIVE BEHAVIOR OF GUSSET PLATE CONNECTIONS*

DEGREE FOR WHICH THESIS WAS PRESENTED MASTER OF SCIENCE

YEAR THIS DEGREE GRANTED Fall 1987

Permission is hereby granted to THE UNIVERSITY OF ALBERTA LIBRARY to reproduce single copies of this thesis and to lend or sell such copies for private, scholarly or scientific research purposes only.

The author reserves other publication rights, and neither the thesis nor extensive extracts from it may be printed or otherwise reproduced without the author's written permission.

(SIGNED) .....

PERMANENT ADDRESS:

Civil Engineering

.....

.....

DATED July 15 19 87

THE UNIVERSITY OF ALBERTA

FACULTY OF GRADUATE STUDIES AND RESEARCH

The undersigned certify that they have read, and recommend to the Faculty of Graduate Studies and Research, for acceptance, a thesis entitled Compressive Behavior of Gusset Plate Connections submitted by Shou-Zon Hu in partial fulfilment of the requirements for the degree of Master of Science.

.....

Supervisor

.....

.....

Date July 10, 1987

ABSTRACT

The compressive behavior and buckling strength of thin-walled gusset plate connections were examined on the basis of an experimental investigation of full-scale diagonal bracing connections. Such connections are commonly used to transfer forces from a bracing member to the beam and column through the gusset plate. A total of 14 tests were run on six connection specimens. Plate thickness, geometric configuration, boundary conditions, eccentricity and reinforcement were considered in planning the tests. All concentrically loaded tests failed in plate buckling. The tests with eccentricity failed in bending yielding of the splice plates. The test results were evaluated based on load and deformation data. Attempts were made to correlate the eccentric loading test results with the beam-column formulas and the concentric loading test results with the finite element program BASP. Comparisons are shown to be in reasonable agreement. Current design practices are discussed briefly and found to be very unconservative compared with test results. A parametric study was undertaken by using different thickness and size of gusset plates, different thickness of splice plate and different boundary conditions. A tentative design guideline for gusset plate loaded in compression is proposed based on test results and parametric studies. A suggestion for further studies also is proposed.

ACKNOWLEDGEMENT

This investigation was made possible by a grant provided by the Canadian Steel Construction Council and supplemented by the Natural Sciences and Engineering Research Council of Canada Grant No. A4727.

The author wishes to express his sincere appreciation to the advice of Dr. J.J. Cheng.

Gratefully acknowledged are the comments and criticisms of Professors G.L. Kulak and J.S. Kennedy, who served on the examining committee.

The guidance of the Project Coordinator, M.I. Gilmor, and the contributions of L. Burden and R. Helfrich in carrying out the testing program is also greatfully acknowledged.

Table of Contents

List of Tables

List of Figures

1. INTRODUCTION

1.1 General

One of the most common methods of connecting two or more members together is by a gusset plate which is used to transfer forces from one member to the other such as connections in trusses or in braced steel frames. Figure 1.1 shows a typical connection in a Warren truss using double gusset plates to transfer forces among members. In the case of braced frames, either tensile or compressive loads from a bracing member which is designed to resist lateral forces are transferred to the beam and column through the gusset plate. The gusset plate is normally bolted to the bracing member and connected to the column and beam by bolts or welds. A splice plate may, or may not, be used, depending upon the member geometry. Figure 1.2 illustrates such a connection. Although it is customay to assume that the members in gusset plate connections are loaded only in their axial direction, the delivery of these loads will produce bending, shear and normal forces in the gusset plate.

Despite the popularity of this type of connection, the gusset plate has received relatively little attention in terms of strength, behavior and design investigations. Current design specifications only mention the design philosophy (CAN3-S6-M78 1978) and have no specific formulas for evaluating the dimension and thickness of a gusset plate. The traditional method of gusset plate design (Kulak

et al. 1987) is primarily based on the elastic analysis and the strength of materials, combined with the experience, past practice and the engineer's intuition. Thus, variable margins of safety of the gusset plate may result from the assumptions that were used in the design.

Recently, a few analytical and experimental studies have been conducted to determine the behavior and ultimate strength of the gusset plates loaded in tension (Bjorhovde et al. 1983; Richard et al. 1983) which aimed at providing a rational design method with a consistent factor of safety against failure. However, these studies did not address the problems of gusset plate connections in which the load was delivered by compression members, nor the related problem of gusset plate buckling.

A gusset plate loaded in compression increases the complexity of the connection. Common yield stress analysis cannot represent the actual stress distribution because of load concentration, warping of the plate section, local yielding and local eccentricity. All of these may cause buckling or crippling in the area of gusset plate adjacent to the diagonal member or to the spliced location. In addition, due to the uncertainty of the boundary conditions, the prediction of the buckling load becomes extremely difficult. In addition, compressive stresses along free edges of gusset plates may cause local buckling and insufficient gusset plate thickness may cause unacceptable deformations in the connection.

1.2 Objective and Scope

It can be seen from the above discussion that there is little research, either theoretical or experimental, on the compressive strength of gusset plates. Therefore, a research project sponsored by the Canadian Steel Construction Council was initiated to investigate the behavior and strength of gusset plates loaded in compression. The main objectives of the project are following:

1. Provide experimental data for the various design parameters.
2. Evaluate current design methods.
3. Compare the test results with the analytical studies using finite element programs.
4. Establish preliminary design rules, if possible.
5. Identify the areas requiring further investigation.

Because of the complexity of the problem, the research program developed to fulfill these purposes was primarily one of experimental investigations. The tests results are compared both with the current design practices and analytical studies using finite element programs. The scope of the investigation is limited to the following:

1. Single gusset plate connections of a diagonal bracing in steel frames were used.
2. Forces which exist in the beam and column were neglected.
3. The variables chosen for investigation are plate thickness, plate size, boundary condition and

eccentricity.

4. It was planned that the gusset plate in most of the tests would fail in elastic buckling.

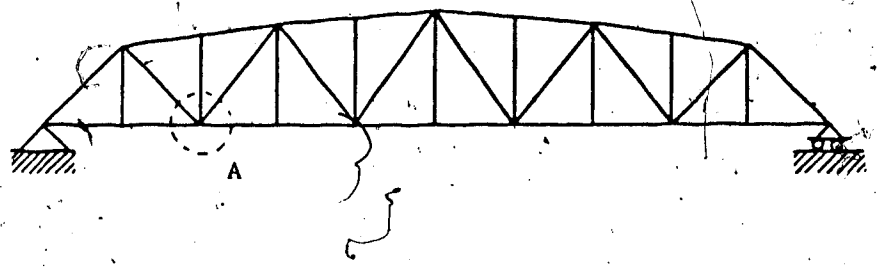

Truss Outline

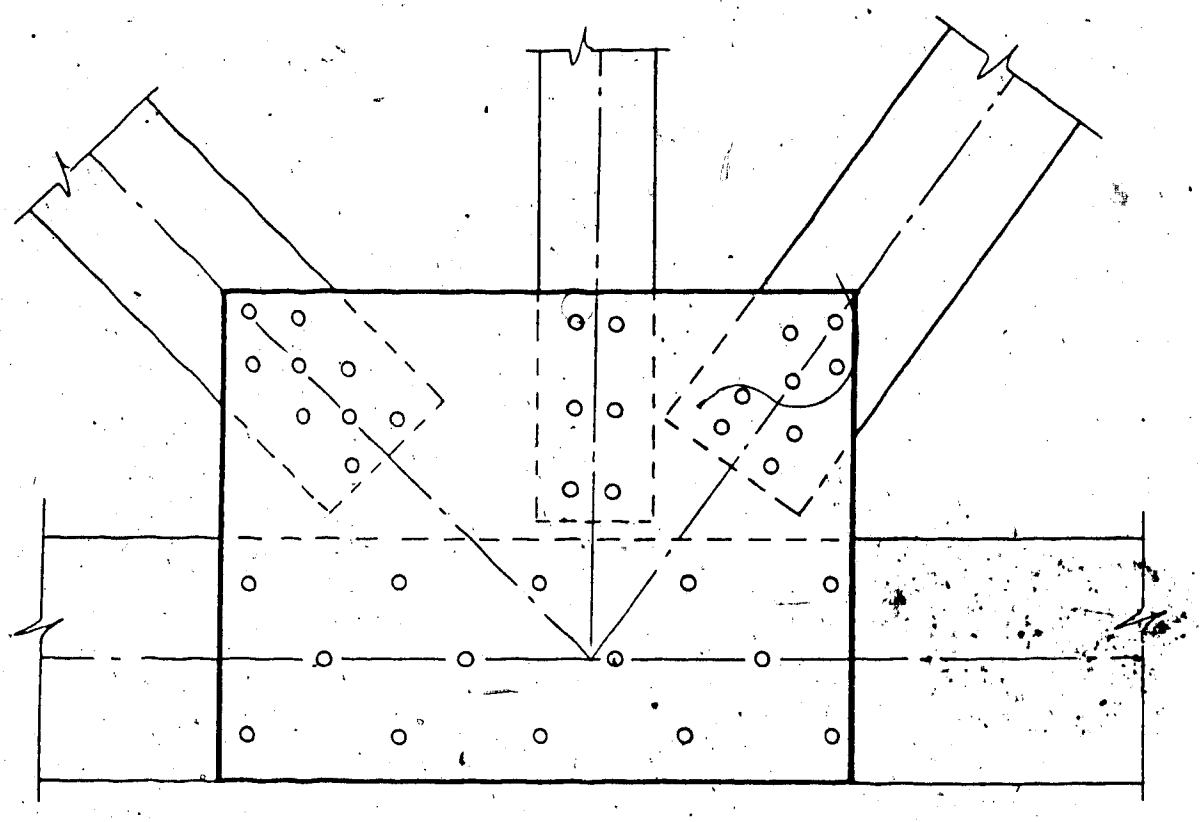

Connection A

Figure 1.1 Typical Gusset Plate Connection in a Warren Truss

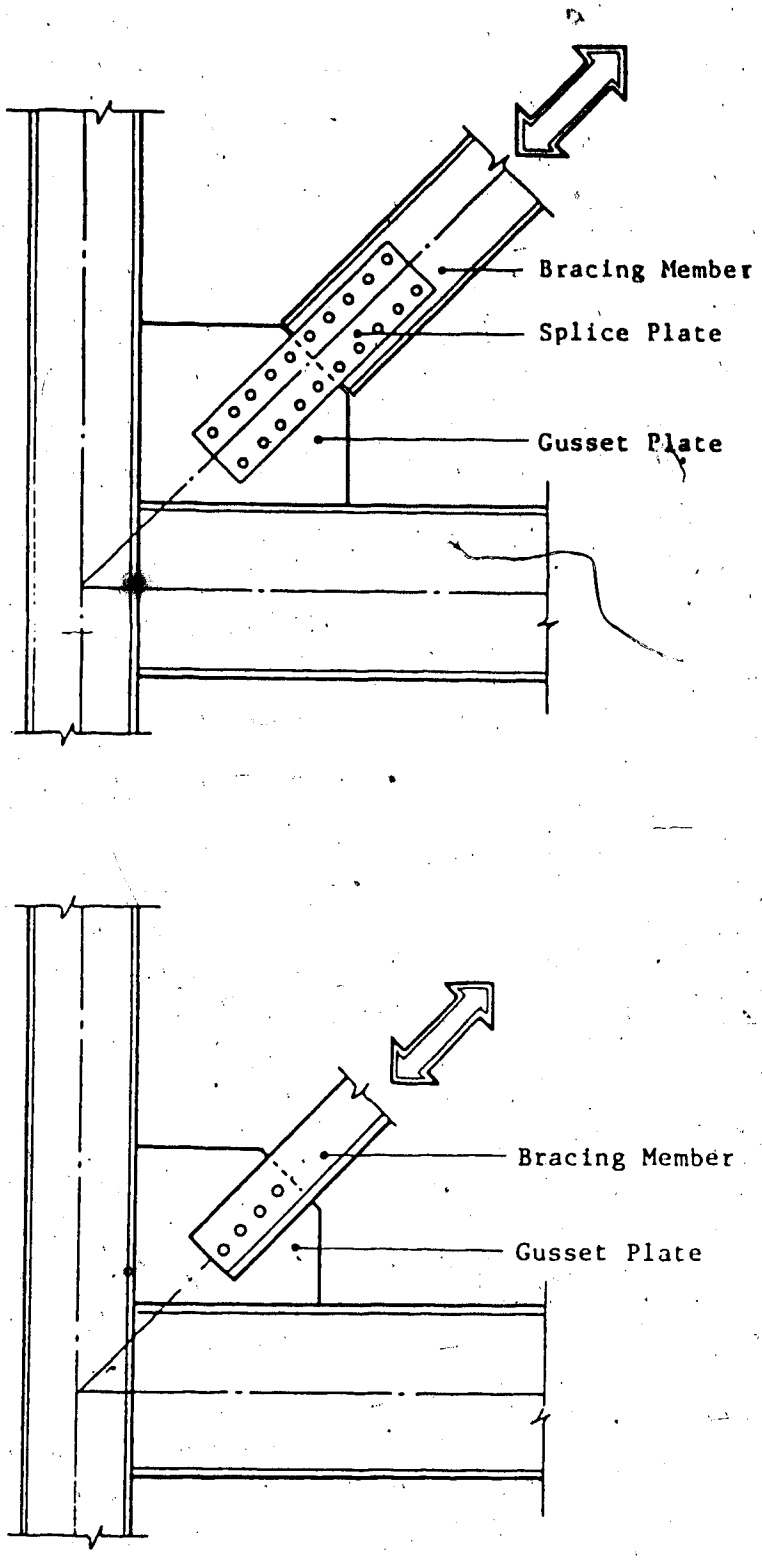

Figure 1.2 Typical Connections in a Braced Steel Frame

2. LITERATURE REVIEW

2.1 Introduction

As mentioned in Chapter 1, the current design method of gusset plates is mainly the result of experience, general practice and the engineer's intuition. Current design specifications only give the design philosophy and have no specific formulas for evaluating the dimension and the thickness of gusset plates. The CAN3-S6-M78, Design of Highway Bridges(1978) states in clause 7.13.4.1 :

.....They (gusset plates) shall be of ample thickness to resist shear, direct stress, and flexure acting on the weakest or critical section.

It is easily understood that a rational design method of the gusset plates is of significant interest.

In this chapter past work done on gusset plate connections is reviewed. A few studies, both experimental and analytical, have been conducted recently to determine the general behavior and to evaluate the ultimate strength of gusset plate connections and these are also reviewed. Current design practices are discussed.

2.2 Analytical and Experimental Works in Gusset Plates

In 1952 Whitmore(1952) investigated the stress distribution pattern on a scale ratio of 1:4 aluminum gusset plate model which represented a prototype of Warren truss joint. Based on this test, it was found that the maximum tensile and compressive stresses were near the ends of tension and compression diagonals, as shown on Fig. 2.1. Whitmore also concluded that using the beam formulas which calculated the direct, bending, and shearing stresses on a plane through the end of the diagonals gave misleading results. There was a significant difference between the calculated and observed stresses particularly at the edges of the plate, as shown in Fig. 2.2. Based on these observations, he introduced the well-known effective width concept to calculate the maximum normal stress in the plate, in which it was assumed that the stresses were uniformly distributed over an area at the end of each diagonal member and using a spread out angle of 30 degrees. This concept gives a reasonable result comparing to the test result and has since been used as one of the primary tools of gusset plate design. This method is illustrated schematically in Fig. 2.2. A few related studies were conducted by other investigators thereafter.

Irvan(1957) investigated the primary stress in the double plane gusset plates of a Pratt truss in 1957. The locations of the maximum stresses were similar to Whitmore's test results. However, his estimation of the maximum normal

stress was slightly different from Whitmore's. He suggested that the effective width could be found by drawing 30^0 lines from the center of gravity of the group of rivets to intersect a line passing through the bottom row of rivets. A further study by Hardin(1958) of a Pratt truss gusset plate with a chord splice was reported in 1958 by using Irvan's method and it confirmed the findings by Irvan. Additional studies were conducted by Davis(1967) and Vasarhelyi(1971), both of whom attempted an elastic finite element study of a specific gusset plate. Davis performed his study on the gusset plate used by Whitmore and confirmed his results. Vasarhelyi evaluated a lower chord joint in a simple Warren truss and noticed that the maximum values of stress in a gusset plate calculated by various simplified methods are only slightly different. On the other hand, he found that the corresponding locations of maximum stress might vary substantially.

Struik(1972) studied the problem in the elastic as well as in the inelastic range using the elastic-plastic finite element analysis. He simulated the fastener holes in an approximate manner by using a special load-deformation relationship for uniaxially loaded plate coupon specimen with holes. The tensile strength of the material was assumed to be 482 kN at a strain of 15%. Reaching the tensile strength in one or more elements was considered to result in failure of the gusset plate and defined the ultimate load. Struik's elastic-plastic analysis indicated that a large and

variable margin of safety against failure is inherent in the current design practice for gusset plates.

Recently, several studies have been conducted to determine the behavior and ultimate strength of gusset plate connections which aimed at providing a rational design method. A test was conducted at the University of Alberta by Bjorhovde(1983) to determine the ultimate strength of gusset plates used in diagonal bracing connections. This study involved testing of full-scale connections between a diagonal bracing member, a beam and a column. A total of six tests were performed by using two different plate thicknesses (3 mm and 10 mm) and three different bracing member orientation angles (30^0, 45^0 and 60^0), as shown in Fig. 2.3. and tried to cover the most common geometries. It was observed that the primary failure of the gusset plate was a tearing across the last row of bolts of the splice connection between the gusset plate and the bracing member in the direction perpendicular to the applied tensile load. Also, it was found that plate buckling as a result of secondary effects appeared to be a significant factor.

Non-linear finite element analyses of gusset plate behavior have been conducted by Richard (1983) and compared with Bjorhovde's test results. It was shown that the area of low strain gradient agreed quite well with the test result and also confirmed that the maximum normal stresses are located in a region near the end of the gusset plate connection. More recently, Hardash and Bjorhovde(1985) at

the University of Arizona studied the results of tests performed on 39 gusset plates. They used the block-shear concept of coped beam-to-column connections for the gusset plate loaded in tension. It was concluded that the governing tensile strength of a gusset plate was to be the one incorporating tensile ultimate stength on the net area between the last row of bolts and a uniform effective shear stress acting on the gross area along the outside bolt lines, as shown schematically in Fig 2.4. At the same time, there was a series of experimental investigations of gusset truss joints conducted by Yamamoto et. al (1985) in Japan for the purpose of providing unified formulas for the gusset plate thickness in a connection with truss-stiffening-girders of suspension bridges in the Honshe-Shikokv Bridge Project. This program was performed to determine the stress distribution, the maximum stress intensity and its location in two types of double plane gusset plates. The results were similar to Whitmore's results. Several equations were proposed. However, this investigation was only dealing with the in-plane elastic behavior and no buckling problem was considered.

2.3 Current Design Method

The current design method of gusset plate is mainly the result of experience, general practice and intuition, combined with some simple provisions in specifications.

The traditional method mentioned is summarized as follows. It is assumed that all fasteners carry an equal share of the member force to determine the number of fasteners required. The planar configuration of the plate then can be selected to place all of the fasteners. Stresses are evaluated on the most critical section by using beam formulas as described previously.

An alternative method is performed by evaluating the critical normal stress using Whitmore's effective width concept. The normal stress at this effective area (Fig.2.2) should not exceed the allowable stress permitted by the appropriate specification.

CAN3-S6-M78 states the gusset plates shall have enough thickness to resist shear, direct stress, and flexure, acting on the weakest or critical section of maximum stress. In order to avoid the possibility of local buckling along free edges of the gusset plate, it limits the length of an unsupported edge of a gusset plate to a maximum value of $945/\sqrt{F_y}$ times its thickness.

The Canadian Standards Association CAN3-S16.1-M84 (Steel Structures for Buildings-Limit State Design) gives a simple equation to check the shear stress in gusset plates. The total factored shear resistance of the gross area of gusset plates is to be taken as : $V_r = 0.50\ \Phi\ A_g\ F_y$, where Φ is resistance factor, A_g is gross area and F_y is yield strength of the plate.

One of common practices to connect tubular members together is to cut up the middle of a tube and then weld the tube to a splice plate. The tube is then connected to other members by bolting or welding the splice plate to a gusset plate, which is connected to the other members as shown in Fig. 2.5. In design practice, some engineers evaluate the thickness of gusset plate of this type by considering the gusset plate as an extension of the bracing member and treating it as an axially loaded compressive member with an estimated effective width. This approach neglects the eccentricity that existed in the connection. The eccentricity of the two plates in the joint causes lateral displacement of the gusset plate and this may initiate a premature failure. An unpublished investigation (Gilmor, M.I., 1985) found that by stiffening the gusset plate to offset the effect of the eccentricity, an increased load carrying capacity resulted. However, the effects of the eccentricity and the stiffeners on the ultimate strength of such connections under compression are still unknown.

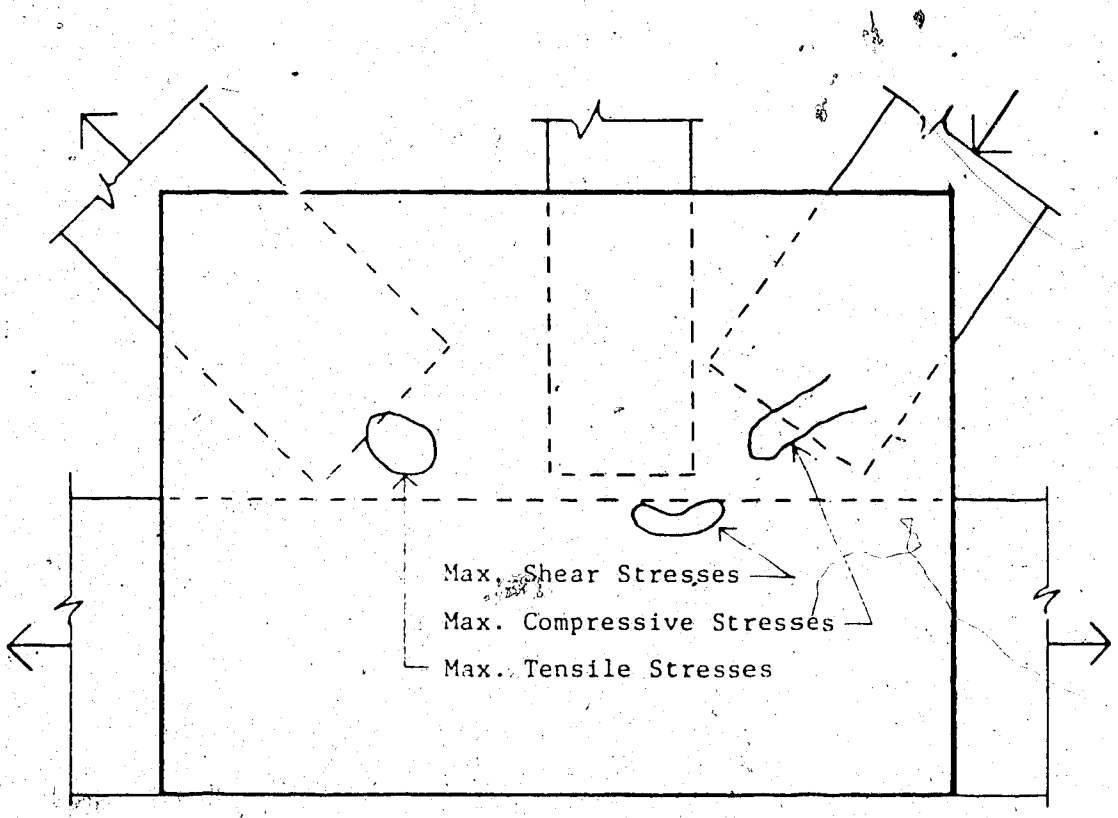

Figure 2.1 Maximum Stresses in Whitmore's Test (Whitmore, 1952)

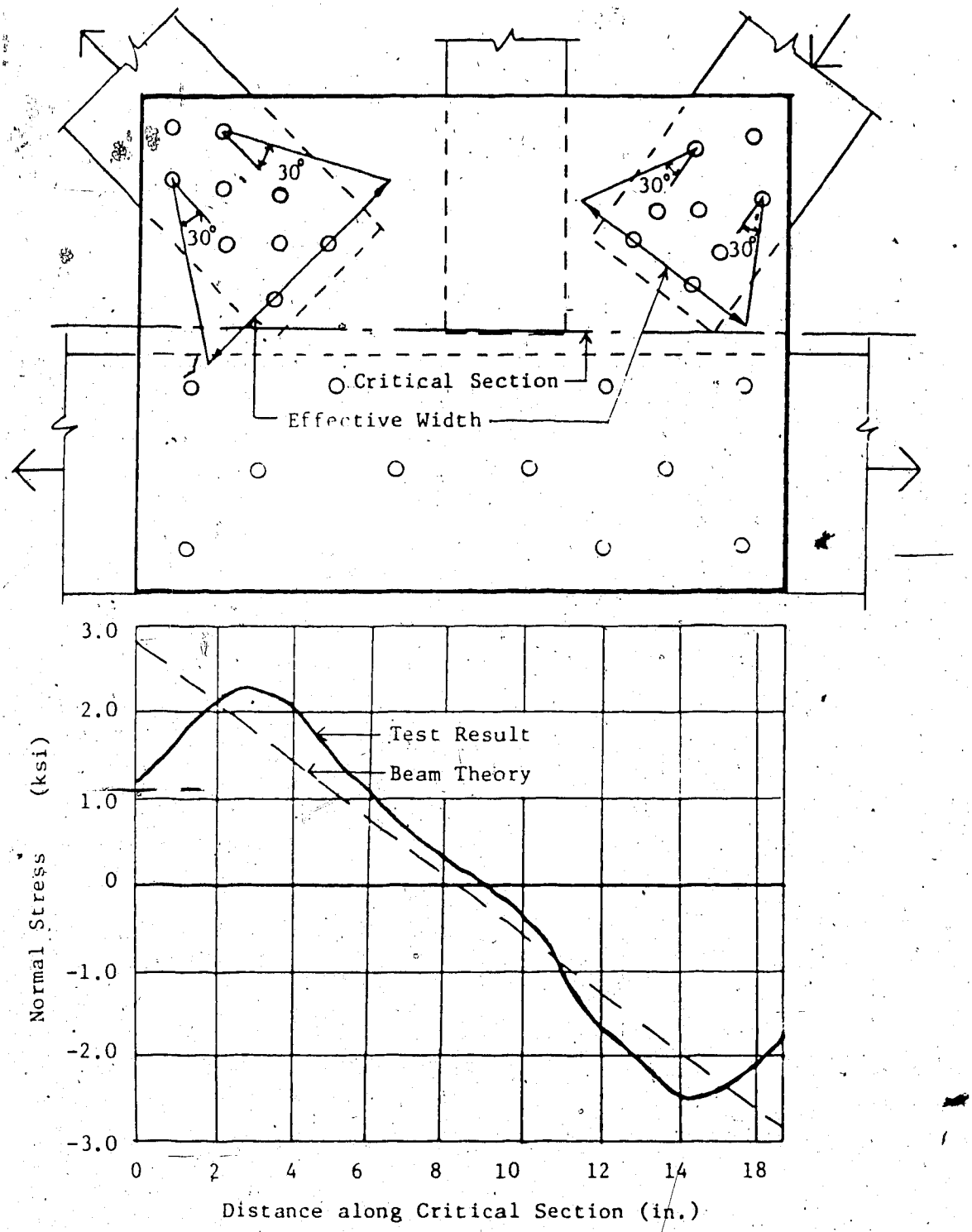

Figure 2.2 Distribution of Vertical Normal Stress on the Critical Section and the Effective Width Concept (Whitmore, 1952)

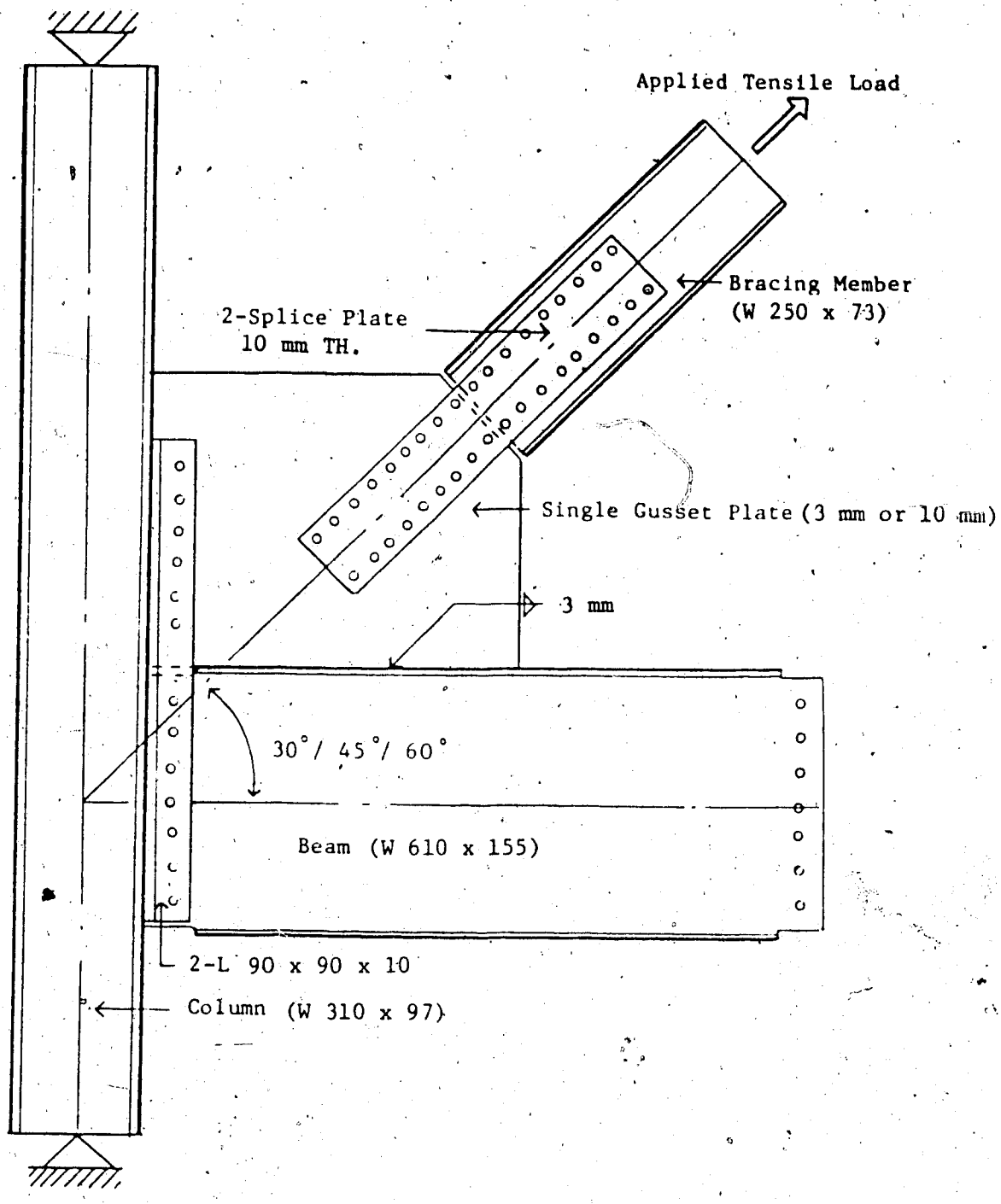

Figure 2.3 Specimens used in Bjorhovde's Test (1983)

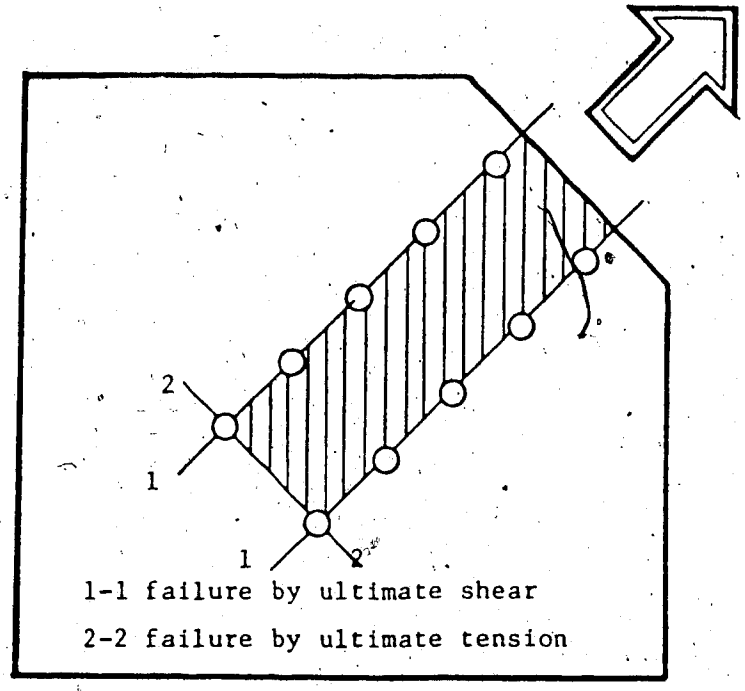

Figure 2.4 Block Shear Model for Gusset Plates in Tension

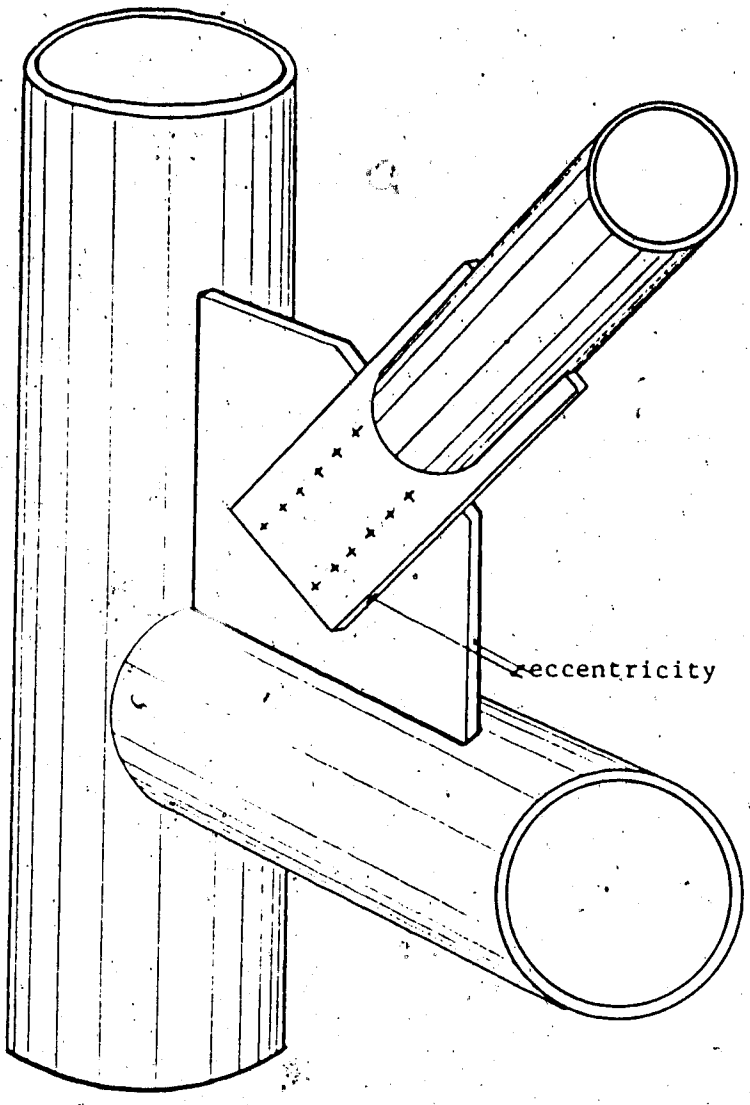

Figure 2.5 Gusset Plate Connections of Unstiffened Tubes

3. EXPERIMENTAL PROGRAM

3.1 Introduction

As mentioned in Chapter 1, the purpose of the experimental program was to investigate the general behavior and the actual failure mode of a gusset plate connection in a braced steel frame under compressive loading. A bracing member subjected to compression in a steel frame may fail either in the bracing member itself or in the gusset plate which connects the bracing member to the beam and the column. The bracing member may be a wide flange section or consist of two angle sections, as shown in Fig. 1.2, and its ultimate load carrying capacity can be readily evaluated by the buckling or yielding criteria (SSRC Guide, 1976). However, the ultimate load-carrying capacity of gusset plates is very difficult to evaluate due to its complicated configuration, boundary condition and residual stress pattern. If a bracing member is strong enough to resist a large compressive load, the bracing system may still fail due to the buckling of gusset plates. In such a case, the bracing member acting as a restraining member provides the rotational restraint to the plate. The assumption was made in designing the experimental program that the gusset plate buckled prior to the failure of the bracing member and the rotational restraint provided by the bracing member is infinite.

3.2 Preliminary Consideration

The experimental program was designed to represent the conditions of actual gusset plate connections. Thus, full-scale single gusset plate connections of a diagonal bracing member at the joint of a beam and a column were used, as shown in Fig.1.2. The variables of this kind of connection include plate thickness, plate size, angle of bracing, type of connection (welded or bolted), cross-section of bracing member, thickness of splice plate, length of splice plate, loading situation, residual stress pattern, etc. In order to simplify the problem, the variables considered in the experimental program are minimized and intended to cover only the most important parameters of such connections.

The test specimens were designed to fail in the elastic buckling; thus, thin plates were used. From basic plate buckling theory, the buckling coefficient is related to the width to depth ratio, the type of loading and the edge boundary conditions. Thus, two different sizes of plate were selected to evaluate the effect of the aspect ratio on the magnitude of the buckling load. The edge boundary conditions were designed to simulate the actual behavior of a gusset plate and divided into two different cases, namely a 'Free Case' and a 'Fixed Case'. The most common bracing angle in practice ranges from 30 to 60 degrees; it was thought that a 45 degree angle should represent this range and be easy to analyze. Also, for the purpose of eliminating the effect of

residual stress on the buckling load, bolted connections were used. Another consideration chosen in this project was the loading condition, including concentric loading and eccentric loading, in order to investigate the effect of eccentricity on the behavior and strength of gusset plates. In the eccentric loading case, different thicknesses of splice plate were used to produce an eccentric loading. The effect of a stiffener used to increase the flexural rigidity of the splice plate and the magnitude of failure load was also examined.

3.3 Specimen Description

Based on the previous considerations, a total of six gusset plate specimens with varying plate thickness and plate size were designed and the actual dimensions are listed in Table 3.1. The thicknesses of splice plates used in each test specimen are also given in Table 3.1. Two different thicknesses of gusset plates (6.7 mm and 3.11 mm) were used in the test specimens. The detail of the two different plate sizes (850 mm x 700 mm and 850 mm x 550 mm) used in the test specimens are shown in Fig 3.1. The gusset plate specimens were designed to be loaded at 45 degree by the bracing member. Plates C1 and C3 were loaded concentrically while plates E5 and E6 were loaded eccentrically. For comparison purposes, plates E5 and E6 have identical cross sectional properties to plates C1 and C3, respectively, but have different loading conditions and

different thickness of splice plates.

In all cases, the bracing member and the gusset plate were connected through splice plates by means of 3/4 in. dia. A325 bolts. Twelve bolts were used in each specimen to ensure no bolt failure prior to specimen failure. To simplify the set-up and reduce the end restraint from the boundary, welded end plates were used in the test specimens. Detail of two different sizes of splice plates and arrangement of bolt holes are shown in Fig. 3.2.

3.4 Test Set-up

A gusset plate connection used in a braced steel frame might deform out of plane due to compressive loading as shown in Fig. 3.3a. The upper end of the gusset plate which connects to the bracing member moves out of plane. However, the lower end of gusset plate, which is welded or bolted to the steel frame, remains in plane due to the restraint provided by the steel frame. This deformed shape can be simulated by the steel frame shown in Fig. 3.3b in which the bracing member and upper end of gusset plate remain in plane while the lower end of gusset plate along with the steel frame moves out of its original plane. To simplify the test set-up, the simulation of Fig. 3.3b was used. The schematic test set-up is shown in Fig. 3.4 and Fig. 3.5 is a photograph of the assembled set-up. To further simplify the test set-up, the forces that exist in the beam and column to balance the compressive load in the bracing member were

neglected. Although this may not reflect the actual forces in the beam and column, the effect of axial load in boundary elements on the buckling strength of a plate generally is negligible and this assumption is used in the current local buckling design criteria. The gusset plate itself was directly welded to the edge plates instead of to the beam and column and it was then bolted to the test frame through these pre-welded edge plates. It was recognized that for a thin plate the boundary conditions would be similar to the direct welding to the beam and column. The test frame consisted of two W310 x 97 beams with 12 mm thick end plates. These beam were welded to a 305 mm x 1100 mm x 12 mm plate. A W 250 x 58 section was bolted to the gusset plate through splice plates to act as a bracing member. To prevent transverse movement and allow the bracing member to move vertically, tension bars were used through the last row of bolt holes and located on the bottom of the bracing member. The tension bars were tightened by turnbuckles and nuts to a pair of auxiliary columns about 5 m away on each side of the test frame. The test frame, with the specimen in place, was then set on a pair of rollers to allow it to move laterally. To prevent sudden kicking out of the test frame and to create different boundary conditions, a pair of angle stoppers were located on each side of the test frame. The gap between the stopper and the specimen could be adjusted by a bolt which was placed on the center of the stopper. Following plate buckling, the bolt was losen manually until

it reached its maximum allowable displacement which was limited by the turning over of the rollers. The gap also could be eliminated by tightened the bolt which created the case of fixed boundary condition. The magnitude of the applied load and the vertical displacements of the specimens were monitored by the MTS test machine.

3.5 Instrumentation

The specimens were instrumented using linear variable displacement transducers (LVDT), strain gages and a dial gage to measure displacements and strains. In order to measure strain in the gusset plates, strain gages were placed on each specimen in pairs, one on either side of the gusset plate. The location of the strain gages was decided on the basis of previous tension test experience (Bjorhovde, 1983) and the predicted results using the finite element method (Richard, 1983). A pair of rosette gages was placed on the possible maximum normal stress point. For the specimens subjected to an eccentric load, an additional pair of strain gages was put on the location where a plastic hinge could possibly form. The locations of the strain gages are shown in Figs. 3.6 and 3.7.

The buckling shapes of the plates were monitored by three sets of LVDTs which recorded the deformed shapes of two free edges and the center line of the loading path as shown in Figs. 3.8 and 3.9. Two LVDTs were placed on the bottom of test frame to measure the possible twisting of

test frame. These LVDTs were placed on a temporary frame which was located about 4 m away on the east side of the specimen and connected to the specimens via brass wires as shown in Fig. 3.10. An LVDT was placed on the conjunction of bracing member and gusset plate to measure the vertical shortening of gusset plate.

A dial gage was located on the bottom of the west side of the test frame to monitor the test process as shown on the lower left corner in Figs. 3.8 and 3.9. Each of the strain gages, LVTDs, MTS load cell and MTS stroke was then assigned a specified channel connecting to the data acquisition system.

3.6 Test Procedure

Fourteen tests were run on these six specimens in order to best utilize the material. These tests were divided into two different categories - concentric loading (plates C1 to C4) and eccentric loading (plates E5 and E6).

Eight concentric loading tests were run on the plates C1 to C4 for the series C, in which two tests were conducted for each plate. These corresponded to the 'Free Case' and 'Fixed Case', respectively. The free case allowed the bottom of the test frame to move laterally and fixed case did not allow such movement, but for both cases the rotation at the bottom of the test frame was prohibited. The test procedure was generally the same for plates C1 to C4. First, the specimen was tested in the free case. The plate was loaded

in increments until the load versus lateral displacement curve became nonlinear. Stroke control was then used. The test was terminated when the predeterminated maximum lateral displacement was reached or the maximum load was obtained and unloading occurred. The maximum allowable lateral displacement of the roller underneath the test frame was 50 mm. To prevent sudden kicking out of the specimen due to energy release of the friction built up within the rollers, a pair of angle stoppers was put on each side of the test frame. The test specimen sprang back to its original position when the load was removed and stoppers were provided subsequently at the roller locations in order to prevent movement of the bottom of the specimen. A new test, corresponding to the fixed case, was then conducted until the specimen reached its ultimate load.

For the series E, six eccentric loading tests were performed on the two gusset plates E5 and E6, in which three cases were tested on each plate. these were called 'Free without Stiffener', 'Free with Stiffener' and 'Fixed with Stiffener', respectively. The details to produce the eccentricity and to reinforce the splice plate by using a stiffener for different cases are shown in Fig. 3.11. The test procedure followed the sequence of the above three cases. For the case of free without stiffener, the bottom of the specimen was free to move until it reached its ultimate load. To conducted the second case, the specimen was then forced back to its original position and stiffeners were

added at the splice plate location, as shown in Fig. 3.11 (TYPE B and C) and the specimen was reloaded again until it reached the maximum load. For the last case, fixed with stiffener, the specimen was moved back to its original location and a stopper was provided at the bottom of the rollers and the test procedure was the same as before.

Table 3.1 Geometric Properties of Test Specimens

Test Specimen	Thickness mm	Size mm x mm	Thickness of Splice Plate Used, mm
C1	6.70	850 x 550	13.0
C2	3.11	850 x 550	13.0
C3	6.70	850 x 700	13.0
C4	3.11	850 x 700	13.0
E5	6.70	850 x 550	8.1
E6	6.70	850 x 700	8.1

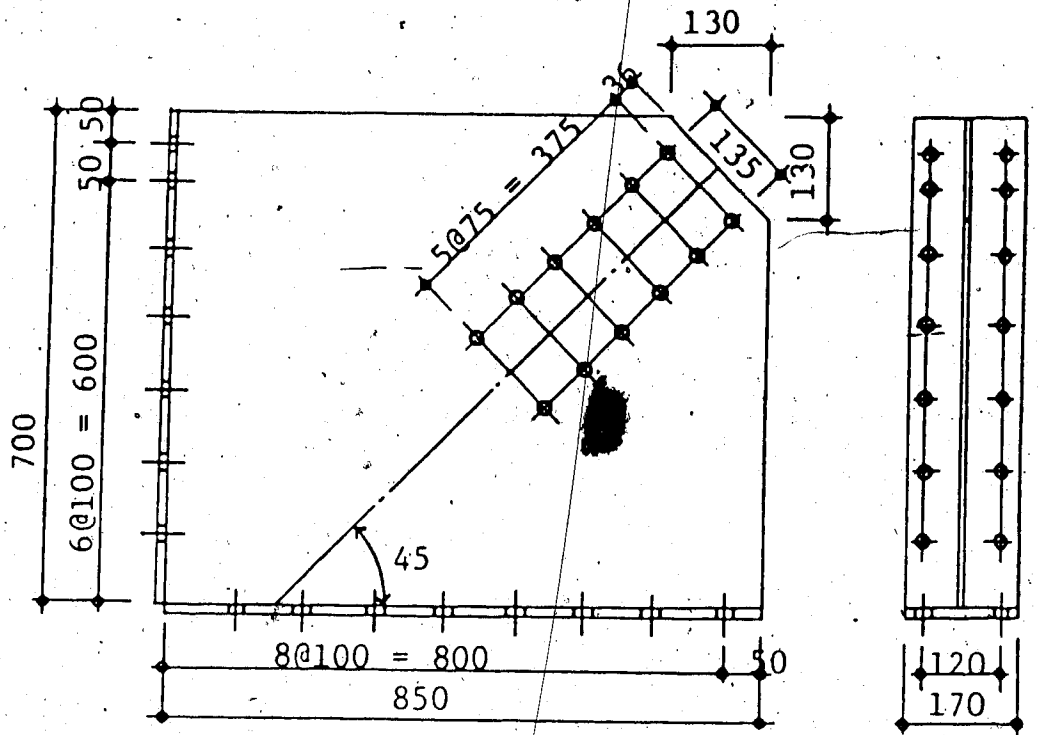

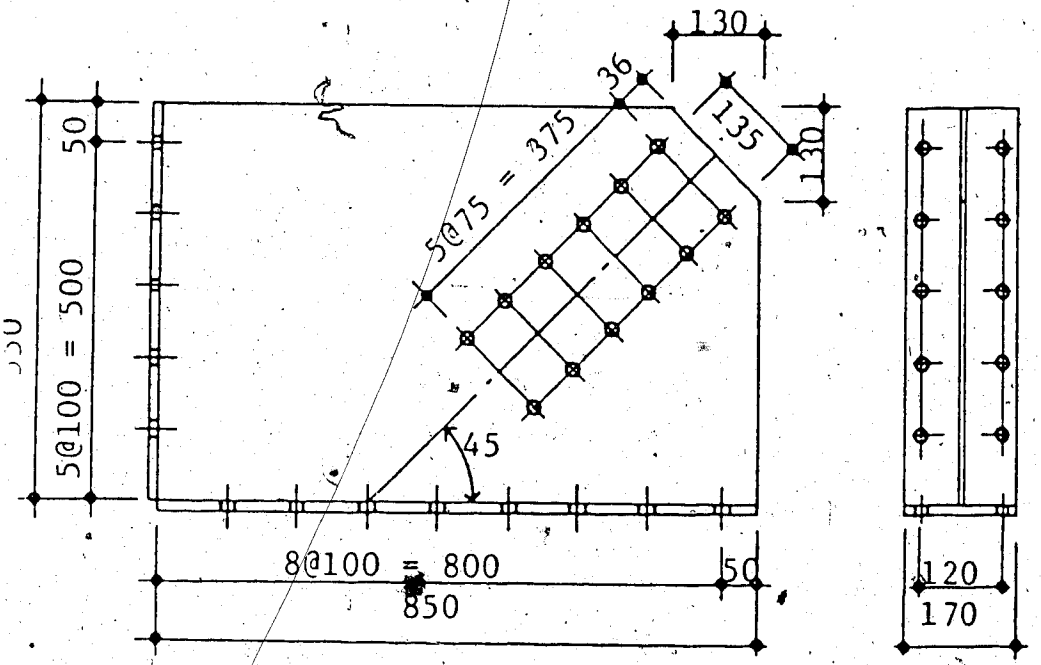

Figure 3.1 Detail of the Test Specimens

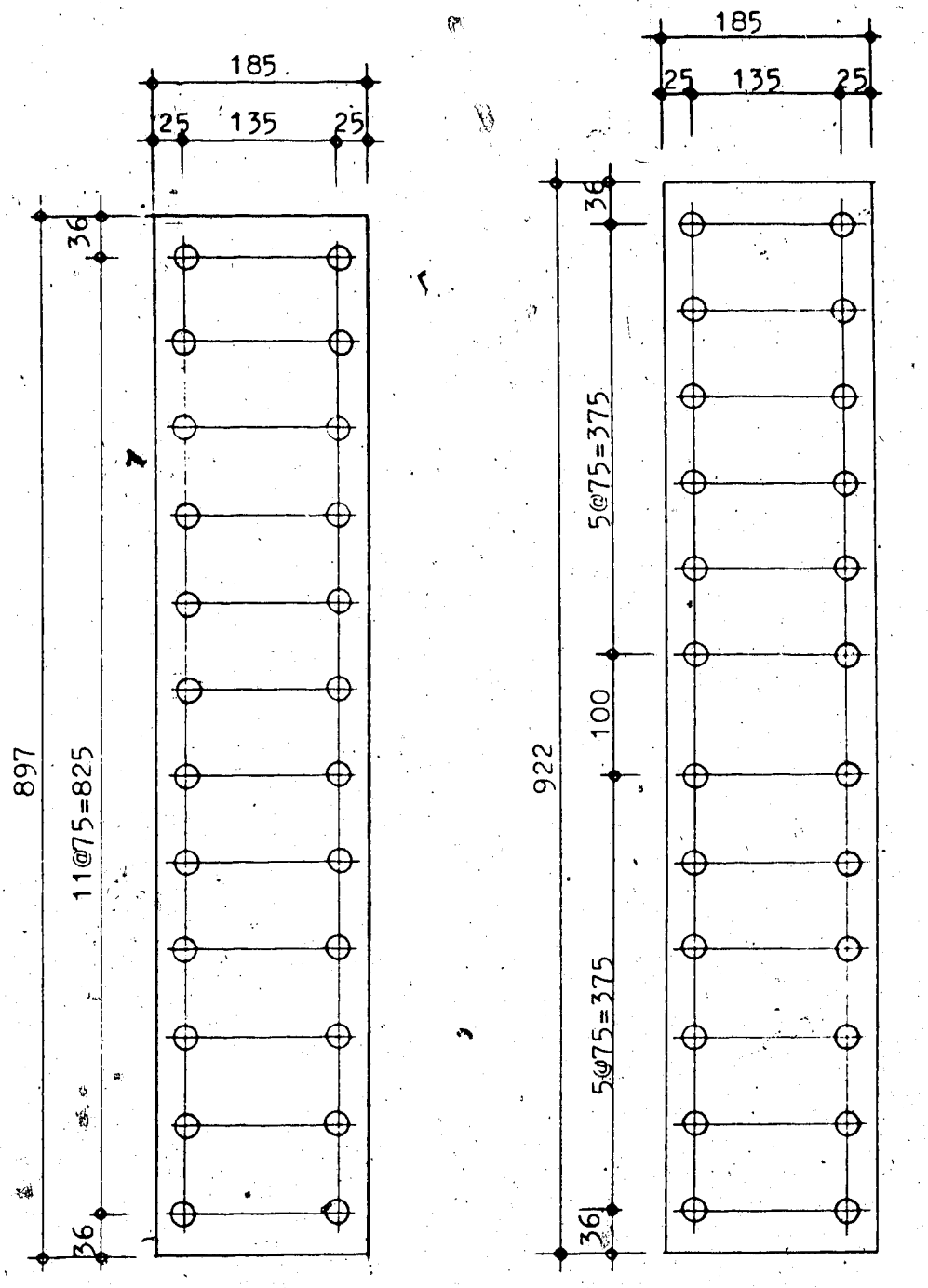

(a) for concentric loading specimens

(b) for eccentric loading specimens

Figure 3.2 Detail of the Splice Plates

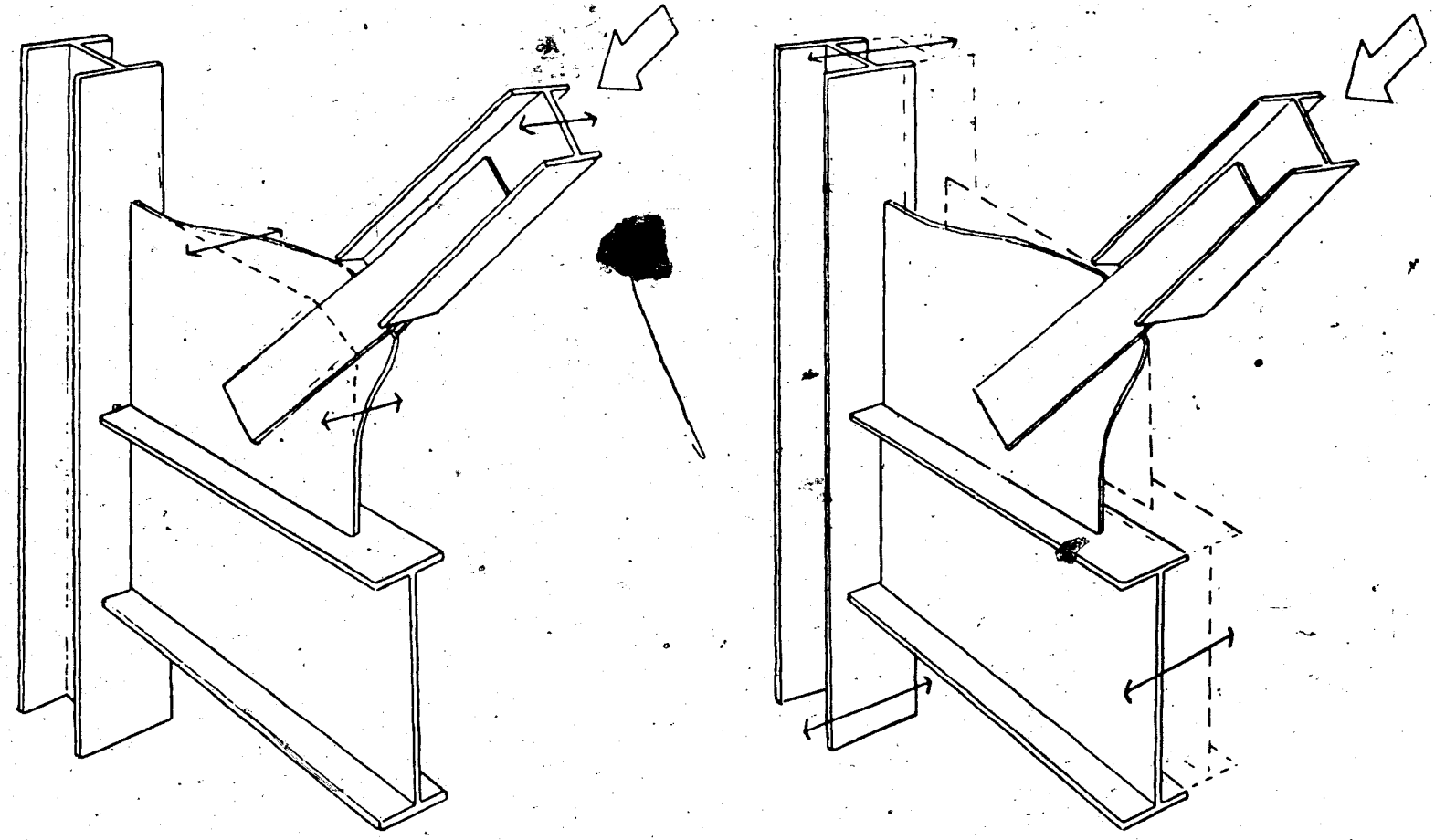

(a) bracing member and upper end of gusset plate deformed out of plane due to buckling

(b) steel frame and lower end of gusset plate move out of plane

Figure 3.3 Simulation of Boundary Conditions

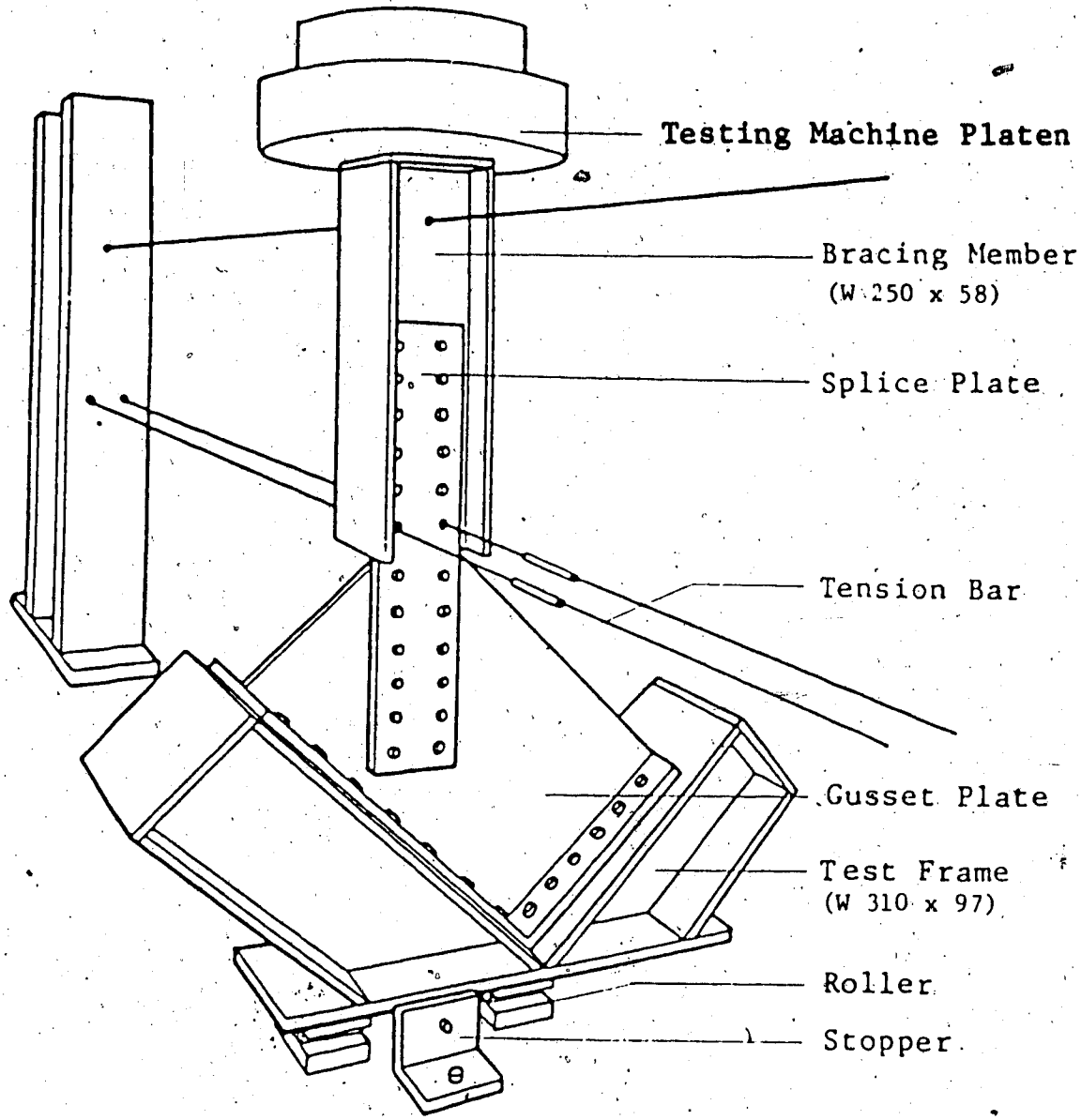

Figure 3.4 Schematic Test Set-Up

Figure 3.5 Test Set-Up

LEGEND

Strain Gage

Rosette Gage

Strain Gage applied only to E5 and E6

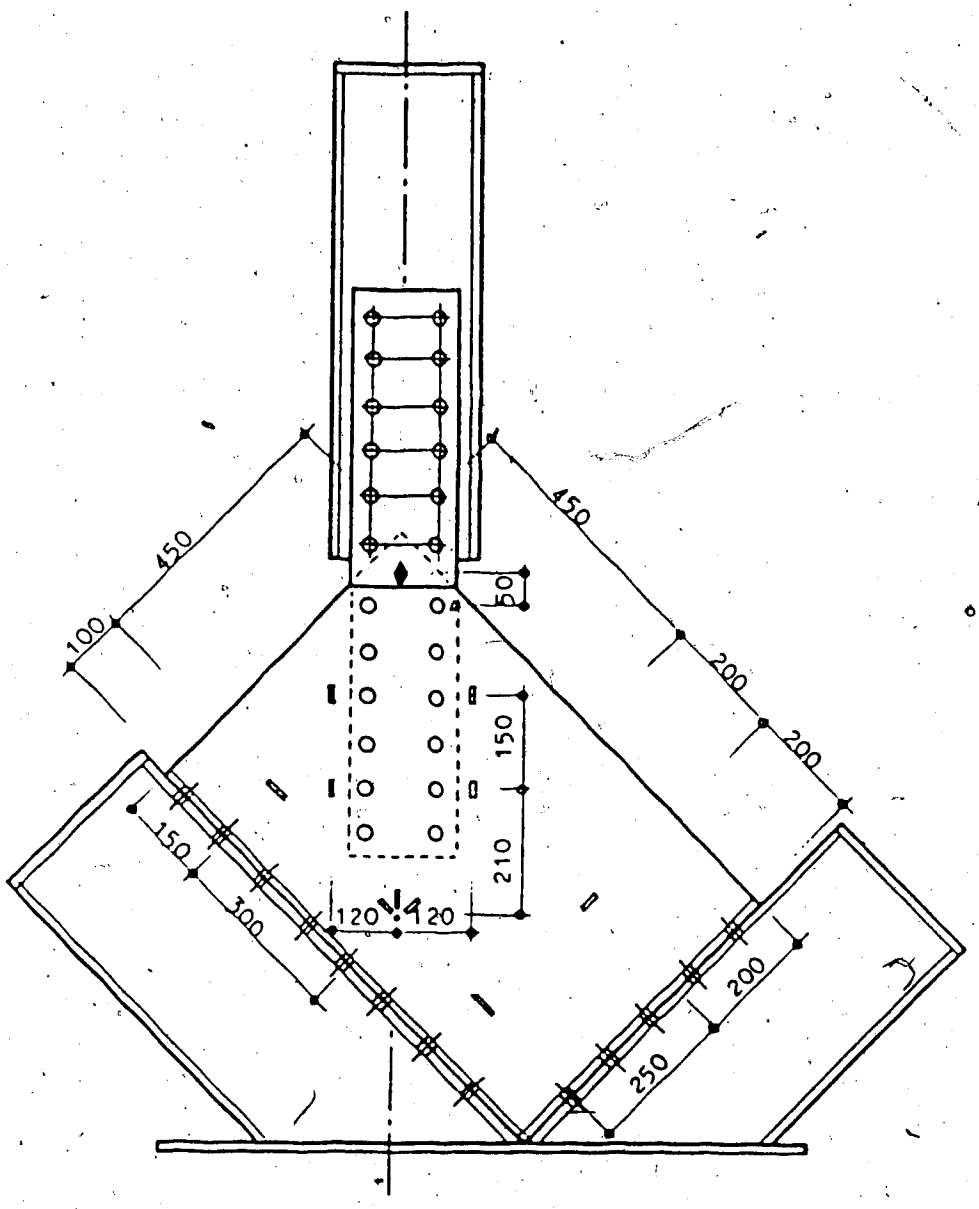

Figure 3.6 Strain Gage Locations of 850 mm x 550 mm Plates

LEGEND

▯ Strain Gage

Rosette Gage

♦ Strain Gage applied only to E5 and E6

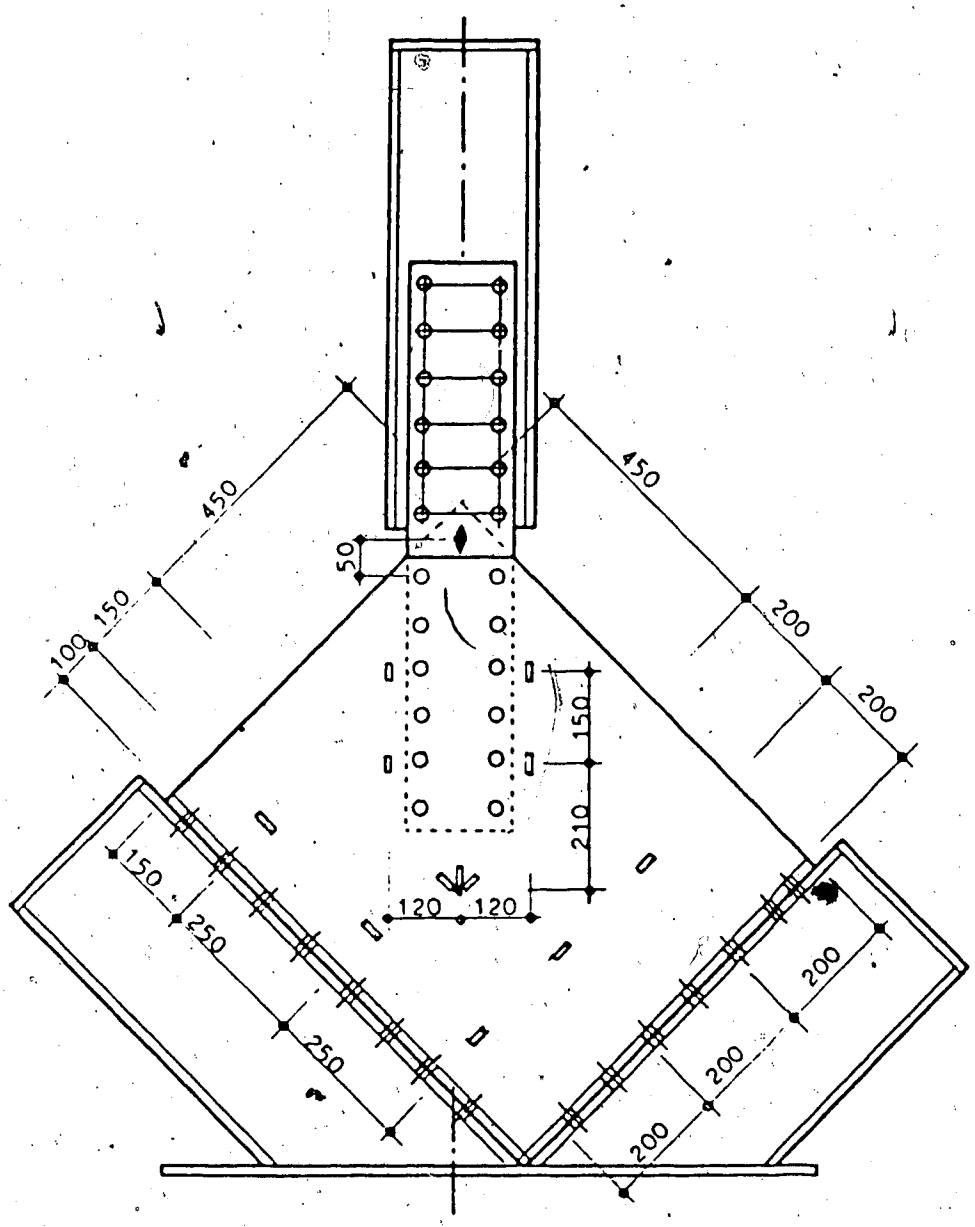

Figure 3.7 Strain Gage Locations of 850 mm x 700 mm Plates

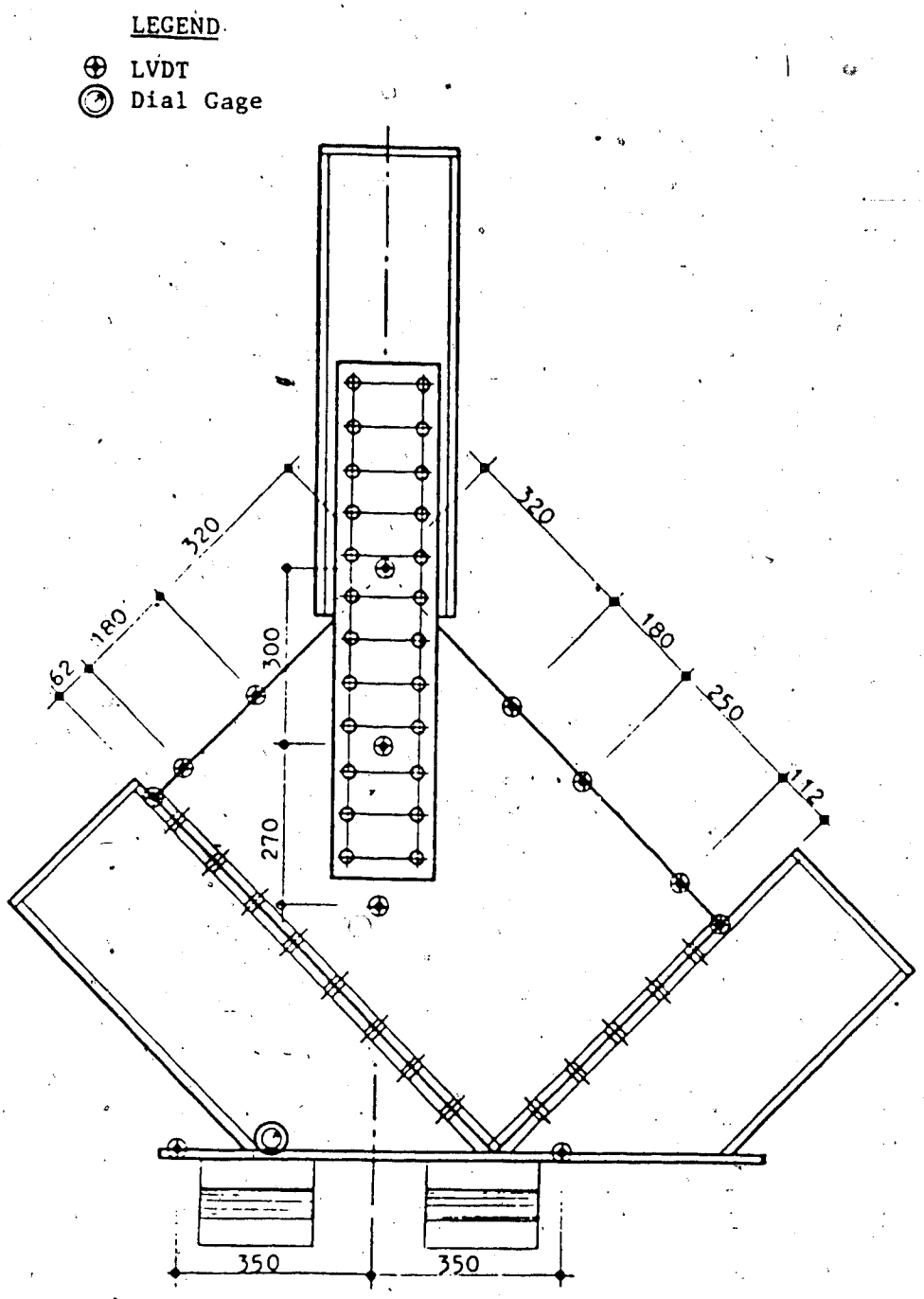

Figure 3.8 LVDT and Dial Gage Locations of 850 mm x 550 mm Plates

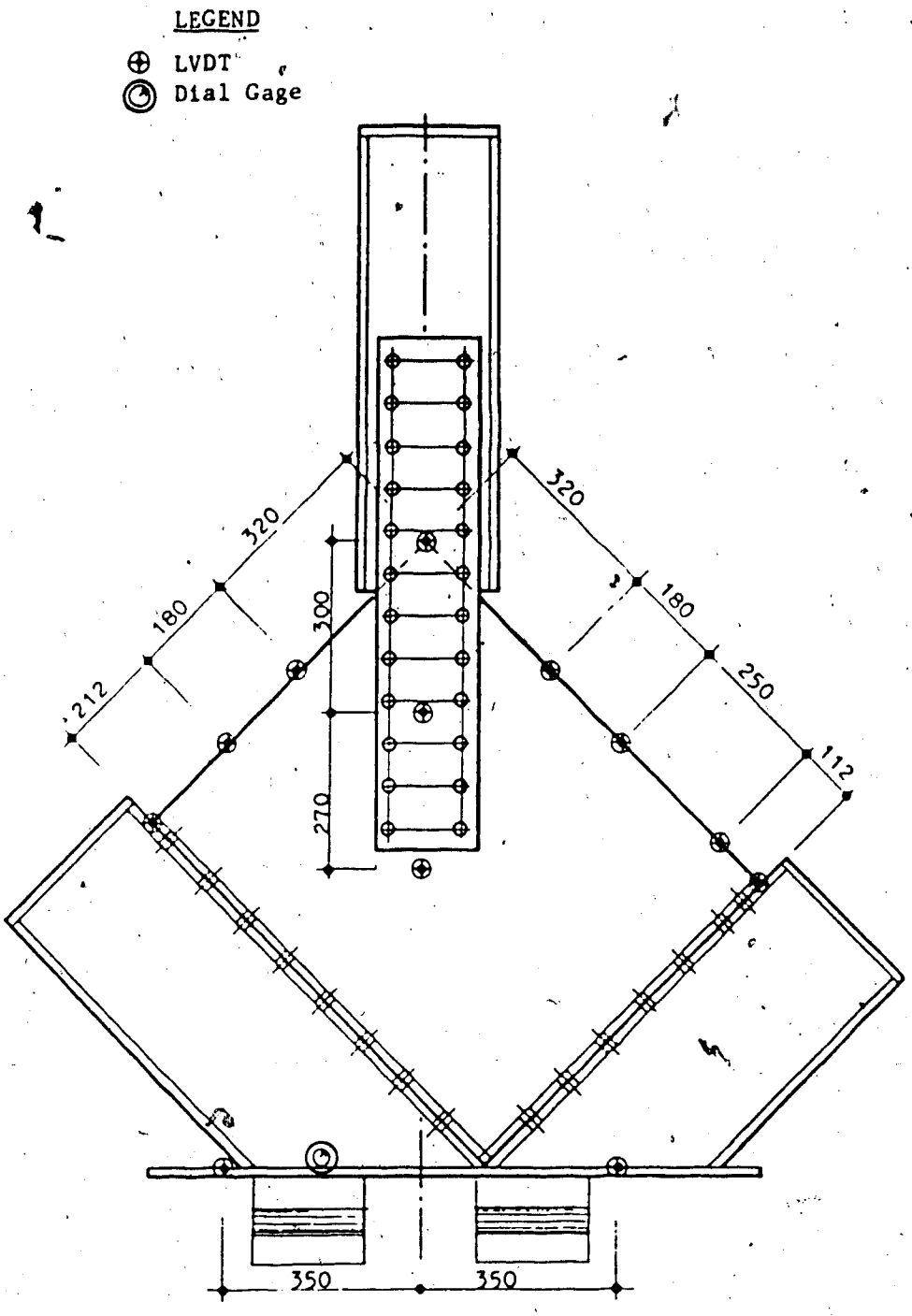

Figure 3.9 LVDT and Dial Gage Locations of 850 mm x 700 mm Plates

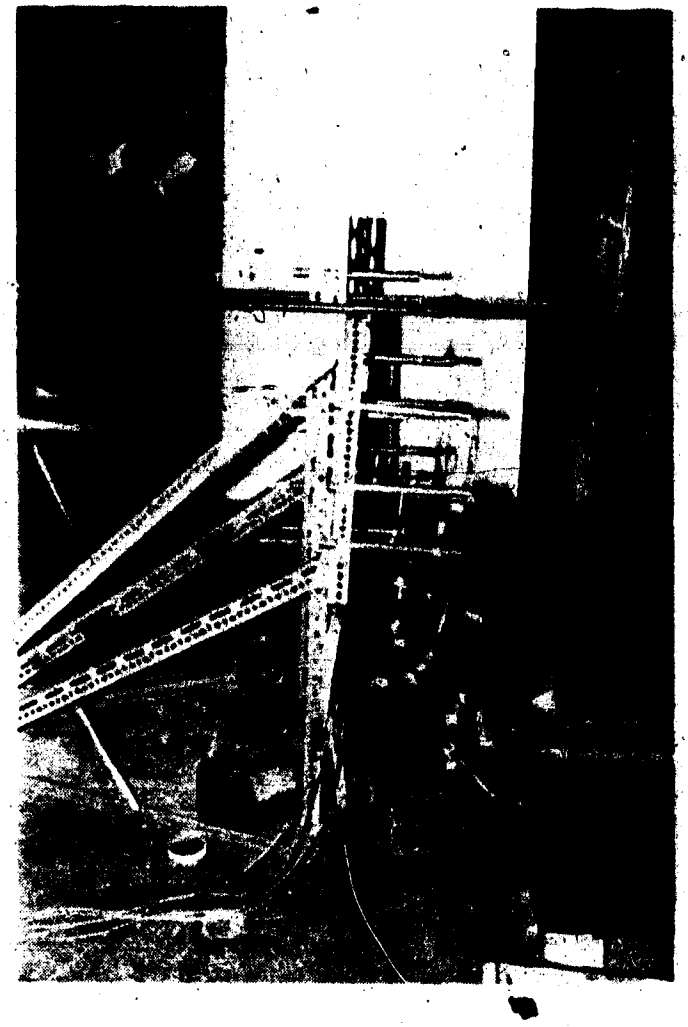

Figure 3.10 Supporting Frame of LVDTs

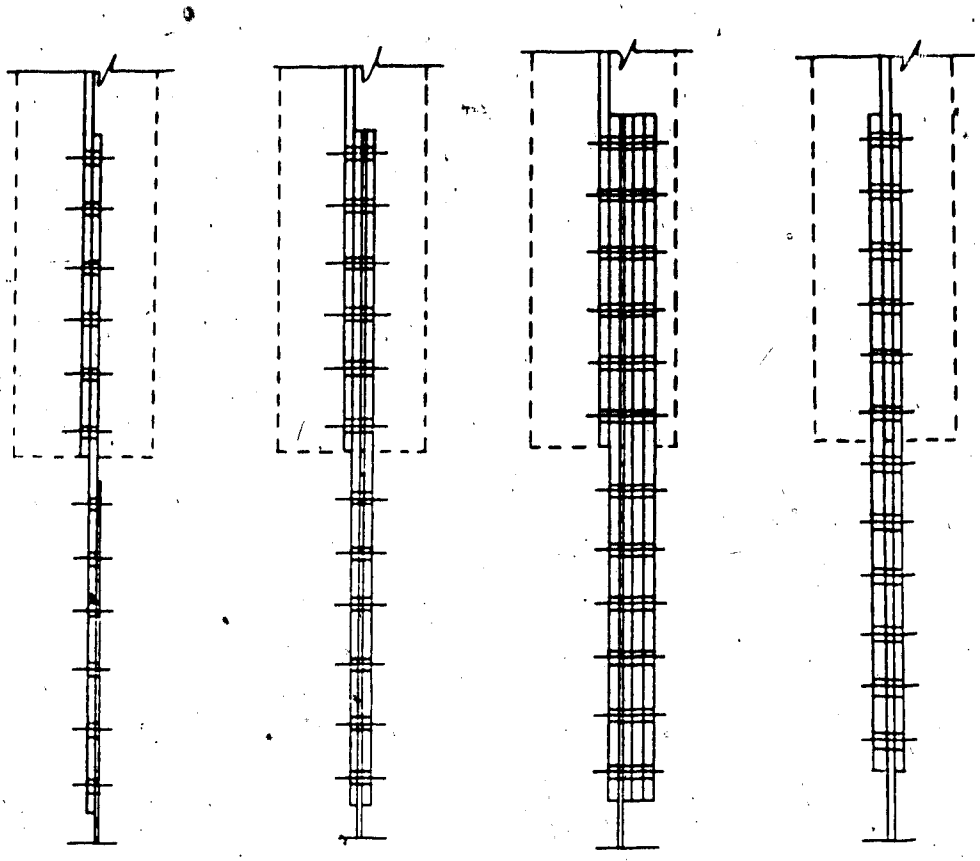

TYPE A TYPE B TYPE C TYPE D

Series	Cases	Type
Concentric Loading	both Free and Fixed Cases	D
Eccentric Loading	Free w/o Stiffener	A
	Free and Fixed w/ Stiffener for E5	B
	Free and Fixed w/ Stiffener for E6	C

Figure 3.11 Detail of Splice Plate and Stiffeners for Each Case

4. EXPERIMENTAL RESULT

4.1 Introduction

The results of the experimental program are presented in this chapter. The material properties of the test specimen are presented in Section 4.2. Section 4.3 describes the general behavior and the results of the test of the concentric loading. A description of the eccentric loading test is presented in Section 4.4. The summary of the maximum load, P_{max}, obtained from each test is given in Table 5.1 and will be further compared and discussed in Chapter 5.

4.2 Material Properties

Table 4.1 lists the values of elastic modulus, static yield point and ultimate strength as determined from tensile tests on the coupons taken from the material used in the test specimens. Two coupon tests were performed on each different thickness of plate, and the average values are reported. These coupon tests were conducted according to the ASTM standard (ASTM 1985).

4.3 Concentric Loading Test Results

As mentioned in Chapter 3, eight tests were run on four gusset plates in this series. Two tests were conducted on each plate with different boundary conditions, namely 'Free Case' and 'Fixed Case'. The test results of 'Free Case' are discussed first in this section followed by the results of

'Fixed Case'.

4.3.1 Free Case

In this case, the boundary conditions on the upper end of test specimens were designed to prevent both rotation and translation, while on the lower end rotation was fixed with translation permitted.

4.3.1.1 General Observation

All specimens in this case failed as a result of overall buckling of the plates themselves. When the applied load reached a certain value, the gusset plate started to buckle by the bottom of the test frame moving laterally out of its original position.

The maximum lateral deflection occurred at the bottom of the test frame. The LVDTs at these locations showed that both rollers had the same amount of displacement and no twist of the test frame was recorded. The other two LVTDs located on the end of both free edge of gusset plate also showed the same amount of displacement which indicated that no tilting occurred in the test frame. The buckling shapes of the specimens along two free edges and the center line of splice plate were plotted using the LVDT data from each location, normalized by the maximum displacement, as shown in Fig. 4.1. The photograph of the deflected shape taken from the short free edge of the plate C2 is shown in Fig. 4.2. They are very similar to the buckling shape of a

slender column with upper end fixed both in rotation and translation and lower end fixed in rotation but free in translation. They will be further compared with analytical solutions in Chapter 5.

The bolted connection was properly designed to ensure that no bolts failed before the maximum load of the plate was reached. No slip occurred between the splice plate and gusset plate and no yield line was observed either on the splice plate or on the gusset plate during the tests.

After unloading, the 6.7 mm gusset plates sprang back to their initial position with little residual lateral displacement. However, the 3.11 mm gusset plates recovered only part of their lateral displacement. There was a large residual displacement.

4.3.1.2 Behavior During Loading

The axial load versus vertical displacement curves are plotted in Figures 4.3 to 4.6, in which the load and stroke displacement from the testing machine are used. Figures 4.7 to 4.10 give the curves of the axial load versus lateral displacement in which the maximum deflection at the bottom of the test frame is used.

From the axial load versus vertical displacement curves, the same thickness of specimens exhibited similar behavior prior to reaching their maximum load. During the initial loading stages, nonlinearity was observed due to the settling of testing fixtures and the

nonuniform bearing at the two ends of the specimen. Following this, linear elastic behavior was observed for the thinner plates C2 and C4 up to a certain value, then the curves gradually turned to their maximum load level, as shown in Figs. 4.4 and 4.6. This can be attributed to the large initial imperfection that existed in the thin-walled specimens. However, a sharp turning to a maximum load after linear elastic portion was observed for the thicker plate C3, as shown in Fig. 4.5.

To prevent sudden failure and the possibility of the specimen kicking out, stroke control was used when curve started to become nonlinear. Tests were stopped either when the load started to decrease or when the lateral displacement reached about 70% of the maximum allowed value (50 mm).

The curves of axial load versus lateral displacement also behaved differently with different plate thicknesses. The curves for the 6.7 mm plates (specimens C1 and C3) show that, before buckling, the plate remained relatively staight. Beyond this point, larger deformations corresponding to an almost constant load were observed. For the 3.11 mm thick plates, which were C2 and C4, the curves gradually turned to their maximum loads, preceeded by only a small linear portion. Again, this can be attributed to the large initial imperfection of the plate section which was induced by the end plate welding and tightening up the specimen to

the test frame. The changing slope shown in Fig. 4.10 of plate C4 probably represents small local buckling due to initial imperfections.

The load versus vertical displacement curve (Fig. 4.3) and the load versus lateral displacement curve (Fig. 4.7) of test C1 show a sudden increase in the maximum loading capacity. It was caused by the bottom of the test frame hit the stopper at the reading #10. The stopper was moved outward slowly at reading #15 and the specimen moved laterally, accompanied by a loading decrease. The specimen was unloaded to approximate 145 kN and reloaded again until the load reached its maximum load.

The Southwell plotting technique (Southwell, 19[illegible] a method for predicting the buckling load in elas[illegible] region without actually loading the specimen to [illegible] was then used to determine the actual buckling load of this plate. The test data of load versus lateral displacement were plotted in the form of lateral displacement over loading versus lateral displacement curve, as shown in Fig. 4.11. The slope of the thick solid line in this plot is expected to represent the actual buckling load of the specimen. The predicted buckling load of 439 kN by the Southwell plot agrees very well with the measured maximum load of 441.7 kN. The dashed line in Fig. 4.7 was determined by using the slope in the Southwell plot (Fig. 4.11) to calculate the

corresponding loading and could be used to represent the actual test curve without interruption of load.

The principal stresses and the principal planes located at the spot of the possible maximum compressive stress were calculated using the rosette gages. The data were based on the average strains of gage readings on both sides of gusset plates. The orientations of the principal plane for the 6.7 mm plates in different loading stages remained constant. For the thinner plates, this angle diverged after the load reached about 80% of its maximum recorded value. The normal compressive stress along the applied load direction at the rosette gage location was also calculated and the curves of load versus normal compressive stress for different plates are presented in Figs. 4.12 to 4.15. Linear elastic behavior existed on the thicker plates before reaching their maximum load. However, nonlinear behavior existed for the thinner plates after the applied load exceeded approximate 80% of the maximum recorded load. None of the average principal stresses of the tests exceeded the yielding strength of the material from this calculation. However, the experimental data show that partial compressive yielding occurred on the west side of plate C2 at the rosette gage location. This was probably due to the large lateral displacement of the plate. Comparison of test data with the Whitmore model and an analytical solution will be further

discussed in Chapter 5.

.3.2 Fixed Case

The same plates were again used to perform the second et of tests with different boundary conditions. The plates ere adjusted back to their initial loading position. Two toppers were placed on both sides of the test frame. These revented the rollers from moving. In this manner, lateral ranslation of the test frame was prohibited.

4.3.2.1 General Observation

All specimens failed as a result of buckling of the gusset plate. The maximum deflection due to the buckling of the plate occurred at the mid-point of the longer free edge.

The deflected shapes of two free edges and the centerline of the loading path show the idealized fixed-fixed end boundary condition for the thinner plates (C2 and C4), as shown in Fig. 4.16. Relatively large rotations were observed on the upper end of the gusset plate for the thicker specimens at the conjunction of the gusset plate and bracing member, as shown in Fig. 4.16. In plotting the results, these deflected shapes were normalized by the largest lateral deformation, which was located on the center of the longer free edge. The photograph of the buckled shape taken from the longer free edge of specimen C2 is shown in Fig. 4.17. The comparison with an analytical solution

will also be discussed in Chapter 5.

Compressive yield was observed on the splice plate near the top row of bolts connecting the splice plates to the gusset plate for both plate C1 and C3. This was due to the high axial load and the large lateral deformation of the gusset plate. It indicated that the rotation at this location was gradually developed as the load increased. No yield line was observed on the plates C2 and C4. The buckling shapes of centerline for these two specimens also indicated that only relative small rotations were developed at this location due to the relative thinner thicknesses of the gusset plate and the splice plate.

4.3.2.2 Behavior During Loading

The curves of the axial load versus vertical displacement are plotted in Figures 4.18 to 4.21. Figures 4.22 to 4.25 give the curves of the axial load versus lateral displacement in which the lateral displacement at the mid-point of the longer free edge was used. The same behavior as previous case was observed in these curves. However, after reaching the maximum load, the load started to drop instead of remaining constant, as shown in the free cases. This phenomenon could be attributed to the partial yielding of the splice plate which reduced the rotational restraint at the upper end of the gusset plate.

The load versus lateral displacement curve for plate C4 (Fig. 4.25) is different from other tests. The reason was that before reaching the maximum load the plate was deflected in one direction due to the large initial imperfection. After reaching its maximum load, the plate sprang back to opposite direction with a sharp decreasing load. In order to illustrate the behavior further, both mid-point lateral deflection of the longer and shorter free edges are shown in Fig. 4.25. The curves of average normal compressive stress at the point of rosette gage versus load show that specimens behaved linearly for thicker plates, as shown in Figs. 4.26 and 4.28. On the other hand, the thinner plates behaved nonlinearly at higher load level, as shown in Figs. 4.27 and 4.29. Except for plate C4, the corresponding normal compressive stresses in Figs. 4.26 to 4.28 agree fairly well with the normal compressive stresses in the free cases (Figs. 4.12 to 4.14). None of the strain gage readings exceeded the yield strength of the material.

4.4 Eccentric Loading Test Results

It is customary to neglect the eccentricity in designing gusset plate connections. However, the eccentricity may cause a significant reduction of the load carrying capacity of gusset plates. Six tests were run on two plate specimens, E5 and E6, with eccentricity. Their dimensions and thicknesses were identical to the plate C1

nd C3, respectively. Three tests were conducted on each pecimen, namely, 'Free Case without Sitffener','Free Case ith Stiffener' and 'Fixed Case with Stiffener'. These will e discussed below in sequence. Because of the similarity of he load versus displacement (both vertical and lateral) urves to the concentric loading case, the curves of this ase will not be discussed in this section. However, all the urves are given in Appendix A for completeness.

.4.1 Free Case without Stiffener

Tests were conducted on plates E5 and E6 with a ccentricity of 12 mm in order to demonstrate the importance f eccentricity of loading.

4.4.1.1 General Observation

In both specimens the bottom of the test frame moved laterally eastward due to the applied eccentric load and produced yielding on the splice plate. Compressive yield lines were observed on the splice plate at the the last row of bolts of the bracing member for both plates. Figure 4.30 shows yield lines at this location for the plate E5. The maximum loads were 80.4 kN and 55.8 kN for plates E5 and E6, respectively. As predicted, the load-carrying capacity decreased significantly below the buckling load as compared with the previous tests of free case of plates C1 and C3 where the maximum loads were 441.7 kN and 380.1 kN, respectively. Specimens failed by yielding resulting

from bending of the splice plates and permanent deformation existed in the splice plate after unloading. A relatively large centerline deflections comparing with the deflection of the free case of the specimens C1 and C3 was observed. The deformed shapes of both specimens are shown in Fig.4.31.

4.4.1.2 Behavior During Loading

The strain gage readings showed that compressive yielding occurred on the east side of splice plate at the conjunction of bracing member and gusset plate for the plate E5 corresponding to its maximum load. On the west side of the splice plate, unloading was recorded. However, the first compressive yield lines were observed at the last row of bolts of the bracing member at the load of 79.5 kN for plate E5. The yield lines were located higher than the strain gage location, as shown in Fig. 4.32 (TYPE A). Therefore, actual yielding took place earlier than the strain gage reading recorded. Similar results were observed for the plate E6. The reason this occurs is because the weakest cross-section is at the last row of bolts. Thus, it is reasonable to assume that the cross-section at the last row of bolts on the bracing member already fully yielded before reaching their maximum load.

4.4.2 Free Case with Stiffener

The same specimens were then stiffened using additional splice plates, as shown in Fig. 3.11 and 4.32, and tested under the same boundary conditions as the previous case in order to evaluate the effect of stiffener.

4.4.2.1 General Observations

For the plate E5, an additional splice plate with thickness of 8.1 mm was placed as shown in Fig. 4.32. The load-carrying capacity increased significantly, to 232.8 kN. This is approximately three times higher than the case without this additional stiffener. However, the ultimate load did not reach the load of the free case of specimen C1. Yield lines formed in the same location (Fig. 4.32 TYPE B) as the free case without stiffener before reaching its maximum load. Again, the plate failed because the load exceeded the combined bending resistance of the splice plate and the stiffener.

Three additional splice plates, each of 8.1 mm thickness, were placed on the east side of the plate E6 to improve the bending resistance of the splice plate. The load-carrying capacity of this specimen also increased significantly, to 338.6 kN, which is approximately 89% of the ultimate load of the free case of plate C3. However, it should be noted that the two specimens (E6 and C3) above had a different arrangement and thickness of the splice plates. This would provide different rotational restraint to the gusset plate. No

yield lines were observed in the splice plate at its maximum load. After the load started to decrease, yield lines were observed at the conjunction of bracing member and gusset plate due to the large lateral displacement.

4.4.2.2 Behavior During Loading

Plates E5 and E6 deformed in opposite directions due to the different arrangement of stiffeners. The yield lines also occurred at different locations.

From the gage reading at the conjunction of bracing member and gusset plate, plate E5 had compressive yield at east side of splice plate after load decreased to 210 kN from its maximum load. The yield lines were first observed at a load of 231 kN before reaching its maximum load. The yield lines were located higher than the strain gage location, as shown in Fig. 4.32 (TYPE B). Again, it could assumed that full yield occurred at the last row of bolts of the bracing member before reaching its maximum load.

For the plate E6, the first yield lines were observed at the maximum load on the conjunction of bracing member and gusset plate right at the location of strain gage, as shown in Fig 4.32 (TYPE C) Because of the failure of the strain gage on the compression side, the strain gage readings indicated that tensile yielding was first recorded at a load corresponding to the maximum load. Therefore, partial yielding at this location changed the boundary condition at the upper end

of the gusset plate and less rotational restraint was provided. Thus, the buckling load was reduced. The specimen failed as a result of the interaction between cross-section strength and structural stability.

4.4.3 Fixed Case with Stiffener

The same plates with the same stiffener were used in another set of tests with different boundary. As mentioned, stoppers were placed on both sides of the test frame and lateral movement was thereby prevented. In this manner, rotation and translation at both the top and bottom ends of the specimens was prohibited.

4.4.3.1 General Observations

The changing of the boundary conditions did increase the maximum load capacity from previous case. The load increased from 232.8 kN to 392.5 kN for plate E5 and from 338.6 kN to 523.2 kN for plate E6.

Plate E5, which has only one piece of stiffener, deformed eastward. Yield lines occurred at the last row of bolts of the bracing member before the maximum load was reached.

Plate E6, which had three pieces of stiffeners placed on the east side of the gusset plate, deformed westward. Yield lines were observed at the conjunction of the bracing member and the gusset plate before reaching its maximum load.

4.4.3.2 Behavior During Loading

From gage readings, first compression yield was recorded in plate E5 on the east side of splice plate at the maximum load level. However, first yield observed was located higher than the strain gage location and took place earlier. Thus, the same conclusion can be drawn, that is, the cross-section at the last row of bolts of the bracing member is fully yielded at maximum loading.

Tensile yield was recorded on east side of splice plate at the load close to the maximum load for plate E6. A large strain, which was approximately twice the yield strain, was recorded at its maximum loading stage, and the cross section at the strain gage location approached full yield.

Table 4.1 Material Properties

Material Used	Elastic Modulus (MPa)	Static Yield Strength (MPa)	Ultimate Strength (MPa)
6.70 mm Gusset Plate	211 000	505	595
3.11 mm Gusset Plate	197 000	240	340
13.0 mm Splice Plate	205 000	260	420
8.1 mm Splice Plate	211 000	305	495

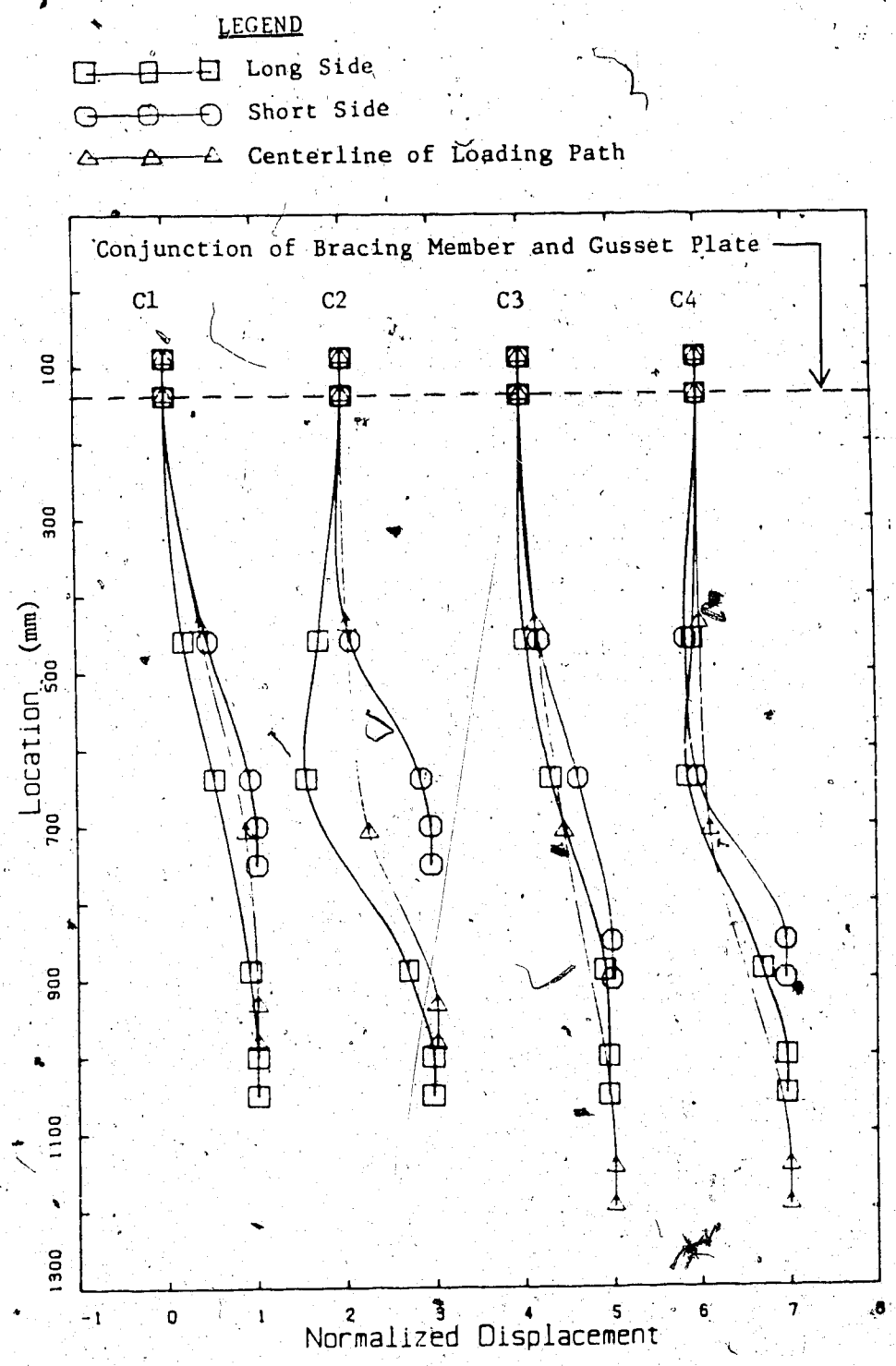

Figure 4.1 Normalized Deflected Shapes of Free Case of Concentric Loading Corresponding to the Maximum Load

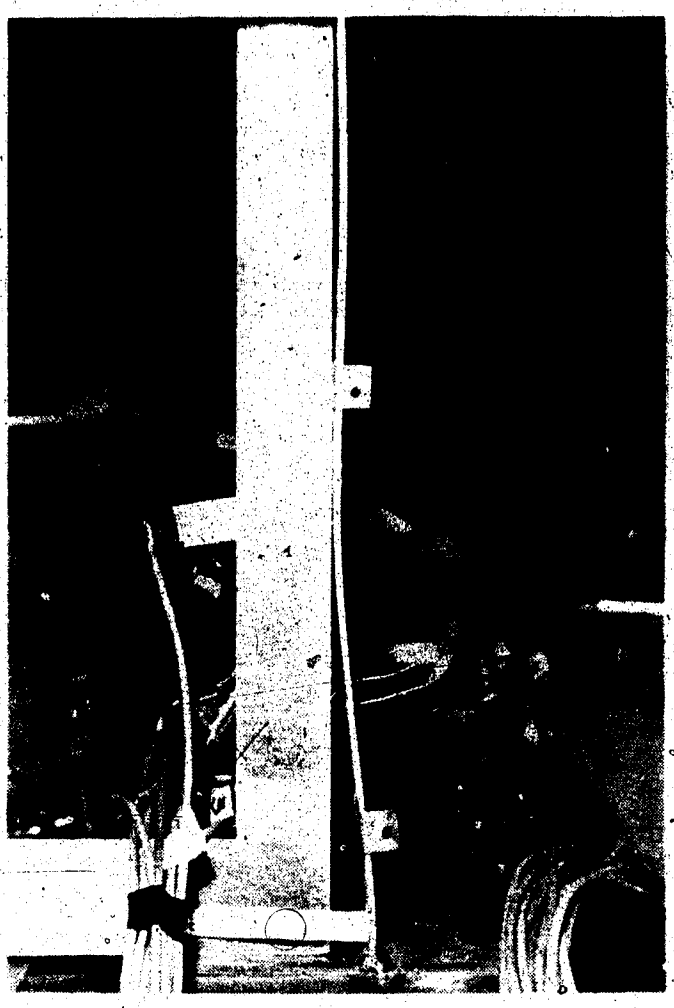

Figure 4.2 Deflected Shape of Short Free Edge of Free Case of Plate C2

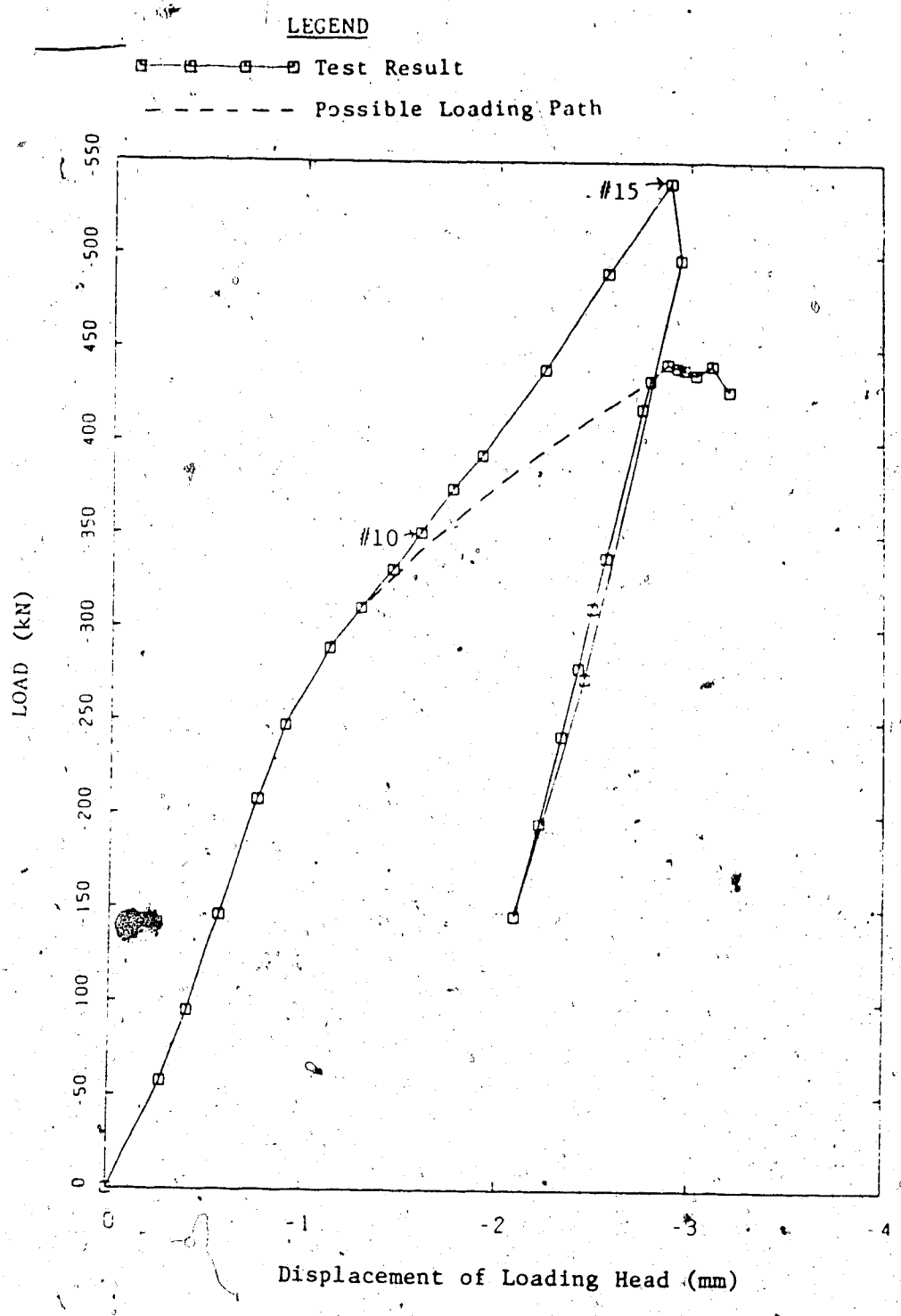

Figure 4.3 Load versus Vertical Displacement Curve for Plate C1 of Free Case

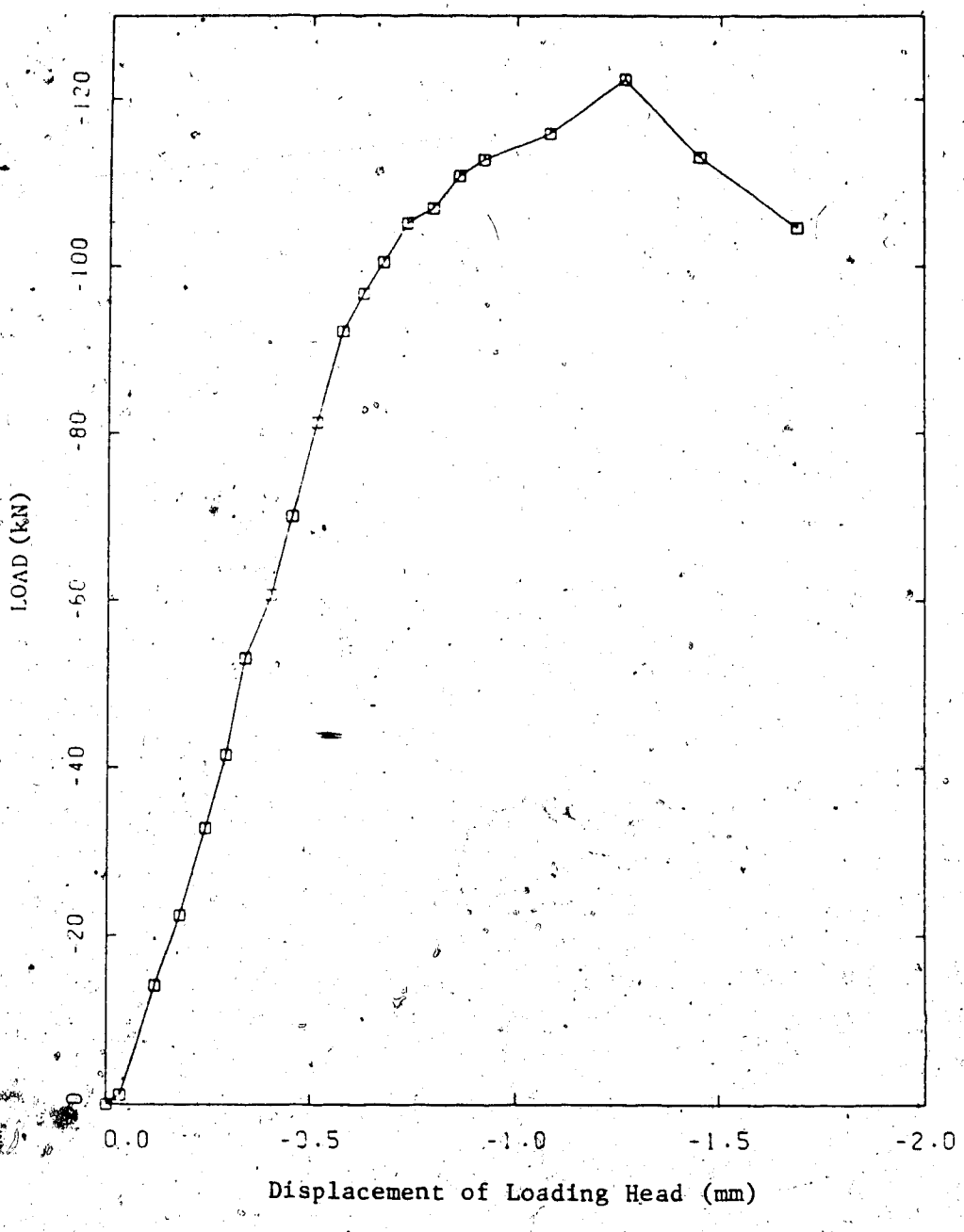

Figure 4.4 Load versus Vertical Displacement Curve for Plate C2 of Free Case

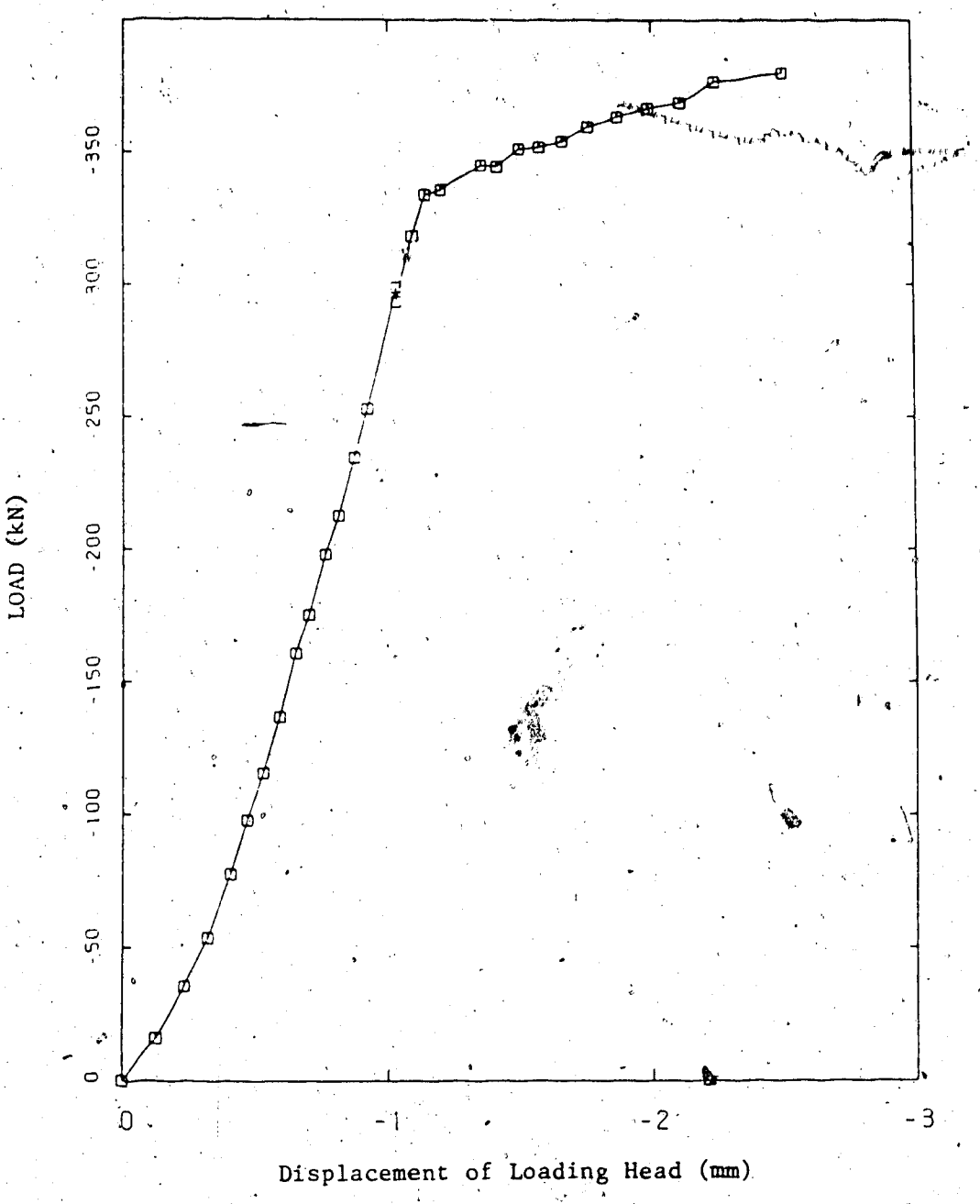

Figure 4.5 Load versus Vertical Displacement Curve for Plate C3 of Free Case

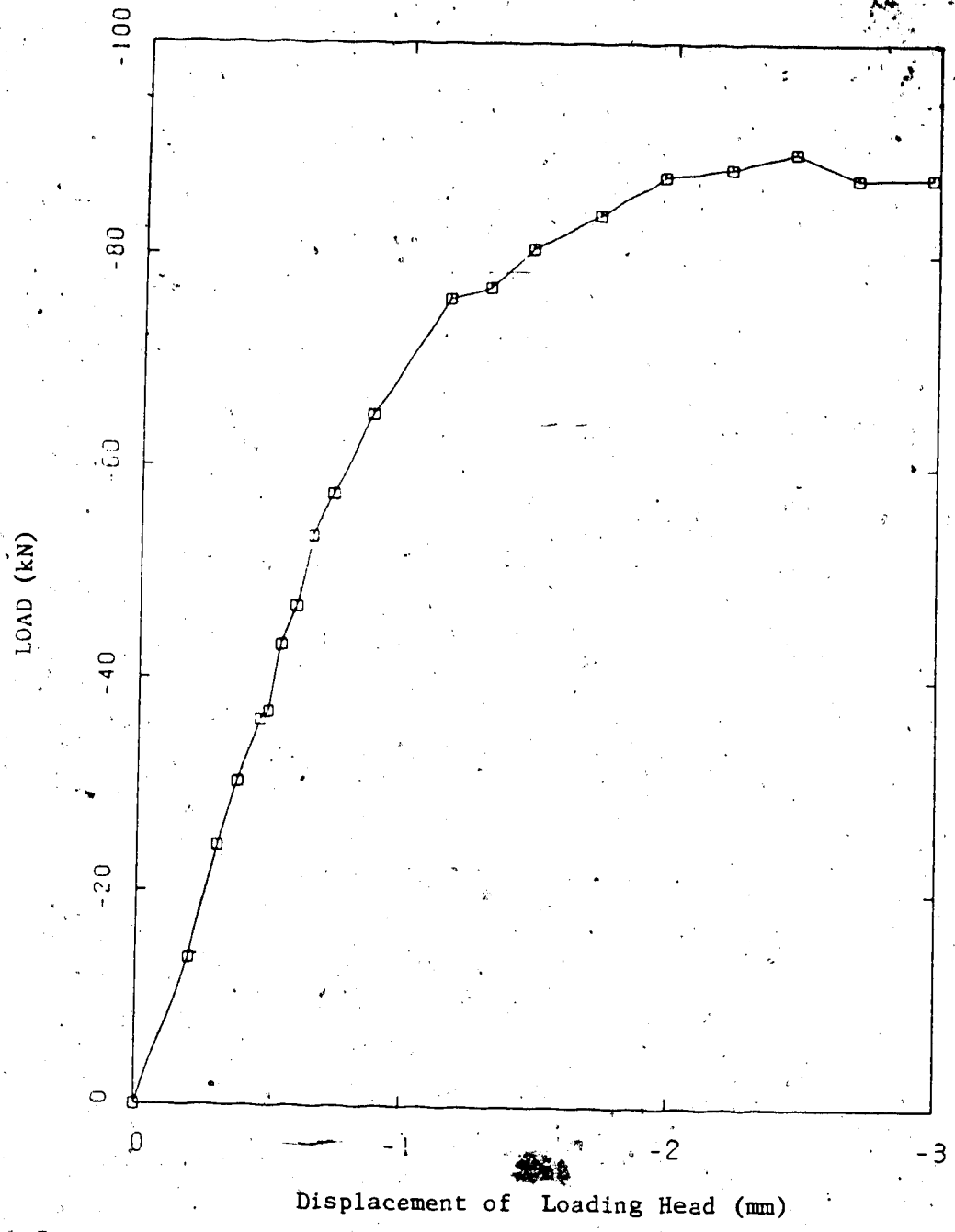

Figure 4.6 Load versus Vertical Displacement Curve for Plate C4 of Free Case

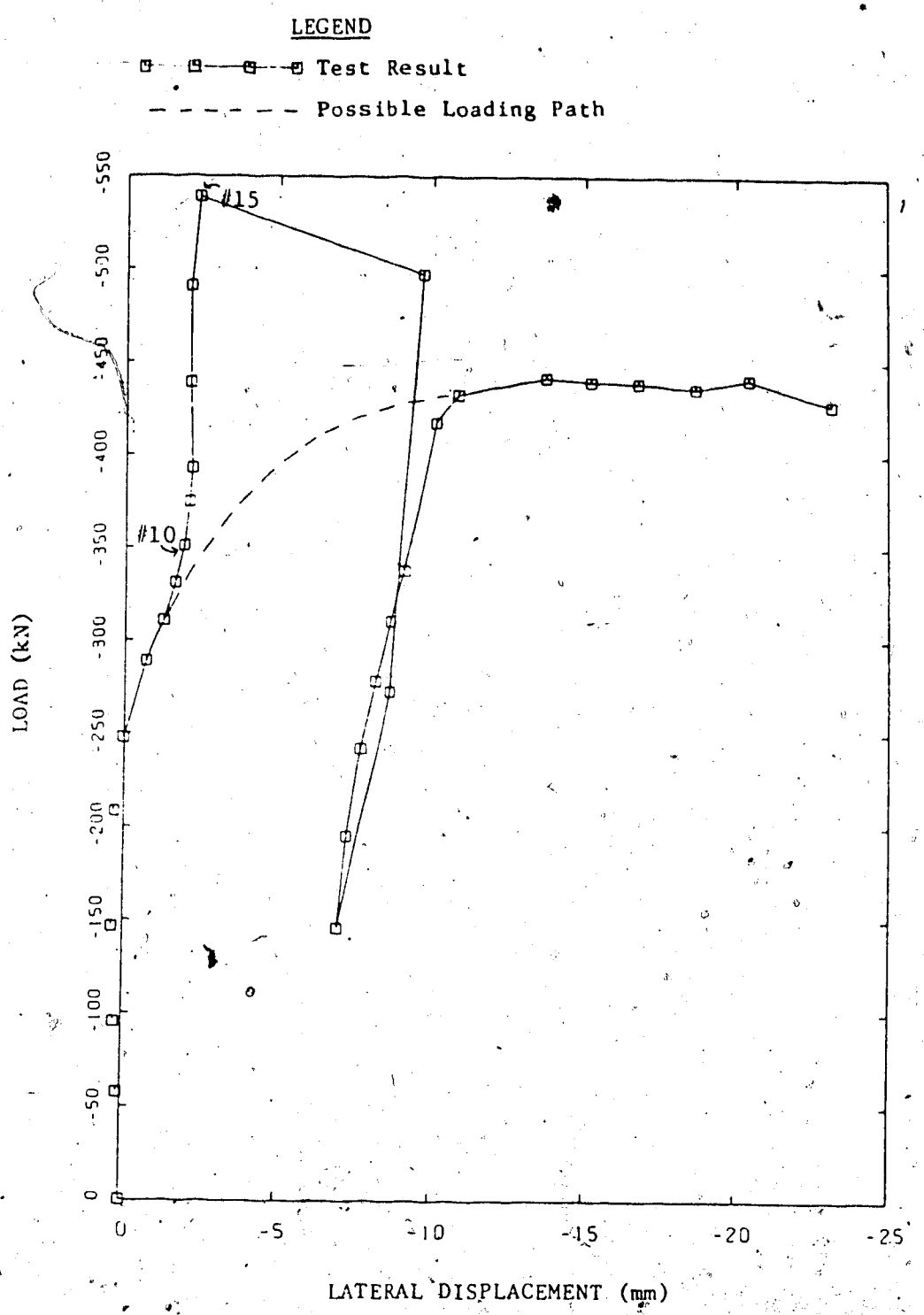

Figure 4.7 Load versus Lateral D[illegible]t Curve for Plate C1 of Fre[illegible]

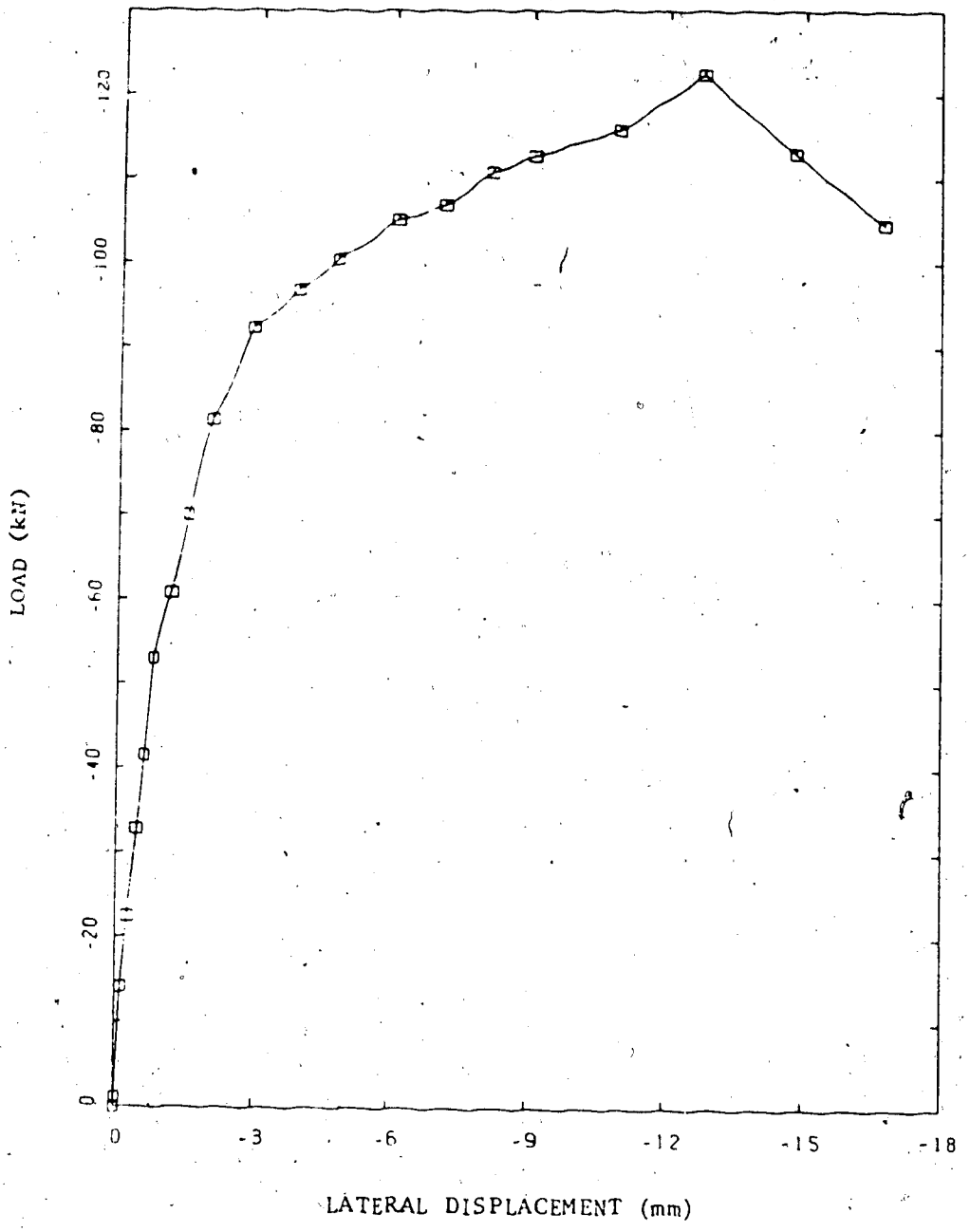

Figure 4.8 Load versus Lateral Displacement Curve for Plate C2 of Free Case

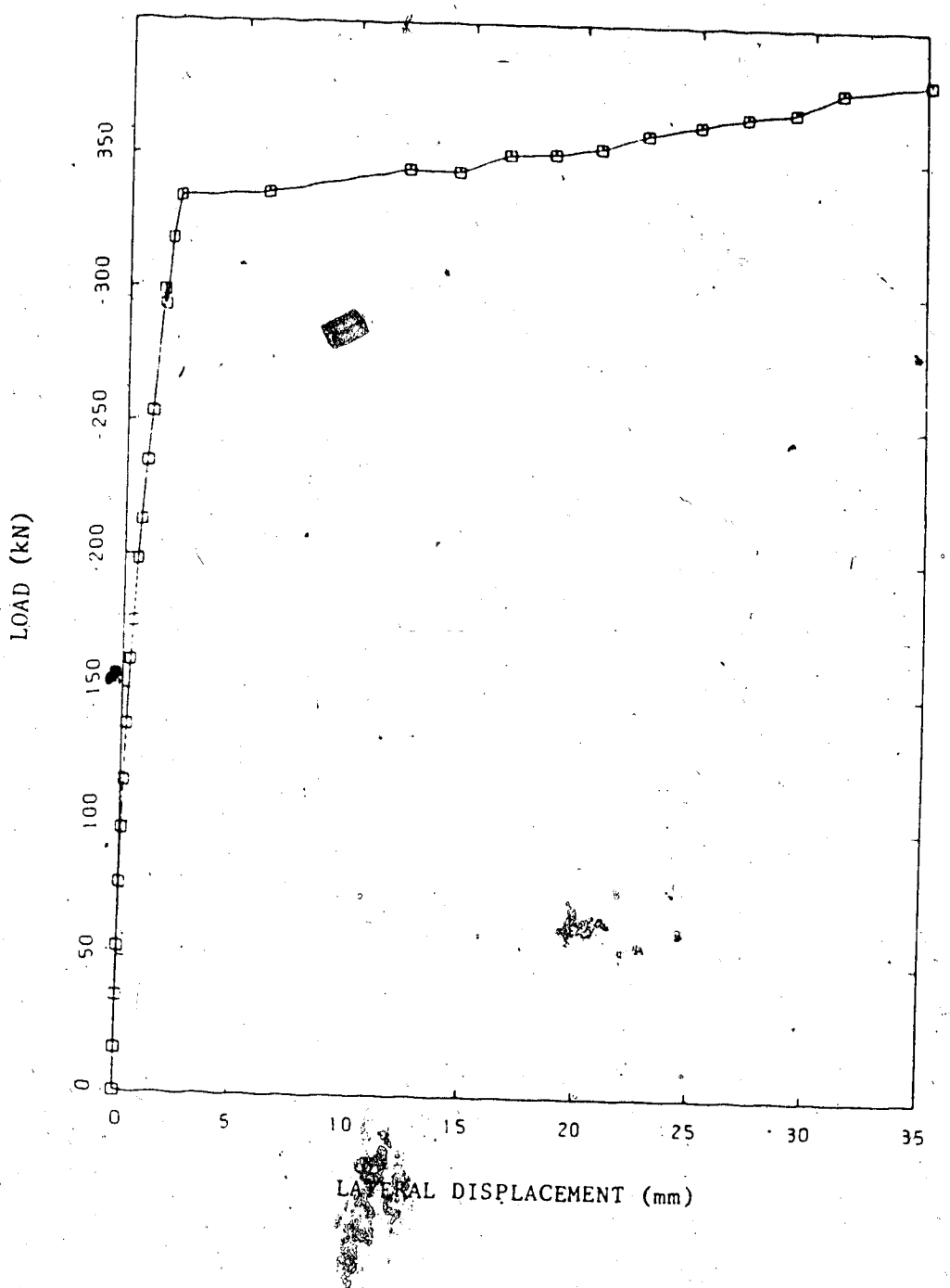

Figure 4.9 Load versus Lateral Displacement Curve for Plate C3 of Free Case

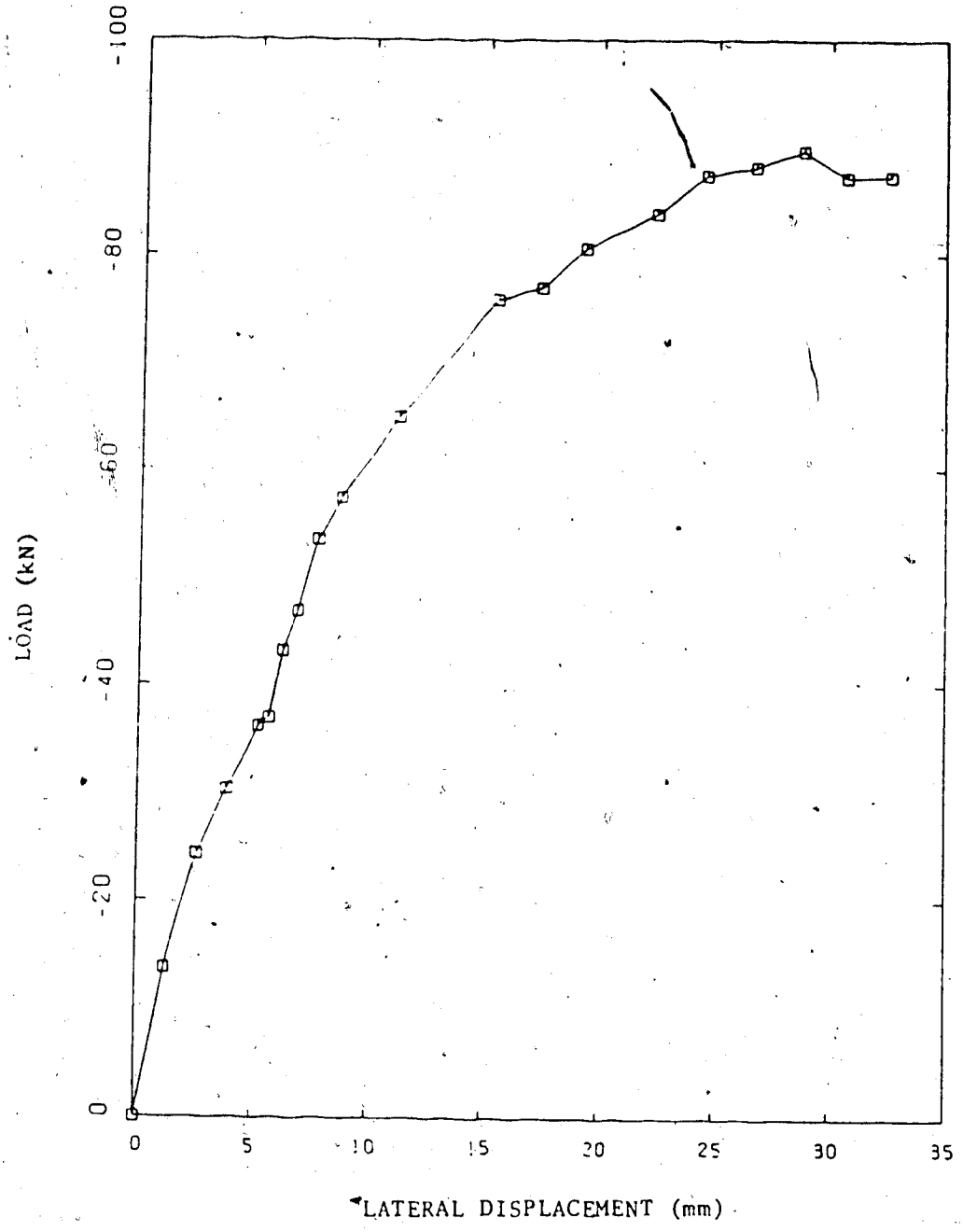

Figure 4.10 Load versus Lateral Displacement Curve for Plate C4 of Free Case

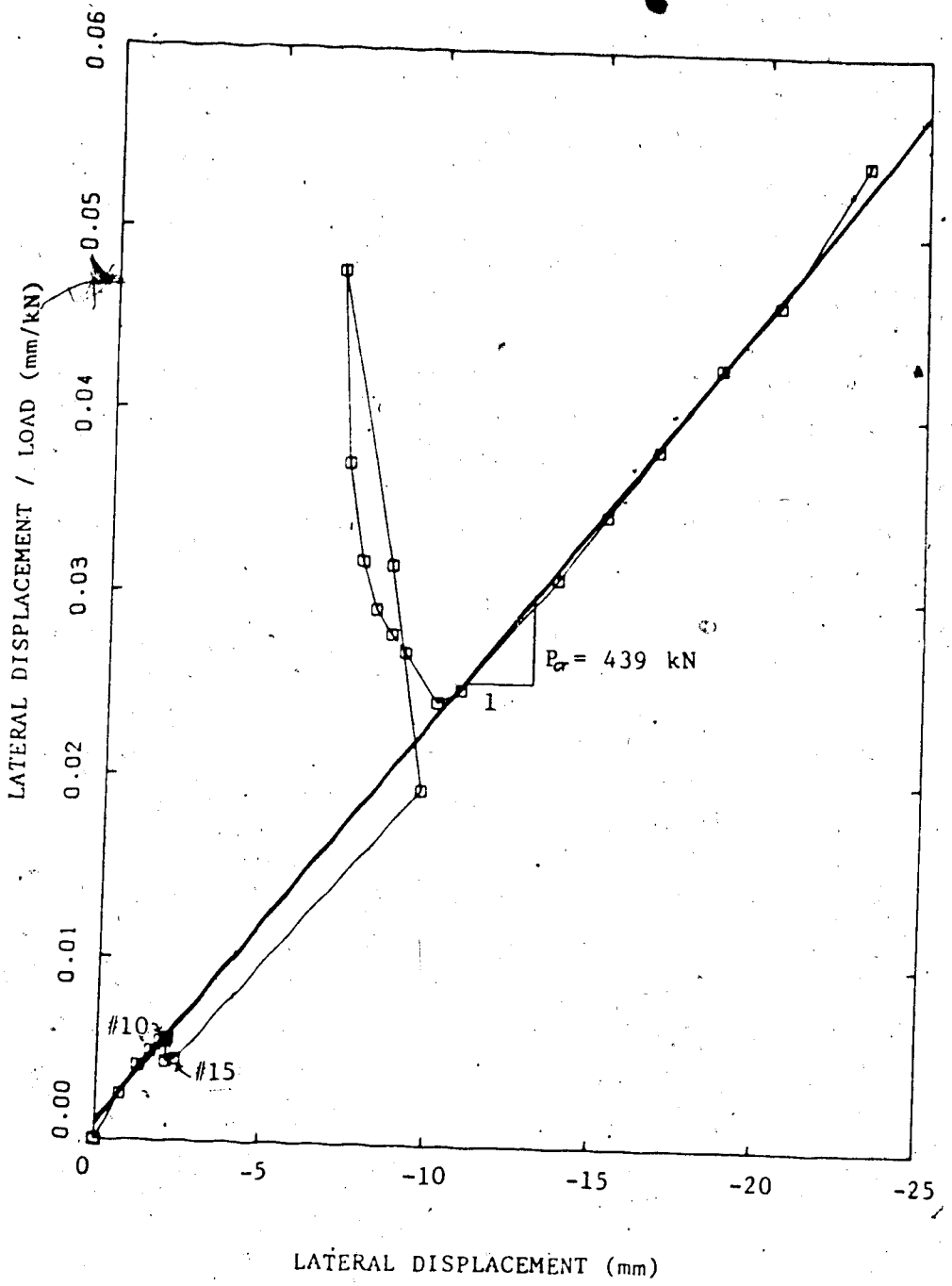

Figure 4.11 Southwell's Plot of Plate C1

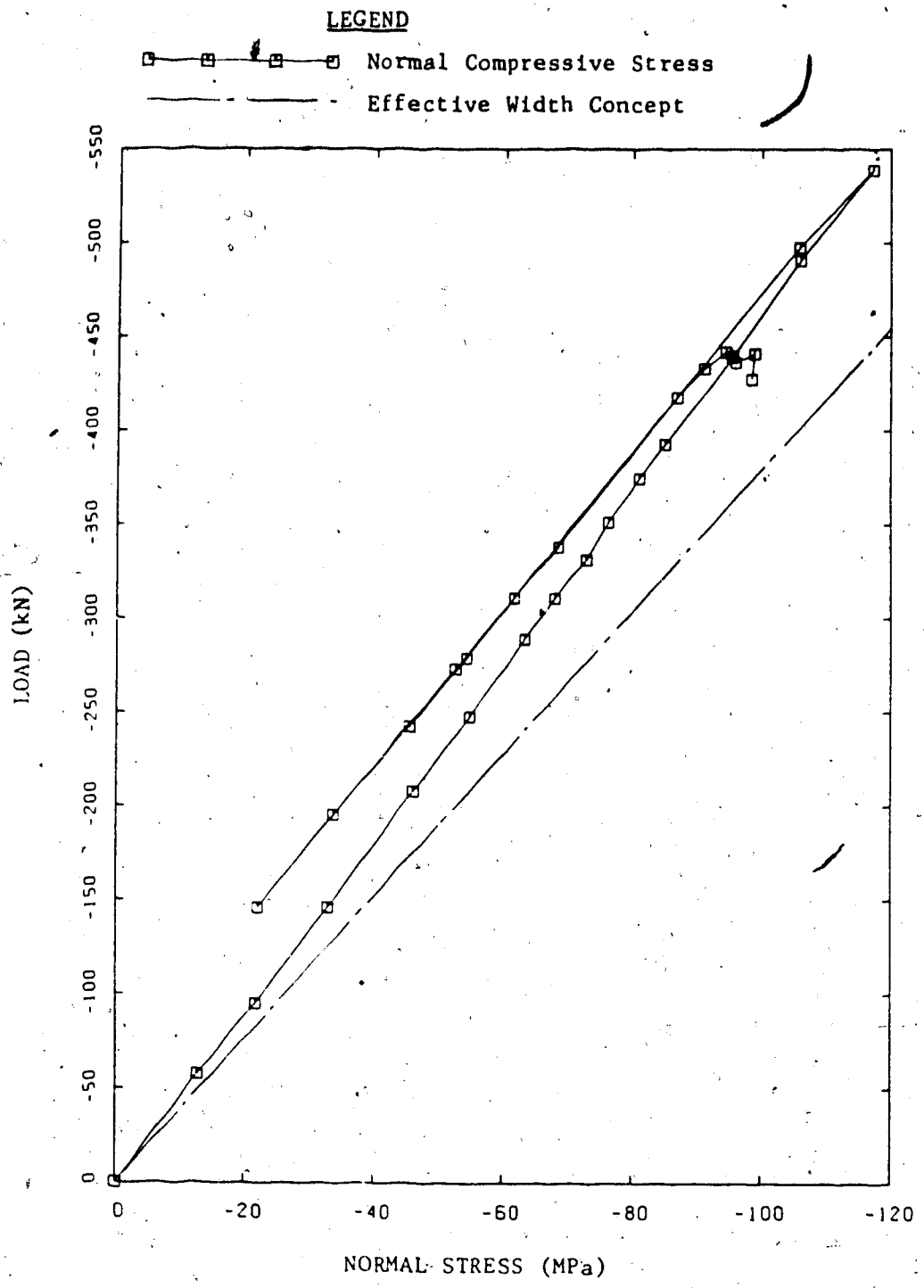

Figure 4.12 Load versus Normal Compressive Stress Curve for Plate C1 of Free Case

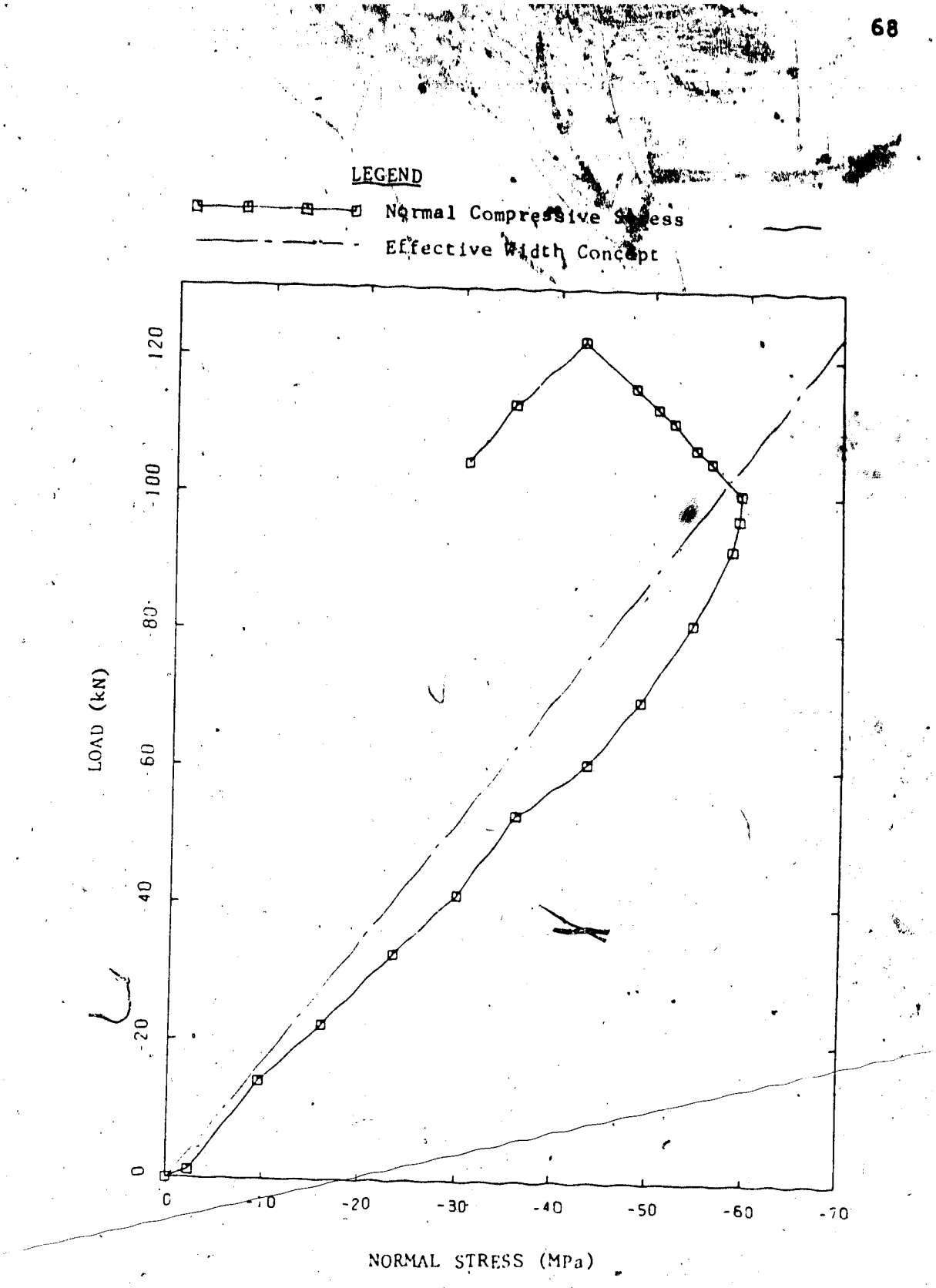

Figure 4.13 Load versus Normal Compressive Stress Curve for Plate C2 of Free Case

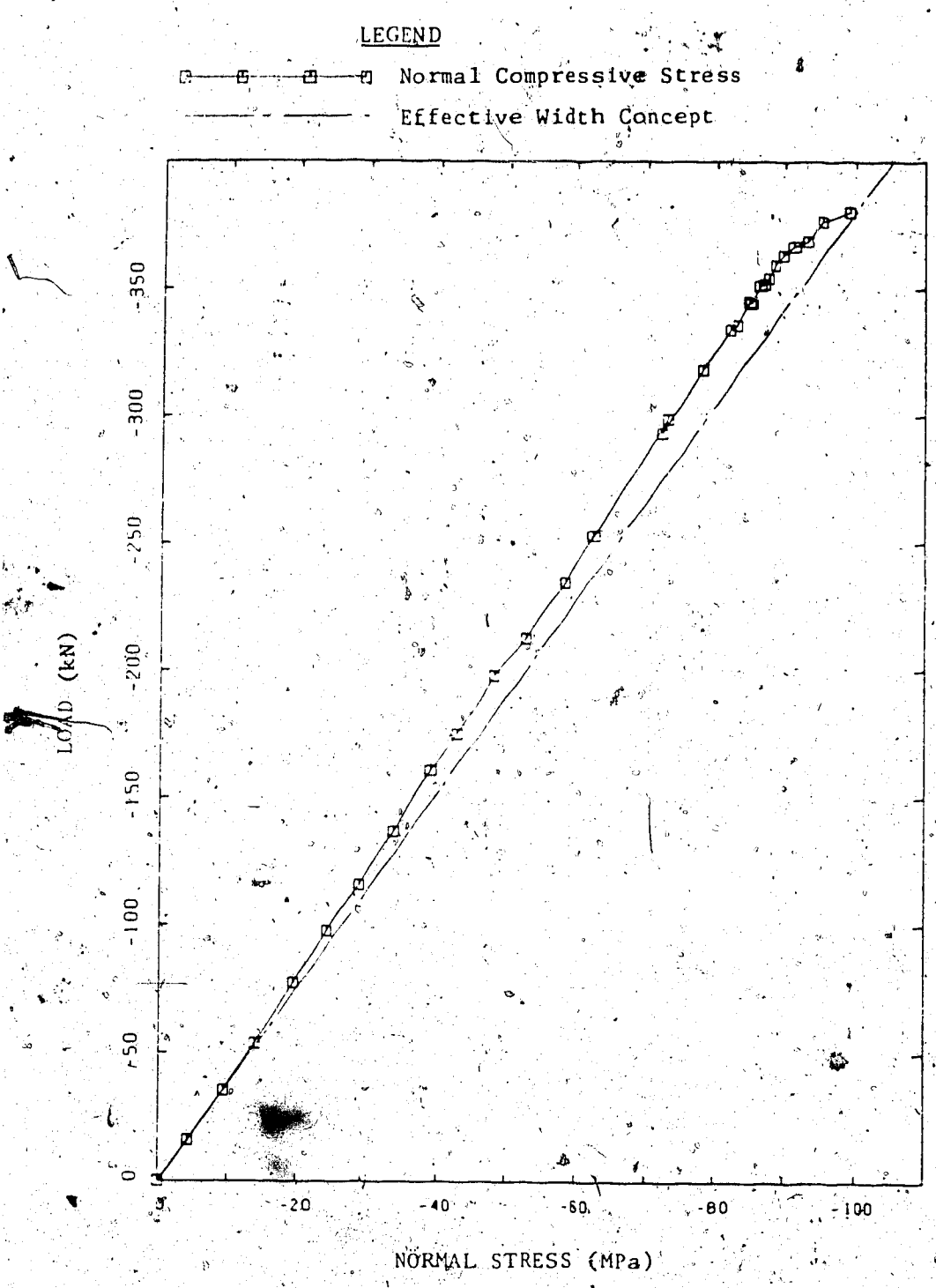

Figure 4.14 Load versus Normal Compressive Stress Curve for Plate C3 of Free Gase

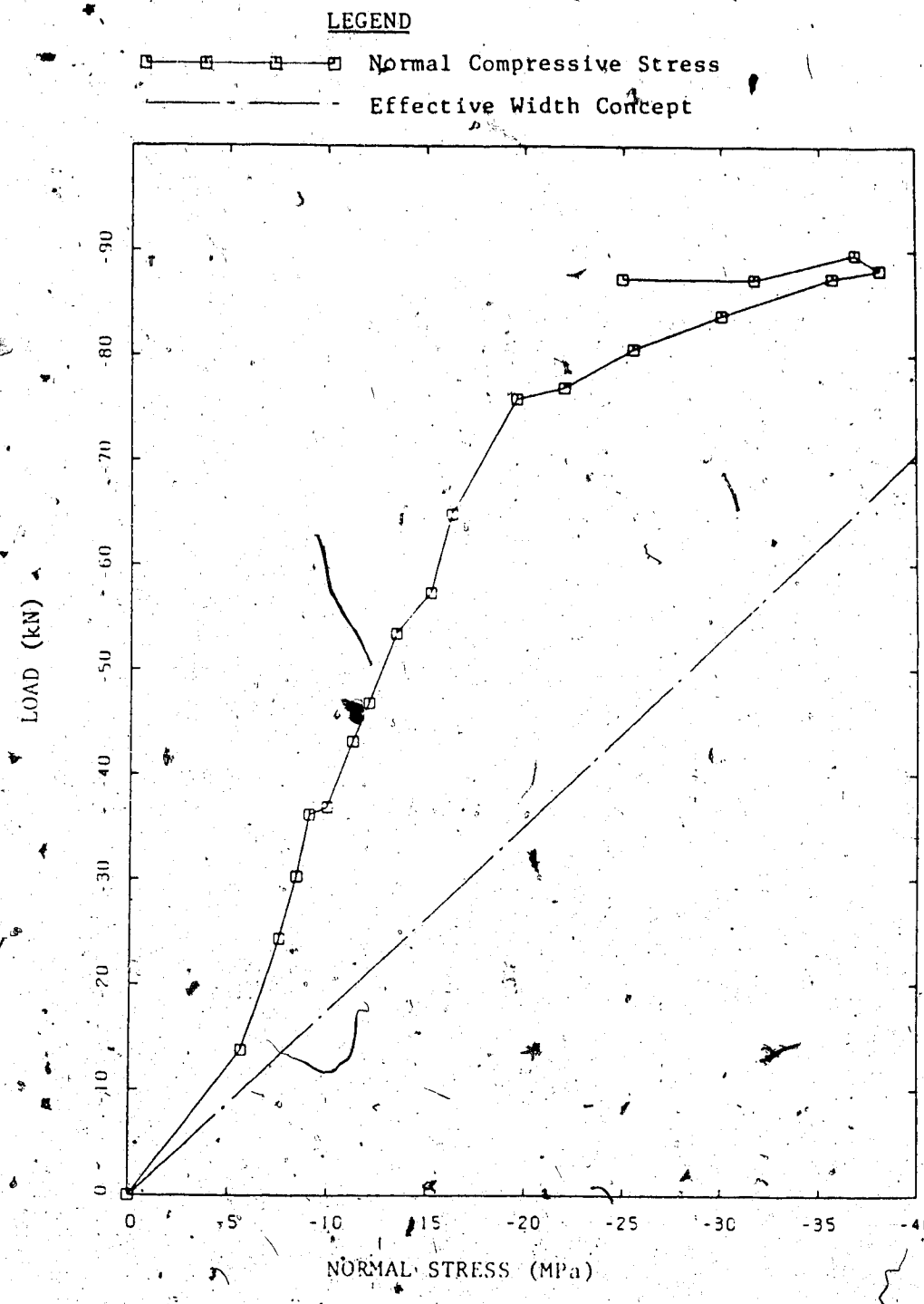

Figure 4.15 Load versus Normal Compressive Stress Curve for Plate C4 of Free Case

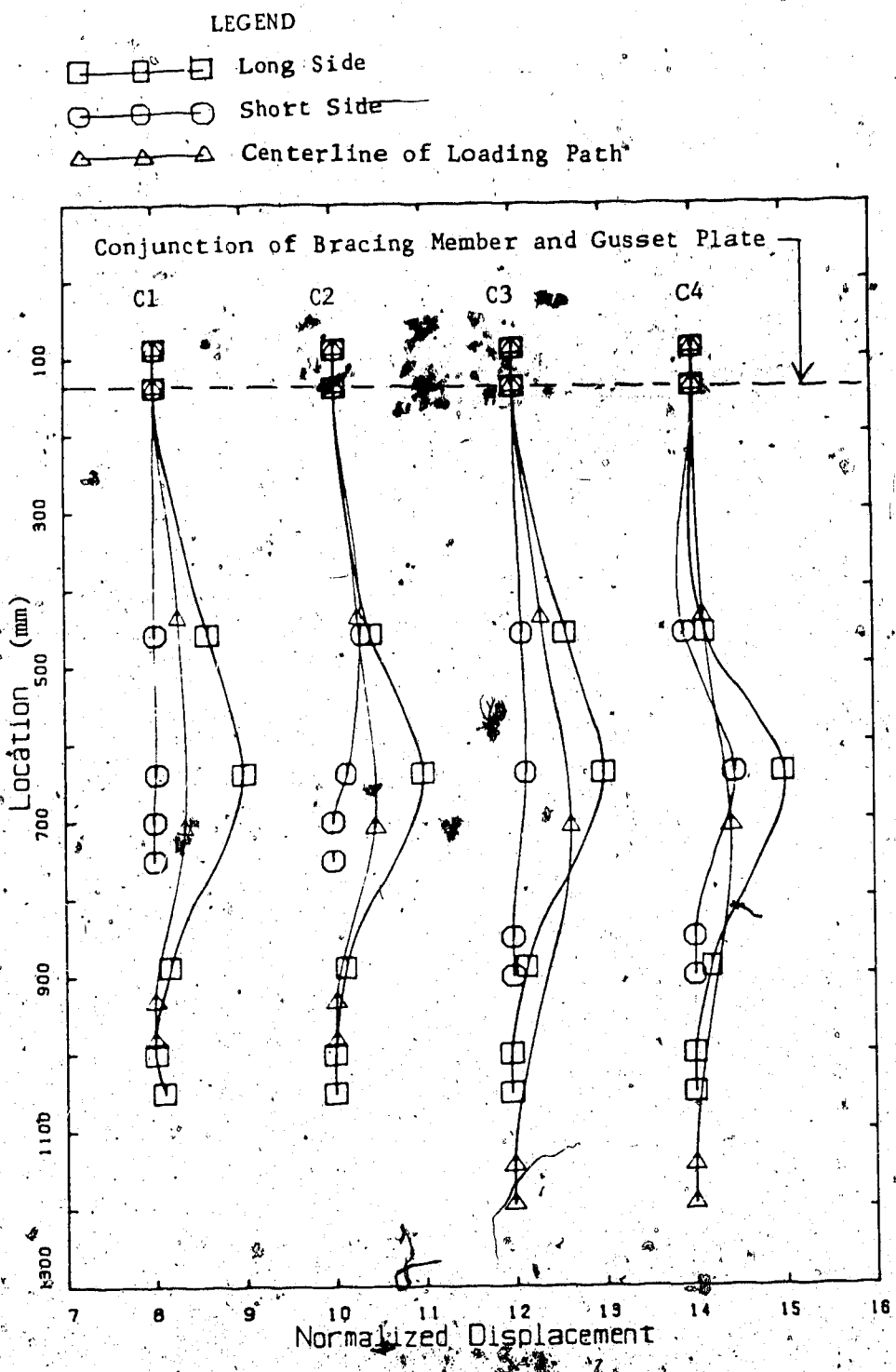

Figure 4.16 Normalized Deflected Shapes of Fixed Case of Concentric Loading Corresponding to the Maximum Load

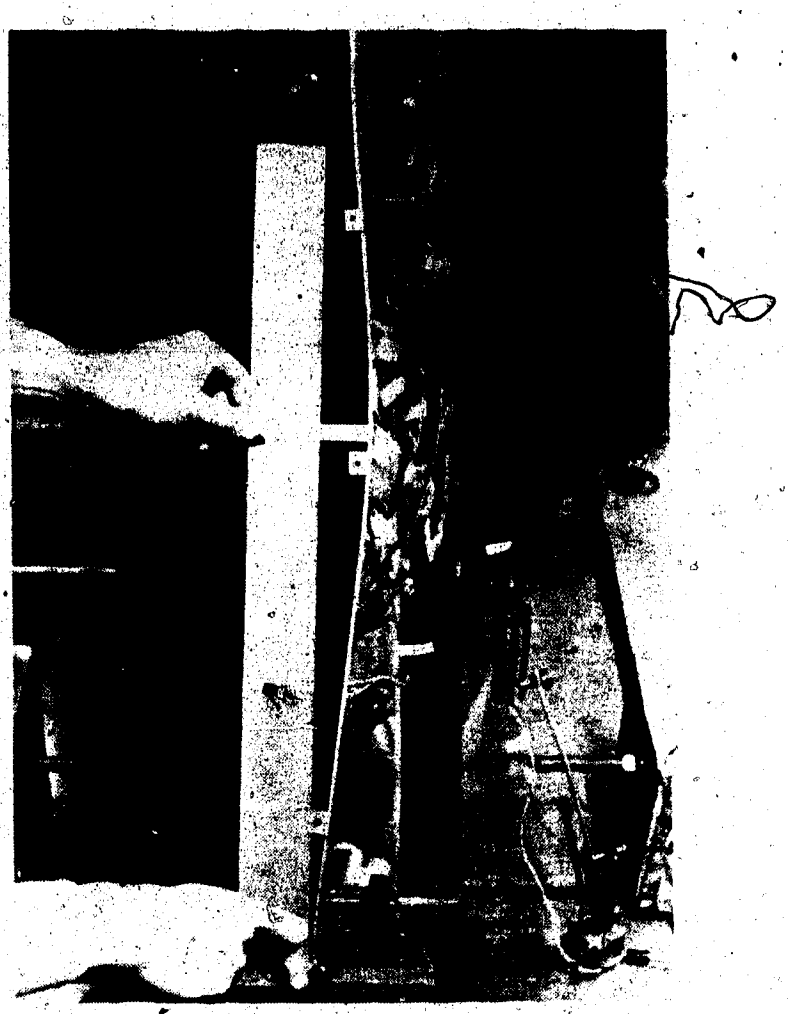

Figure 4.17 Deflected Shape of Long Free Edge of Fixed Case of Plate C2

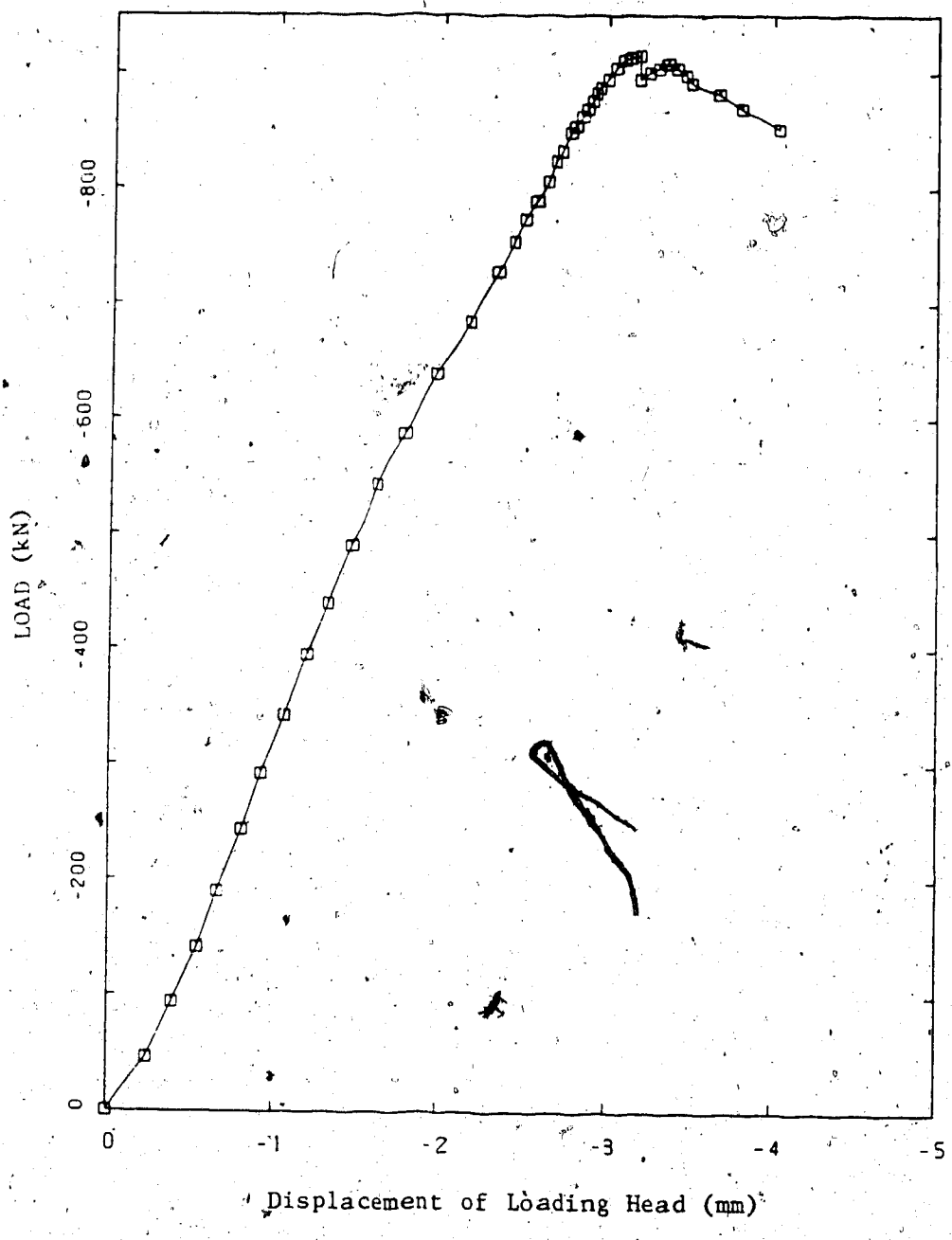

Figure 4.18 Load versus Vertical Displacement Curve for Plate C1 of Fixed Case

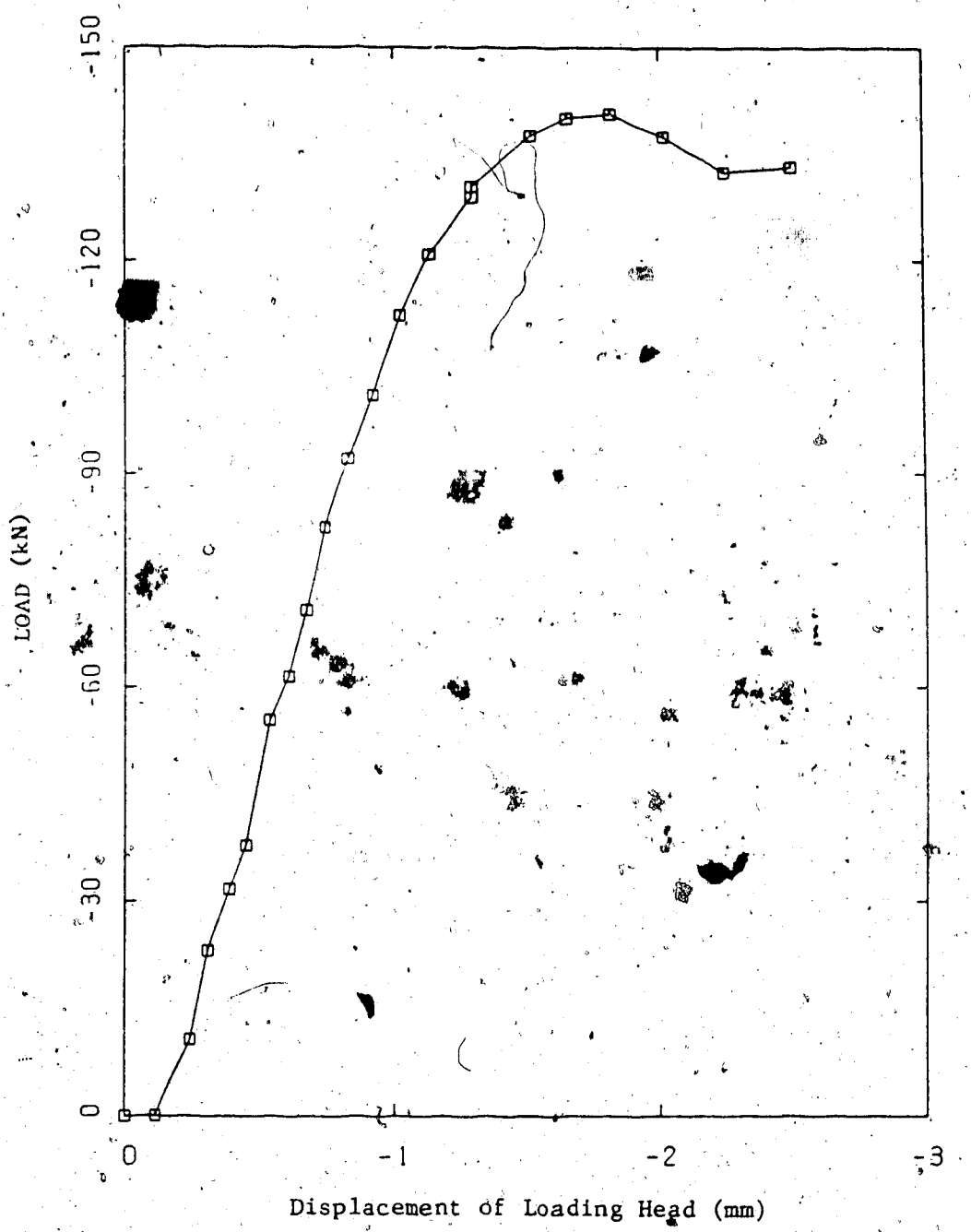

Figure 4.19 Load versus Vertical Displacement Curve for Plate C2 of Fixed Case

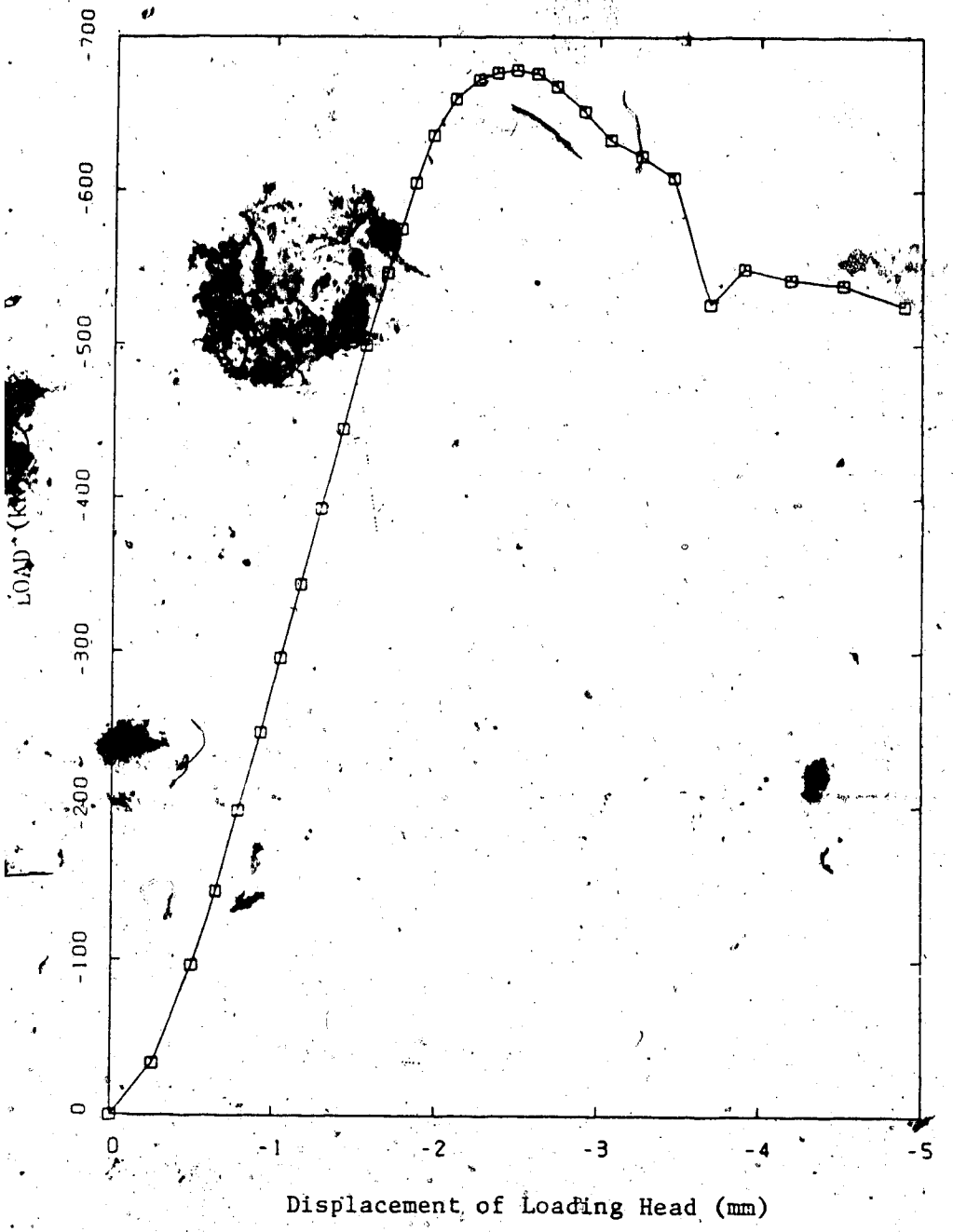

Figure 4.20 Load versus Vertical Displacement Curve for Plate C3 of Fixed Case

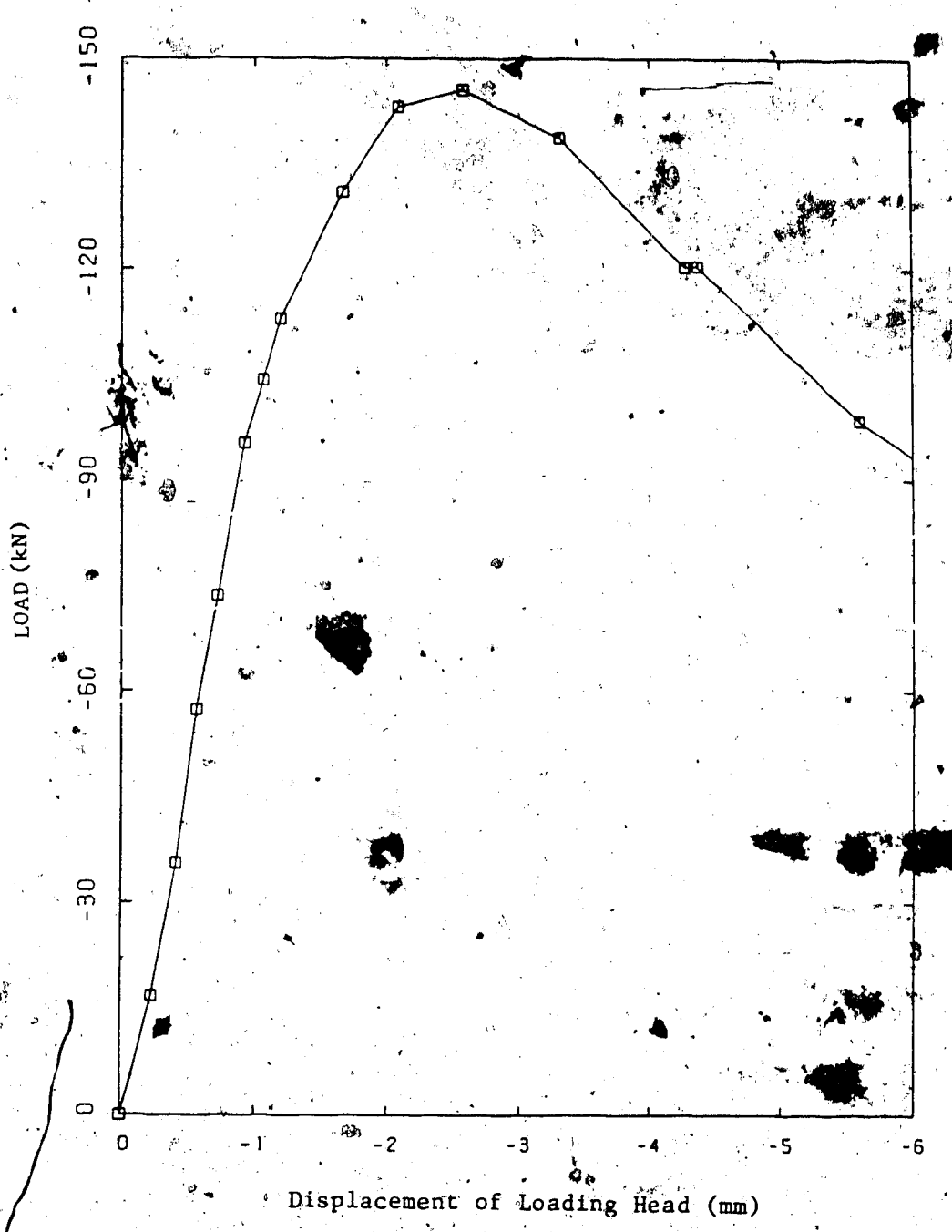

Figure 4.21 Load versus Vertical Displacement Curve for Plate C4 of Fixed Case

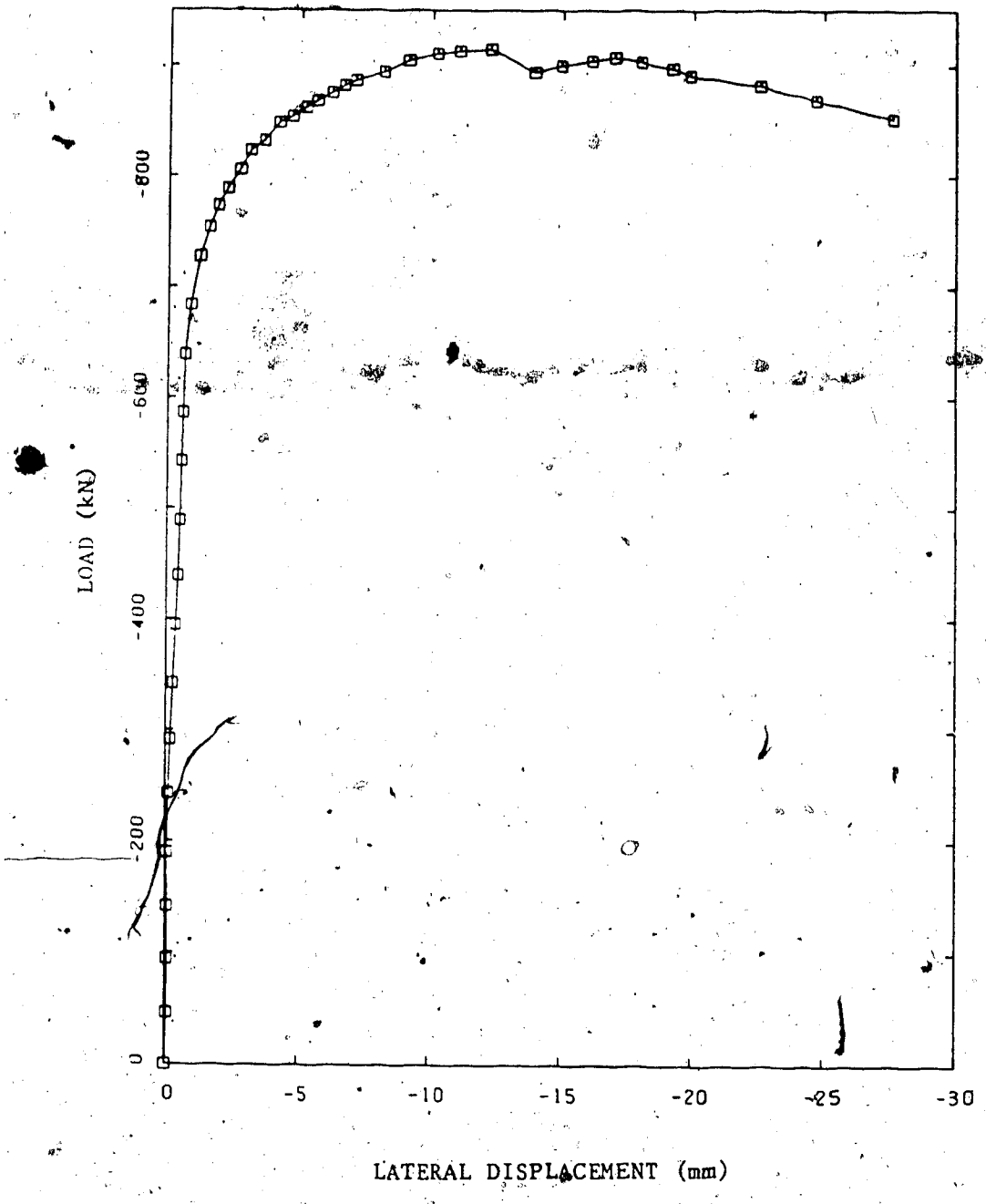

Figure 4.22 Load versus Lateral Displacement Curve for Plate C1 of Fixed Case

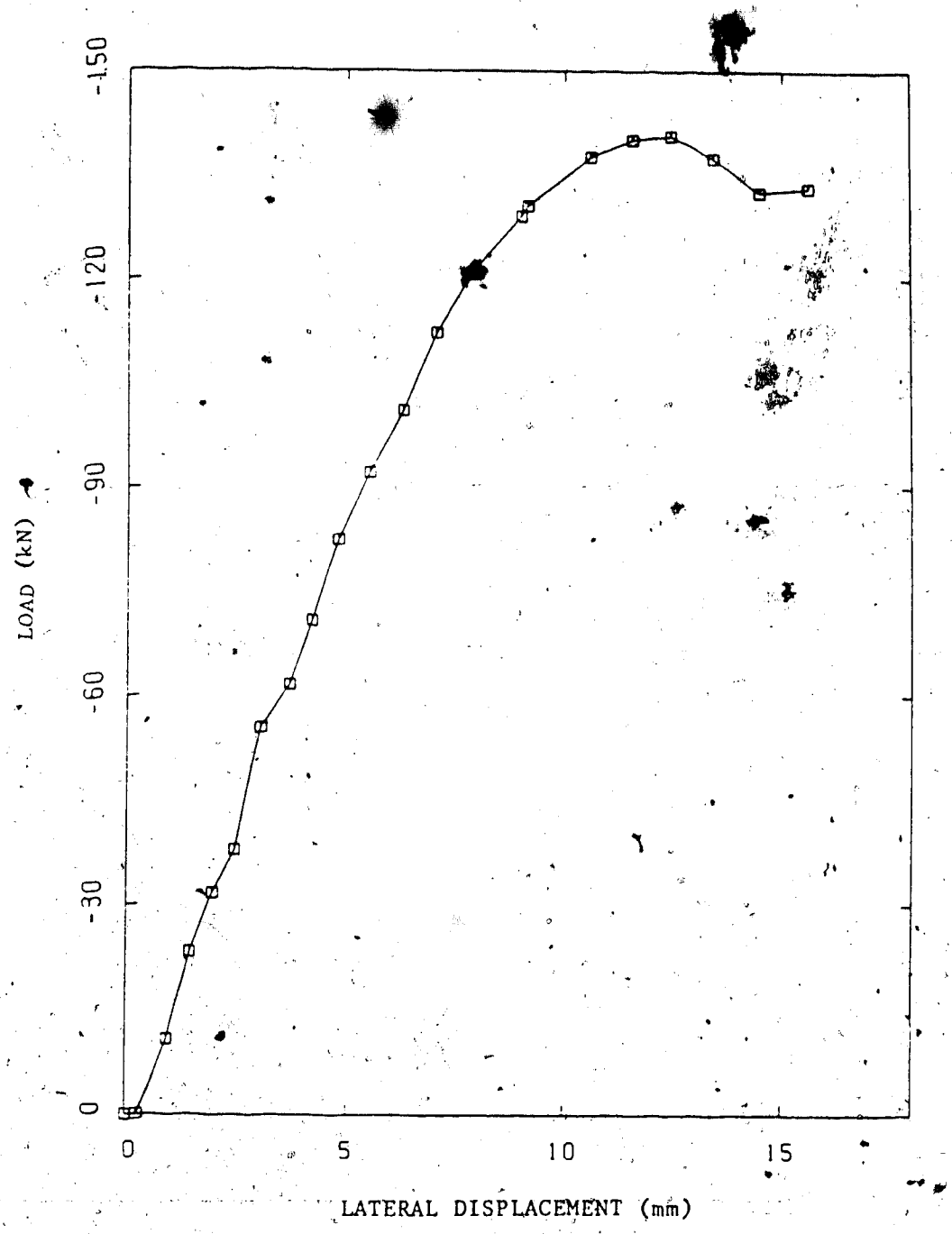

Figure 4.23 Load versus Lateral Displacement Curve for Plate C2 of Fixed Case

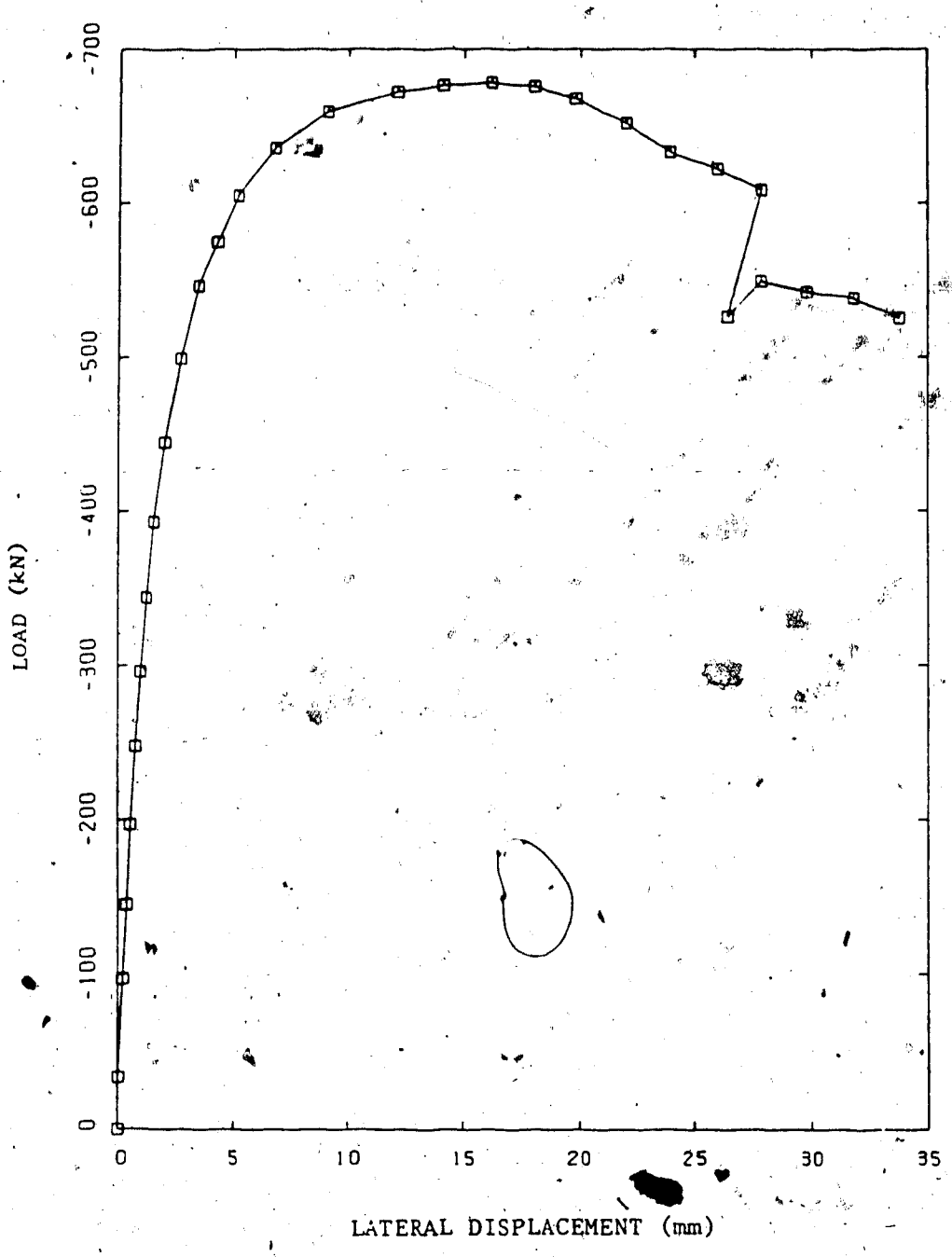

Figure 4.24 Load versus Lateral Displacement Curve for Plate C3 of Fixed Case

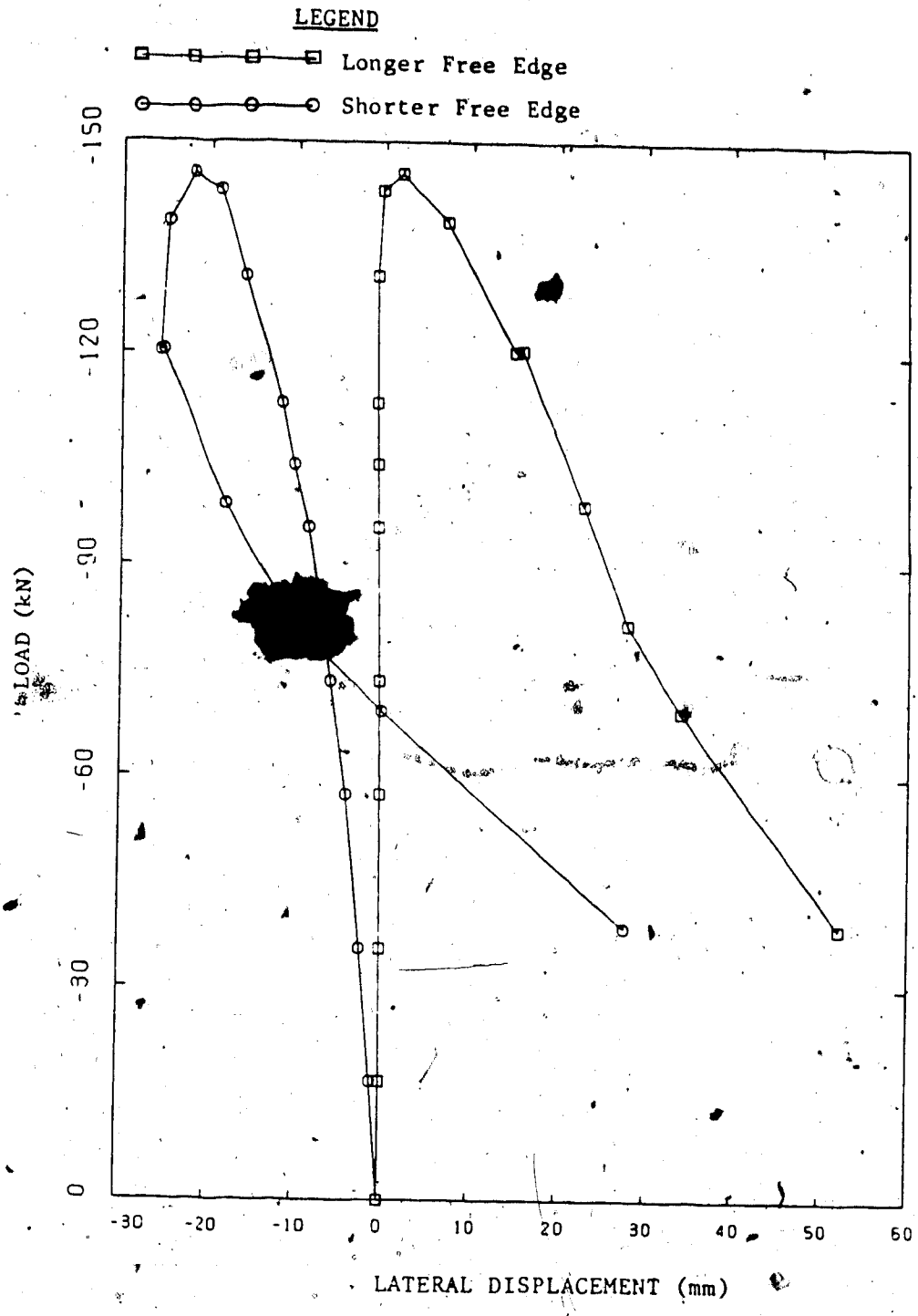

Figure 4.25 Load versus Lateral Displacement Curve for Plate C4 of Fixed Case

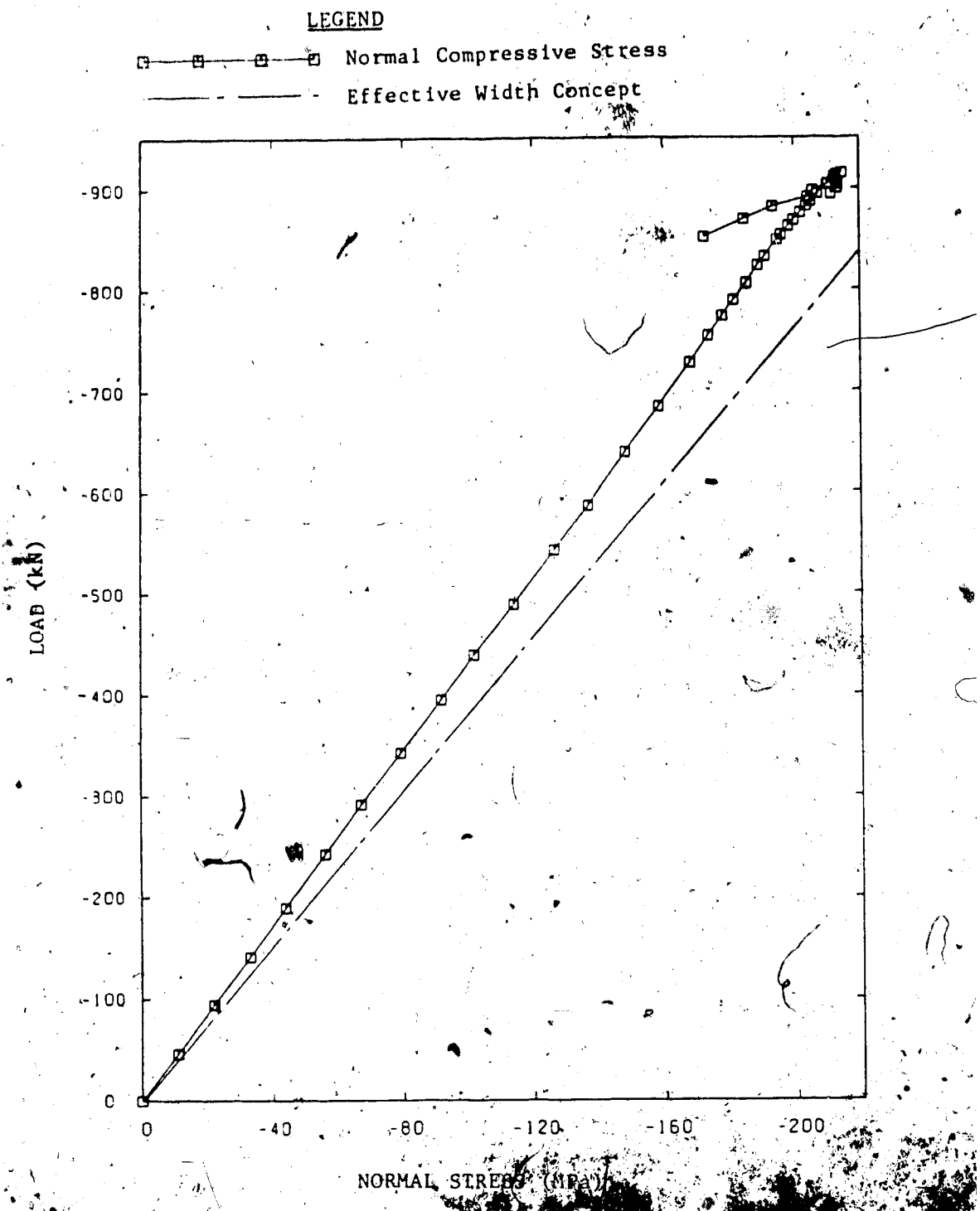

Figure 4.26 Load versus Normal Compressive Stress Curve for Plate C1 of Fixed Case

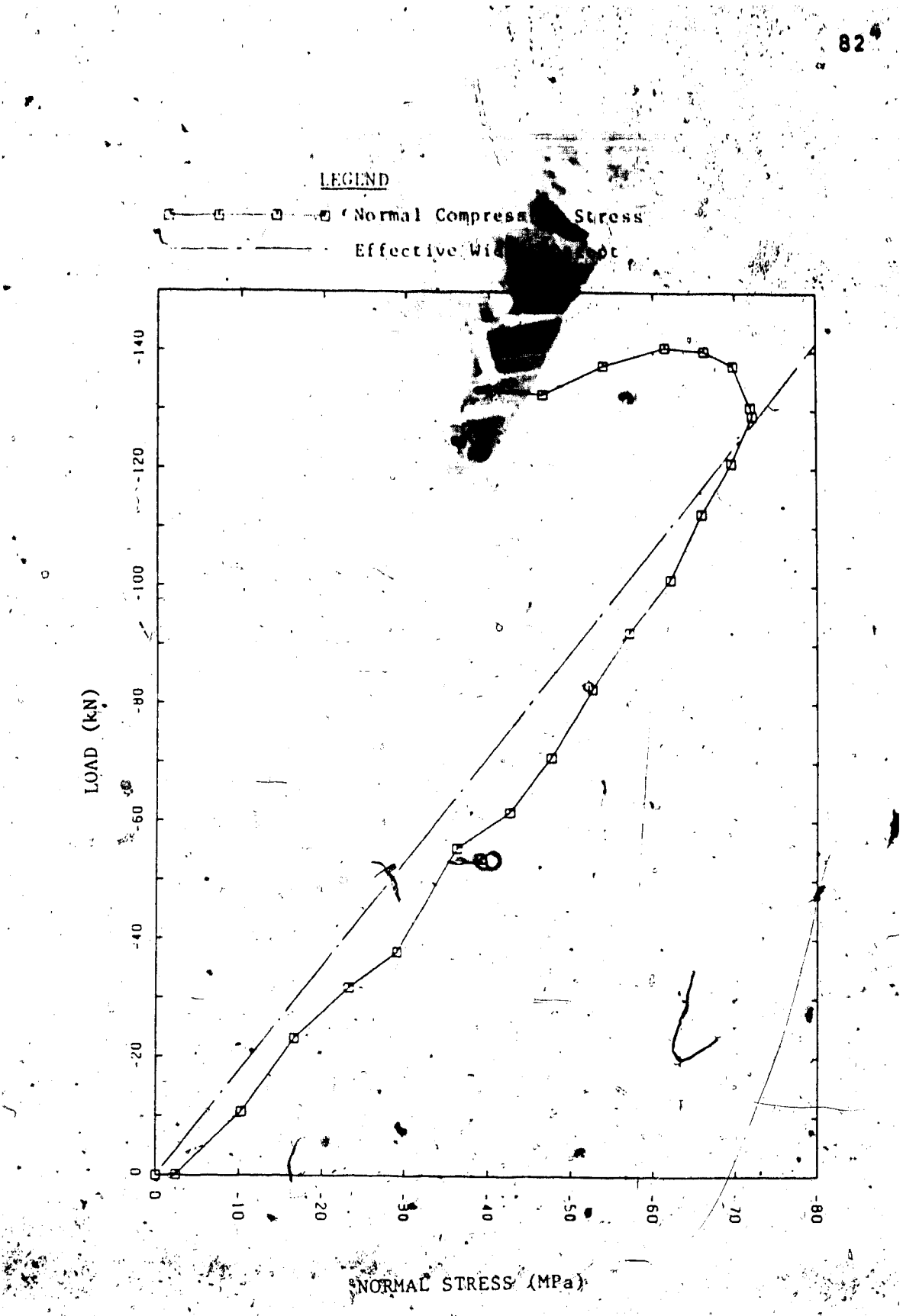

Figure 4.27 Load versus Normal Compressive Stress Curve for Plate C2 of Fixed Case

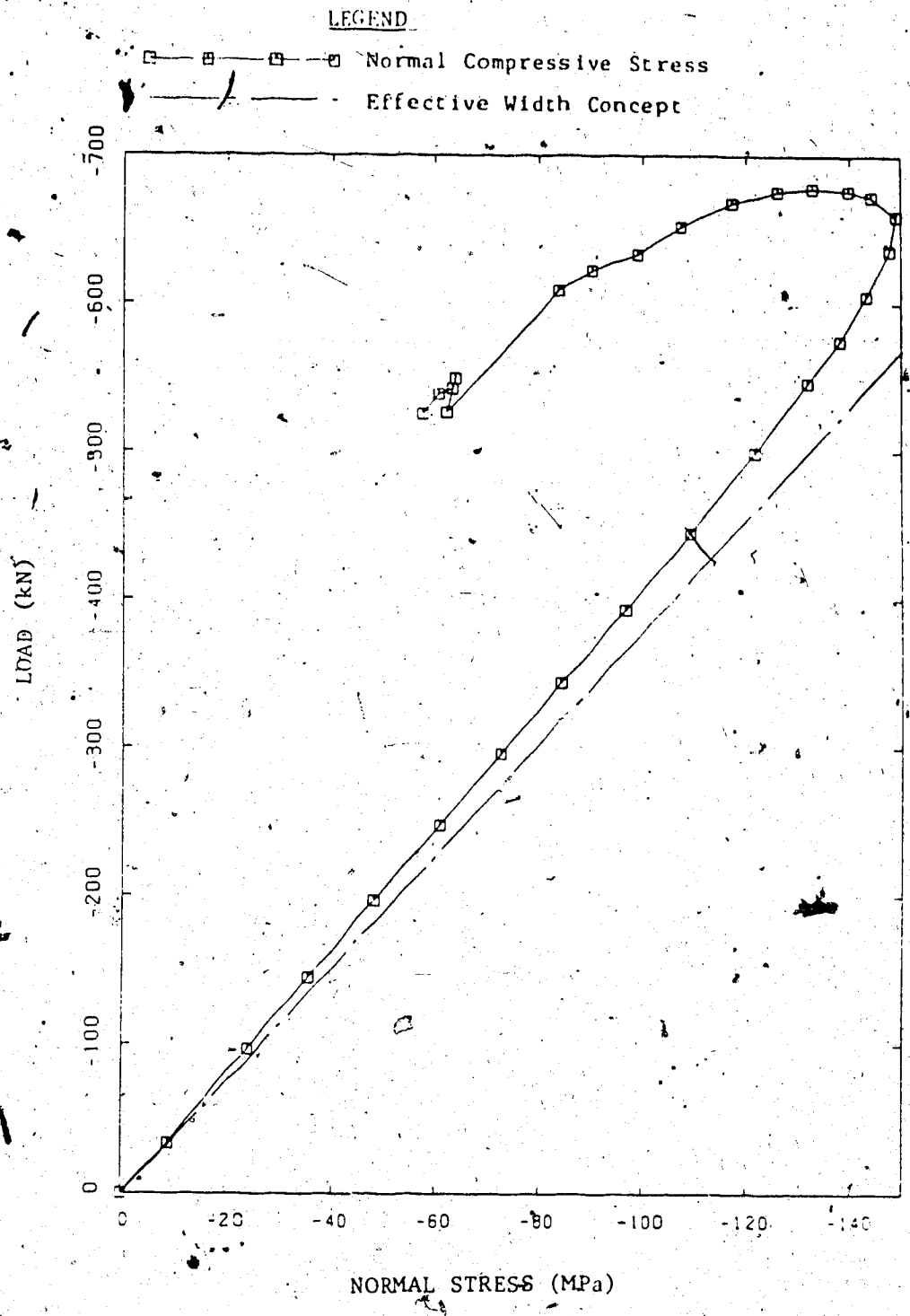

Figure 4.28 Load versus Normal Compressive Stress Curve for Plate C3 of Fixed Case

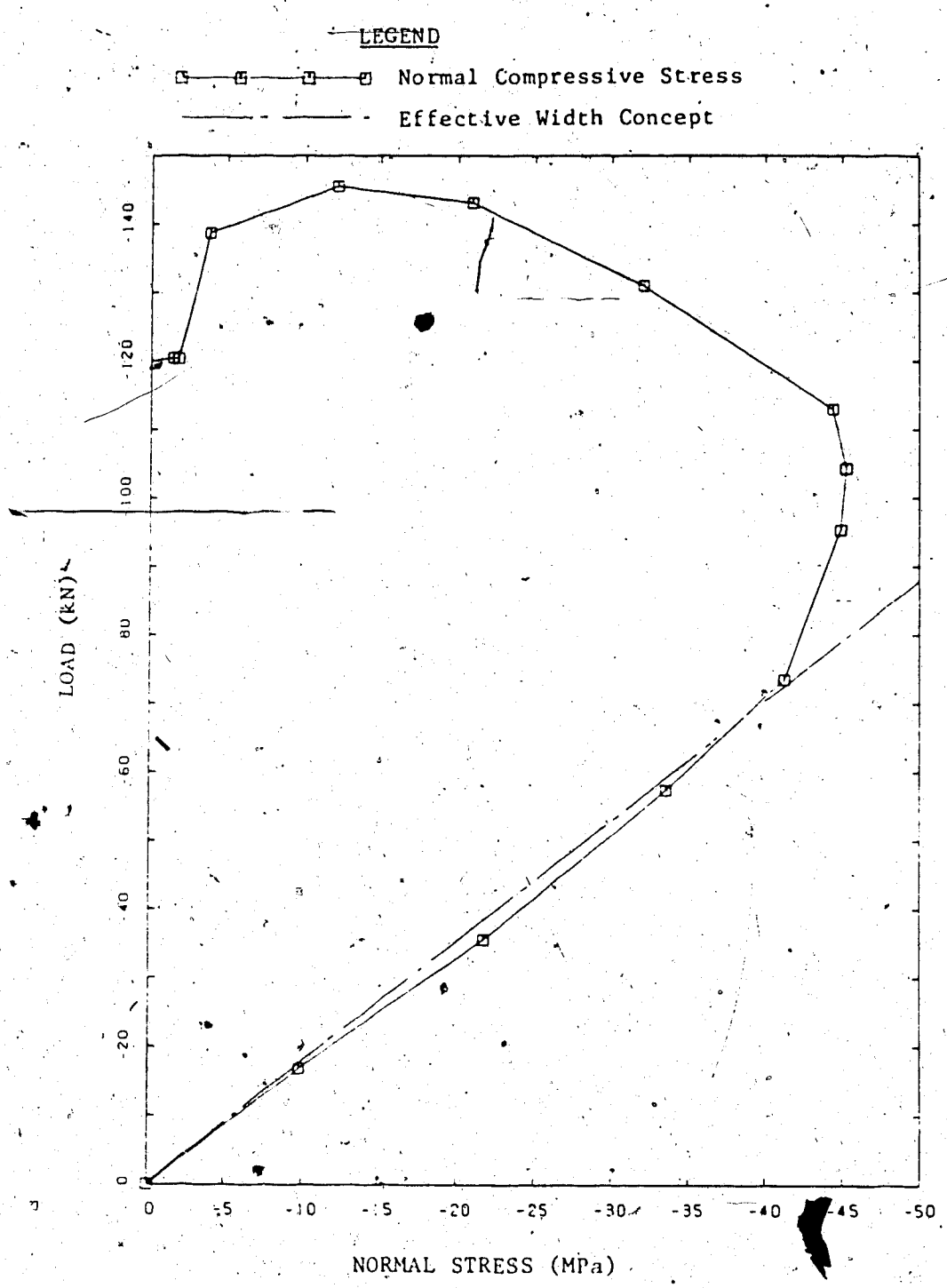

Figure 4.29 Load versus Normal Compressive Stress Curve for Plate C4 of Fixed Case

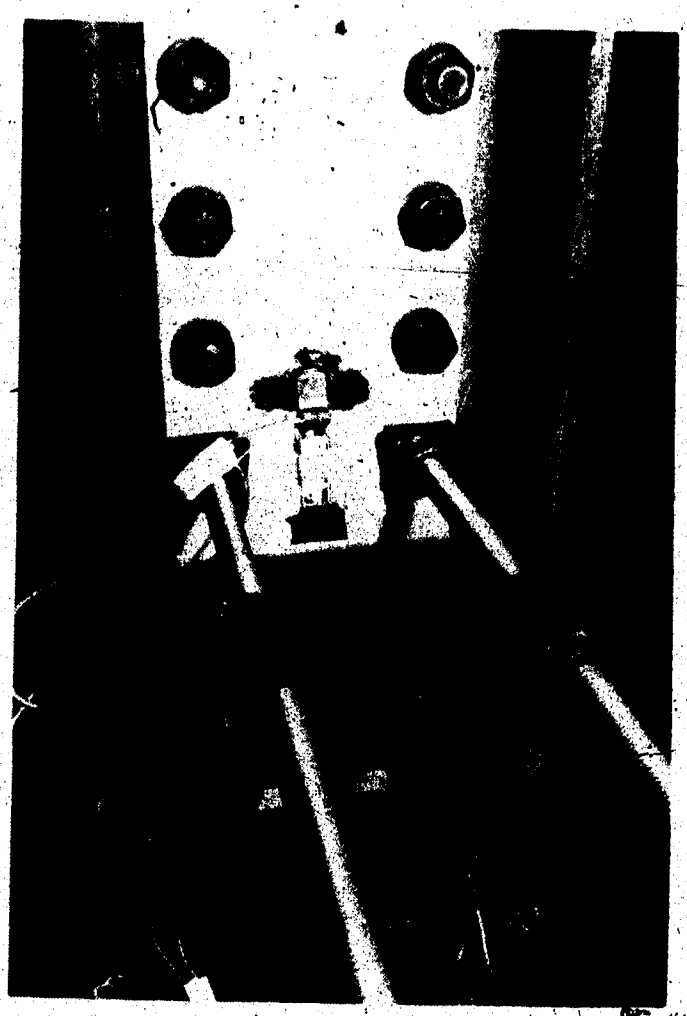

Figure 4.30 Yield Lines on Splice Plate for Plate E5

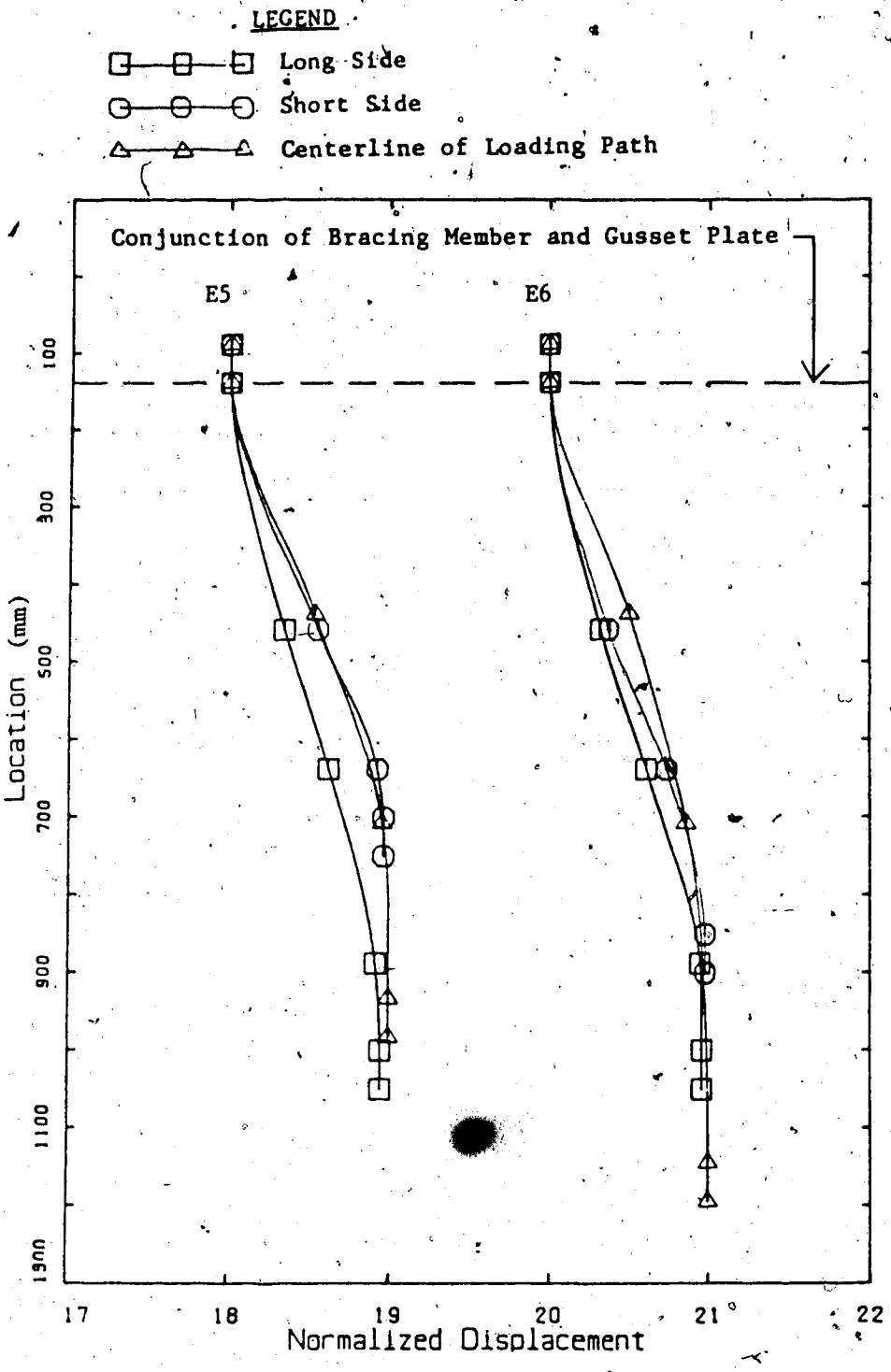

Figure 4.31 Normalized Deflected Shapes of Free Case without Stiffener of Eccentric Loading Corresponding to the Maximum Load

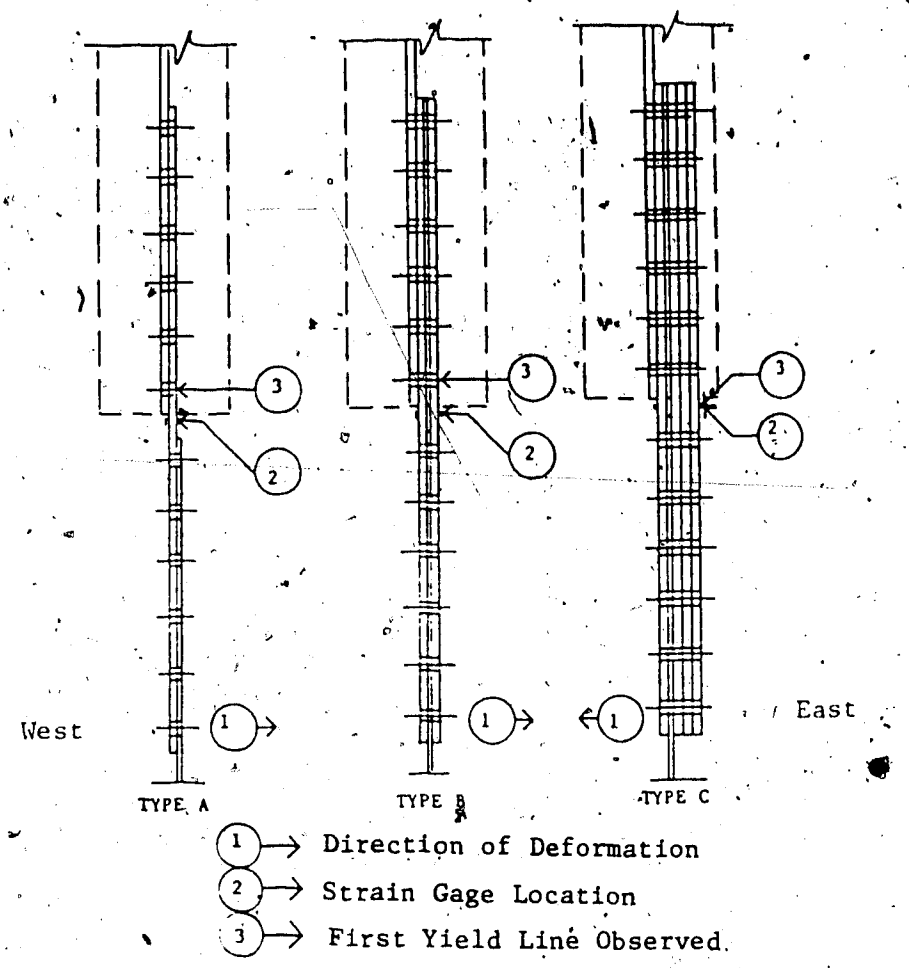

Case	Plate	Pmax (kN)	Yield Lines recorded by Strain Gages	Yield Lines observed	Type
Free w/o Stiffener	E5	80.4	80.4	79.5 (before Pmax)	A
	E6	55.8	46.7 (before Pmax)	46.7 (before Pmax)	A
Free w/ Stiffener	E5	232.8	209.9 (after Pmax)	231.5(before Pmax)	B
	E6	338.6	338.6	after Pmax	C
Fixed w/Stiffener	E5	392.3	392.3	before Pmax	B
	E6	523.3	520.6 (before Pmax)	before Pmax	C

Figure 4.32 Summary of General Behavior and Test Results of Eccentric Loading

5. DISCUSSION OF TEST RESULT

5.1 General

In this chapter comparisons are made between the test results and corresponding values as determined by the current design method presented in Chapter 2 and by the finite element program BASP (Akay et al. 1977) which has capability to handle the buckling analysis of plates. The highest applied loads of each test are first compared with the predicted value using Whitmore's effective width concept. For the concentric loading case, the results are then compared with the BASP results. The beam-column formula for a rectangular cross section is used to evaluate the eccentric loading case and compared with the test results. Typical calculation examples using the effective width concept and the beam-column formula are given in the Appendix B.

5.2 Comparison of Calculation and Test Results

5.2.1 Calculation using Whitmore's Concept

The highest applied load of each test, P_{max}, is used for primary comparison and is summarized in Table 5.1. The corresponding load-carrying capacity of each plate calculated according to the Whitmore's effective width concept is also listed in this Table. As expected, the effective width concept, which is based primarily on the

material strength of a gusset plate at the end of a bracing member gives much higher predicted values than the test value P_{max}, since the test specimens were purposely designed to fail in plate buckling.

Also, this concept gives the same load-carrying capacity for the same thickness of gusset plates no matter what the configuration and the boundary conditions of the plate are, no matter whether the load is concentric or eccentric, and no matter whether the splice plate is stiffened or not.

Even though the ultimate load calculated by the Whitmore effective width concept was substantially different from P_{max}, the in-plane behavior of the gusset plates for either concentric or eccentric case before reaching maximum load is similar to the Whitmore's prediction. Comparison of these stresses for concentric loading tests were shown in Figs. 4.12 to 4.15 for free cases and in Figs. 4.26 to 4.29 for fixed cases. The corresponding normal stress for each loading stage was calculated using Hooke's law and the average strain of the rosette gages on both sides of the gusset plate. The magnitude of the normal compressive stress at the end of the diagonal bracing member measured by the rosette gages agrees reasonably well with the normal compressive stresses calculated by the Whitmore effective width concept. However, a large discrepancy exists for the free case of plate C4 (Fig. 4.15 and 4.29). The possible reason for this is the large initial imperfection of this

specimen, which caused a large deformation in its early loading stages. After buckling or large deformation occurred, these values become meaningless.

5.2.2 Calculation using Finite Element Program

The computer program, BASP, which can handle the linear elastic buckling problem of plates having stiffener elements placed symmetrically about the plate, was originally written by Akay et al.(1977). It was used herein to calculate the buckling loads of the gusset plates and these values are then compared with the test results. In the analysis, the gusset plates are assumed to be fixed at the boundaries of beam and column. The adjacent location of the bracing member and the gusset-plate is assumed to be fixed in rotation but free to move out-of-plane for the free cases and fixed in both rotation and translation for the fixed cases, as shown in Fig. 5.1. The plates were idealized by two-dimensional finite elements. Thicker elements were used for the splice plate locations. The applied loads were assumed uniformly distributed among the bolts on the gusset plate. The problems solved by this program are treated as a linear-elastic buckling problem.

The buckling loads obtained using the BASP program are summarized in Table 5.1. Comparisons with the test results are shown in Figs. 5.2 to 5.5. The abscissas in these plots represent the length of the short free side the gusset plate. The length of the long free side is kept constant at

850 mm. The solid curve represents the results using BASP. It indicates that the buckling load increases as the length decreases. The comparison is shown to be in reasonable agreement. However, large discrepancy exists for the free and fixed cases of the plate C1 and the fixed case of the plate C3. There are two major reasons. One is the simplified assumptions of the splice plate [illegible]s over the splice plate location and the uniform distribution of the applied load. The other is the yielding that occurred in the splice plates due to the high axial load in the spliced plate and the large lateral deformation of the gusset plate. The plate thickness at the splice plate location was assumed to be the total thickness of the splice plates plus the gusset plate. However, there might have been some slight slip between the splice plates and gusset plate, in which case the bending rigidity of the plate would be reduced and, consequently, the rotational restraint at the splice plate location will be decreased. The yielding that occurred at the splice plate also reduced the rotational restraint at the conjunction of the bracing member and the gusset plate, thereby reducing the buckling capacity of the gusset plate. Test results for the 3.11 mm thin-walled gusset plates either in free case or in fixed case agreed fairly well with the BASP results. The reason is that no slip could have occurred between the splice plates and the gusset plates due to the low applied load, and no yielding was observed on the splice plates due to the relatively rigid splice plate as compared to the

stiffness of the gusset plates. Therefore, the assumption of the boundary conditions made in the finite element model is reasonable in these cases.

The contours of maximum compressive stress, based on the in-plane analysis of the BASP program, are shown in Figs. 5.8 to 5.9 for plates C1 to C4. The location of the maximum compressive stress is located at the end of of the compressive diagonal member for the 850 mm x 700 mm plates and is below the end of diagonal member at the point adjacent to the edge plate for the 850 mm x 550 mm plates. The maximum compressive stresses of corresponding load calculated from the rosette gages which are listed on the top of these figures show reasonable agreement with the analytical results. A large discrepancy existed for the free case of plate C4 (Fig. 5.9). The possible reason for this is the large initial imperfection of this specimen, which caused a large deformation in its early loading stages.

The buckling shapes for the free cases using BASP are shown in Fig. 5.10. In the free case of plate C1, which is 850 mm x 550 mm x 6.7 mm in size, the buckling shape of the long free edge is different from the actual deformation shape (Fig. 4.1). The latter case shows less rotational restraint on the upper end of the gusset plate and also gives a lower buckling load. The buckling shapes obtained using the BASP solution for the fixed cases are shown in Fig. 5.11. The difference is that a relatively large deformation along the centerline of gusset plate was

observed in the test results (Fig. 4.16). This indicates less rotational restraint and less bending rigidity at the splice plate location. Consequently, it gave a lower buckling load for the thicker plates. Generally speaking, the buckling shapes of either the free case or fixed case using the BASP analysis were similar to the deformation shape of the test specimens. The rotational restraint at the conjunction of the bracing member and gusset plate was assumed completely prohibited in the finite element model, which increased the buckling load and decreased the height of the inflection point. However, the deformed shapes of test specimens showed that the rotational restraint on the top of the gusset plates was not fully fixed. The splice plates at this location acted as rotational springs and allowed the gusset plate to rotate as the load increased. An analytical study of the effect of the rotational restraint for plates C1 and C3 will be discussed later in the section of parametric studies (Section 5.3).

5.2.3 Eccentric Load using Beam-Column Equation

It was found from the tests conducted on the plates E5 and E6 that the eccentricity initiated the yielding in the splice plate and eventually caused the failure of the connection. The bending moment produced by the eccentricity which was acting on the weak axis of the splice plate would not cause lateral torsional buckling of the plate. Thus, it can be assumed that the splice plate is an isolated

beam-column and is confined in the plane of loading. If the secondary moment due to the lateral displacement is neglected, the ultimate strength of a rectangular beam-column which has a fully plastified cross-section can be used. Thus, the beam-column formulas of a rectangular cross-section can be used to calculate the cross-sectional strength of the splice plates at the location of first yield as:

$$(\frac{P}{P_y})^2+(\frac{M_{pc}}{M_p})=1.0 \qquad [5.1]$$

where M_{pc} is applied bending moment, M_p is plastic moment, P_y is axial compressive load at yield stress and P is applied axial load. The calculated results are listed in Table 5.1.

The results calculated by the beam-column formula give a good indication of the maximum loads obtained from the tests and the actual failure mode occurred. Except for the case of free with stiffener of plate E6, the failure mode of the gusset plates is mainly initiated by the yielding of the cross-section at the conjunction of the bracing member and the gusset plate. This can be confirmed by the yield lines observed in the actual tests. For the case of free with stiffener of plate E6, in which no yield lines were observed until maximum load stage, the failure load was 338.6 kN and approached the buckling load of the free case of plate C3. The failure of this plate could categorized as a stability problem instead of attainment of maximum strength based on

cross-sectional capacity.

Comparing the cases with reinforcement to the cases without reinforcement indicates that the eccentricity could curtail the carrying capacity of gusset plates significantly. However, it also implies that the reduction of the strength due to eccentricity could be minimized or even avoided by providing sufficient stiffeners at the splice plate locations.

5.3 Parametric Studies

The critical stress, σ_{cr}, of a uniaxially loaded plate is directly proportional to the stiffness of the material, E, and varies inversely as the square of the width-thickness ratio, $(b/t)^2$. The equation can be written as:

$$\sigma_{cr} = \frac{k\pi^2 E}{12(1-\nu^2)(b/t)^2} \qquad [5.2]$$

where ν is Poisson's ratio and k is the plate buckling coefficient. The plate buckling coefficient k is a function of the type of stress, the edge support conditions and the depth to width ratio a/b. The specimens used in the tests were an irregular shape and the biaxially loaded plate had a varied thickness. Therefore, it is difficult to evaluate a general form of the critical stress. However, from equation (5.2), the buckling load of a uniform thickness plate is directly proportional to the cube of the thickness, t^3. If splice plates are added onto such plates, their buckling

load will be increased and the rate of increase will depend on the ratio of the thickness of the splice plates to the thickness of the gusset plates. The buckling load will be no longer a function of the cube of the gusset plate thickness but also a function of the splice plate thickness.

In this section a parametric study was undertaken using the following variables so that design rule could be developed:

1. thickness of gusset plates;
2. size of short side of gusset plate (longer side was kept constant at 850 mm).
3. thickness of splice plate with fixed width and length;
4. boundary conditions, with either fixed or free rotational restraint used on the upper end of the gusset plate. Both free cases and fixed cases were studied.

The analytical studies used the same finite element program BASP and the same model as shown in Fig. 5.1 and the material was assumed to be elastic.

The computer results of buckling loads for varied width and thickness of gusset plates are listed in Table 5.2. The table indicates that the buckling load increases as the width decreases. By putting the data in the form of buckling load curves as shown in Figs. 5.12 to 5.14, the buckling loads for both free case and fixed case reached the same magnitude for the same thickness of gusset plates as the width of the gusset plates decreased to its minimum. The minimum width means the gap between the splice plate and the

beam flange vanished, as shown in Figs. 5.12 to 5.14. It implies that by extending the splice plates into the beam or column the buckling strength of the gusset plate will increase significantly.

To evaluate the effect of rotational restraint on the upper end of a gusset plate and the effect of the bending rigidity of the splice plates, the parametric study results are given in Table 5.3 accompanied by the test results. Columns named with rotational restraint and without rotational restraint in Table 5.3 assume a 13 mm splice plate applied on each side of of a gusset plate. The rotational restraint on the upper end of a gusset plate in these two columns is assumed to be fixed or free respectively. Columns named infinite thickness of splice plate and without splice plate in Table 5.3 assume that an infinite thickness of splice plate and no splice plate are used in the finite element model respectively. The infinite rotational restraint is provided in both cases on the upper end of the gusset plate. The rotational restraint on the upper end of a gusset plate performs a very important role in the buckling strength of a gusset plate, as shown in the first two columns of the table. The extreme case was the free case of plate C1, in which the buckling load is 944 kN for fully rotational restraint. After the release of the rotational restraint, the load drops to 150 kN. It could be used to explain the discrepancy between the computer and test results for the free case of plate C1. Partial yielding

observed on the splice plates during the test reduced the rotational restraint on the upper end of the gusset plate and this, in turn, reduced the buckling strength. The results for the infinite thickness splice plate indicate that two 13 mm splice plates in the test specimers provide infinite rotational restraint and bending rigidity for the thinner plates (C2 and C4). However, they are not rigid enough for the thicker plates. Data also shows that as the thickness of splice plate approaches infinite or zero, the buckling loads for different thickness of gusset plates with the same geometric configuration become a function of the thickness cubed of the gusset plate. It implies that the buckling strength of the gusset plates is proportional to the cube of the plate thickness if the flexure stiffness of the splice plates is relatively large.

From the above discussion, four important conclusions can be made:

1. With the same boundary condition, same splice plate and same thickness of the gusset plate, the buckling load increases as the width of the gusset plate decreases.
2. With the same thickness of gusset plate and same splice plate, the buckling load increases and approaches the same magnitude as the width of the gusset plate decreases to its minimum, regardless of the boundary condition on the top end either free or fixed.
3. Rotational restraint on the upper end of a gusset plate is very important. The effect of rotational restraint

depends upon the relative stiffness of the splice plate and gusset plate and the bending stiffness of the bracing member.

4. For the gusset plates with the same boundary conditions and same geometric configuration, the buckling load is affected not only by the thickness of the gusset plates but also the thickness of the splice plate. However, as the thickness of splice plate increases or decreases and approaches infinity or zero, the buckling loads of the gusset plates with different thicknesses are affected only by the thickness of the gusset plates. Their magnitude is proportional to the cube of the gusset plate thickness.

Table 5.1 Summary and Comparison of Test Result

Loading	Case	Plate	Size (mm)	Test Result		Analytical Result		
				Deformed Direction	Pmax (kN)	Effective Width Concept (kN)	BASP (kN)	Beam-Column
Concentric Loading	Free Case	C1	850 x 550 x 6.70	east	441.7	1922	944	
		C2	850 x 550 x 3.11	east	122.4	424	120	
		C3	850 x 700 x 6.70	west	380.1	1922	382	
		C4	850 x 700 x 3.11	west	89.6	424	43	
	Fixed Case	C1	850 x 550 x 6.70	east	914.0	1922	1314	
		C2	850 x 550 x 3.11	west	140.6	424	152	
		C3	850 x 700 x 6.70	west	678.2	1922	1083	
		C4	850 x 700 x 3.11	east	145.5	424	130	
Eccentric Loading	Free w/o Stiffener	E5	850 x 550 x 6.70	east	80.4	1922		81
		E6	850 x 700 x 6.70	east	55.8	1922		81
	Free w/ Stiffener	E5	850 x 550 x 6.70	east	232.8	1922	619 *	317
		E6	850 x 700 x 6.70	west	338.6	1922	402 *	557
	Fixed w/ Stiffener	E5	850 x 550 x 6.70	east	392.5	1922	1121 *	317
		E6	850 x 700 x 6.70	west	523.2	1922	1175 *	557

Note: * It assumes that the splice plates and the stiffeners are placed symmetrically on both sides of the gusset plate.

Table 5.2 Effects of the Thickness and Size of Gusset Plates

Size (mm)	Thickness (mm)					
	3.11	6.70	9.90	3.11	6.70	9.90
	Free Case (kN)			Fixed Case (kN)		
405	330	2564	7270	331	2594	7479
450	211	1788	4086	211	1815	5283
500	170	1413	2899			
550	120	937	2166	152	1314	3729
600	80	622	1670			
650	54	470	1247	134	1126	3036
700	43	382	1042			
750	36	325	906	125	1047	2706
800	31	287	815			
850	28	262	752	107	938	2398

Note: The logger free side of the gusset plate is kept constant at 850 mm

Table 5.3 Effects of Rotational Restraint and Thickness of Splice Plate

Case	Plate	Size (mm x mm x mm)	Test Result (kN)	BASP (kN)			
				w/rotational restraint	w/o rotational restraint	infinite thickness of splice plate	w/o splice plate
Free Case	C1	850 x 550 x 6.70	441.7	944	150	1229	180
	C2	850 x 550 x 3.11	122.4	120		123	18
	C3	850 x 700 x 6.70	380.1	382	82.3	432	113
	C4	850 x 700 x 3.11	89.6	43		43	11
Fixed Case	C1	850 x 550 x 6.70	914.0	1314	1140	1590	519
	C2	850 x 550 x 3.11	140.6	152		159	52
	C3	850 x 700 x 6.70	678.2	1083	589	1330	411
	C4	850 x 700 x 3.11	144.5	130		133	41

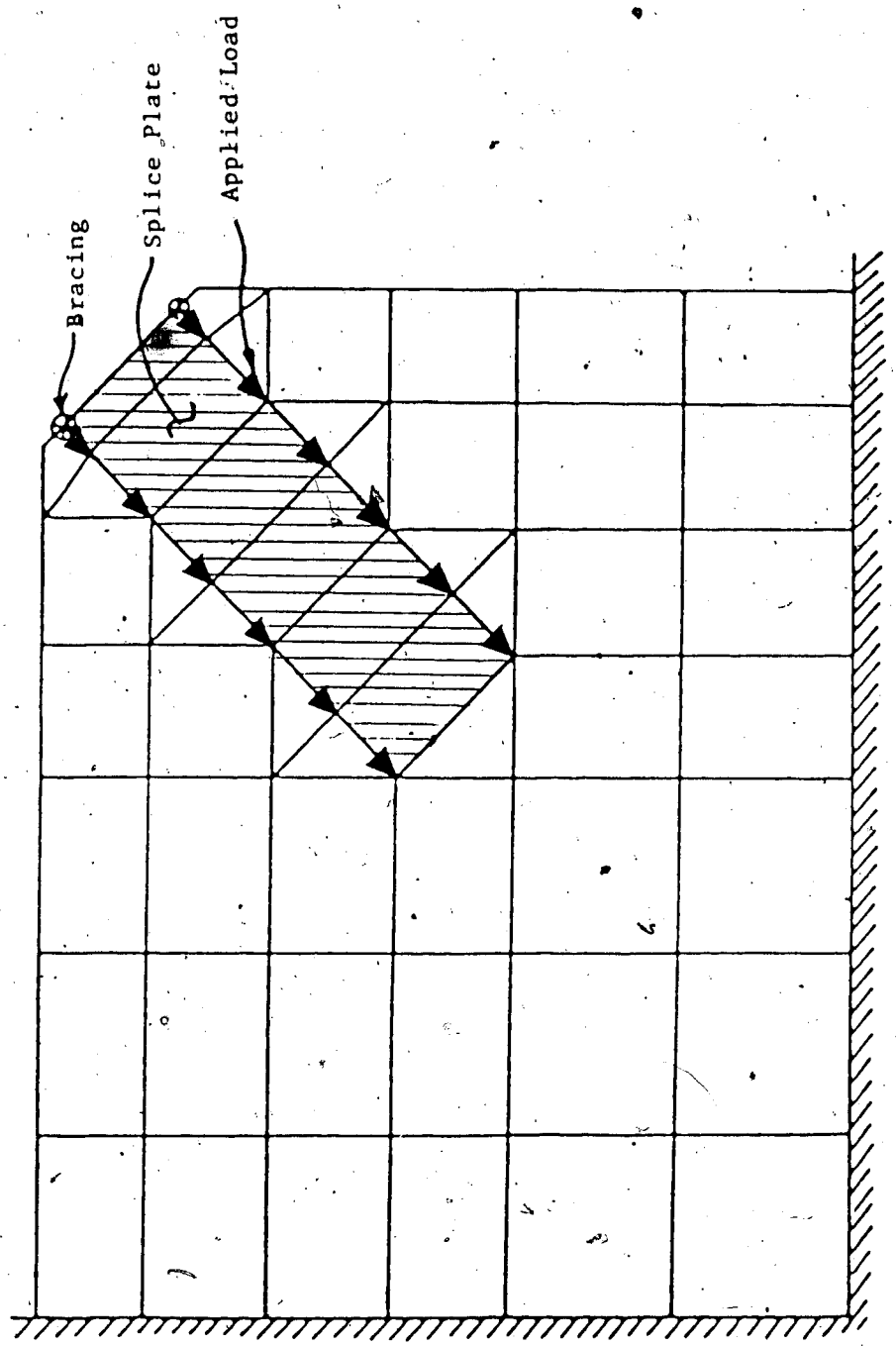

Figure 5.1 Finite Element Model

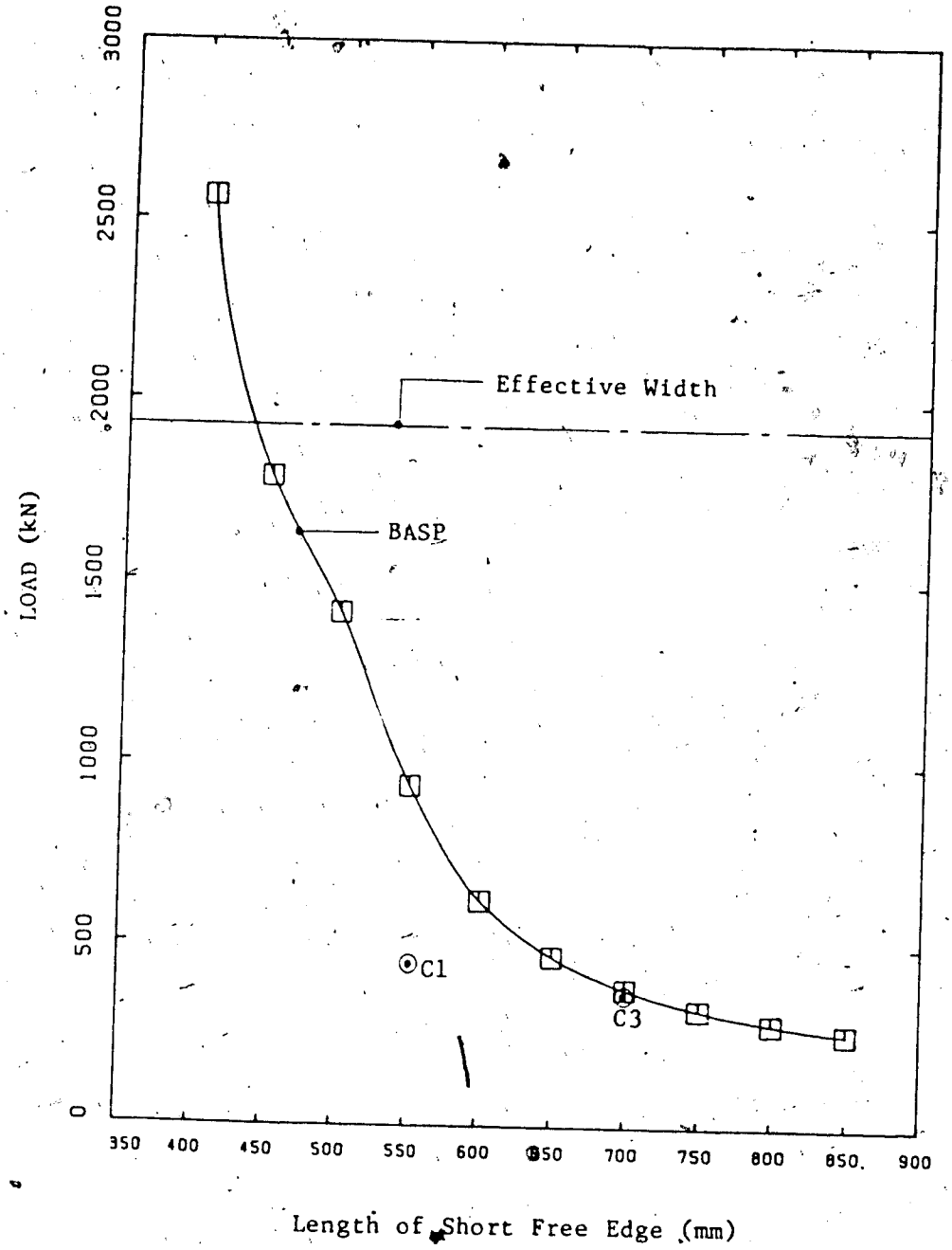

Figure 5.2 Comparison of Test Result for 6.7 mm Plates of Free Case

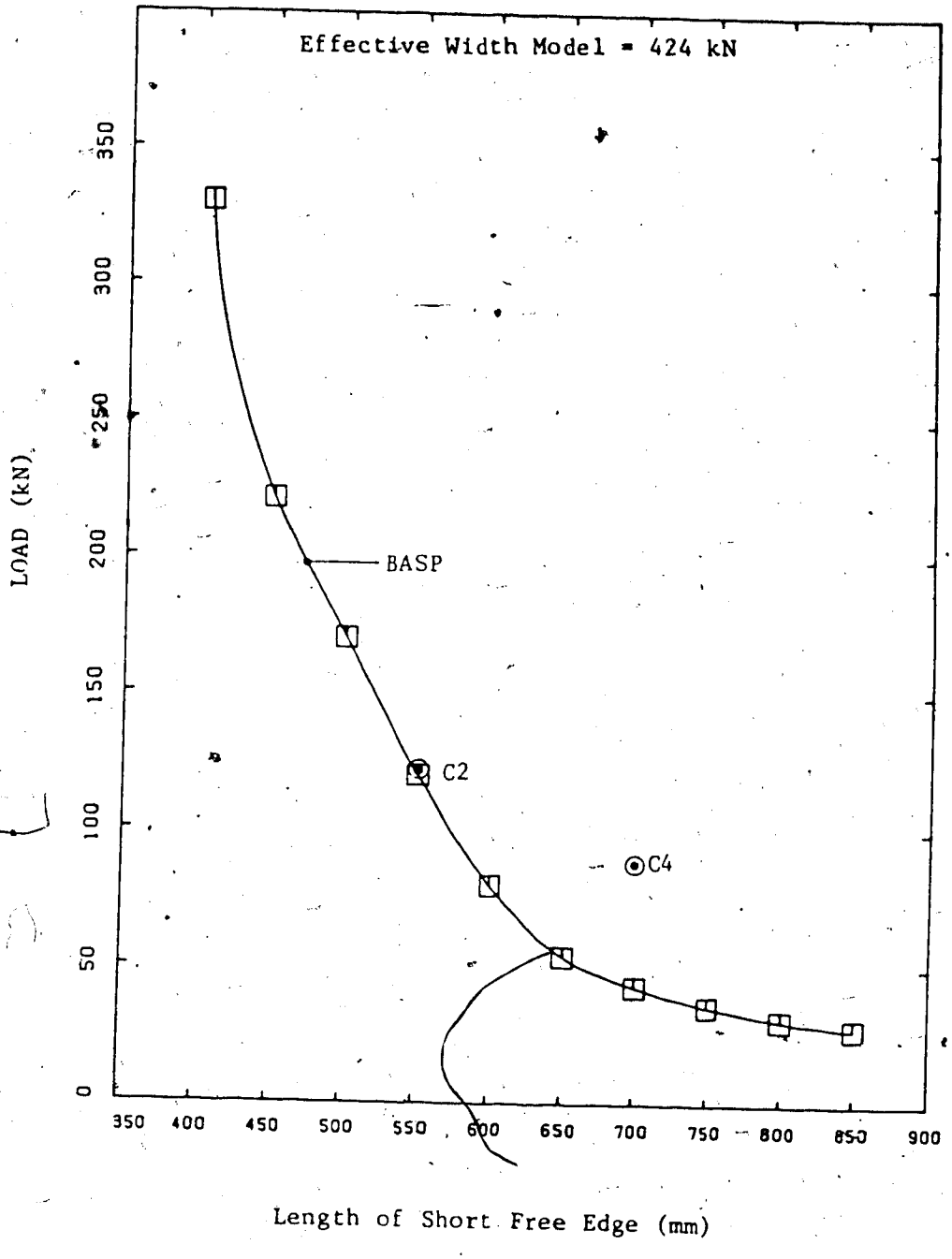

Figure 5.3 Comparison of Test Result for 3.11 mm Plates of Free Case

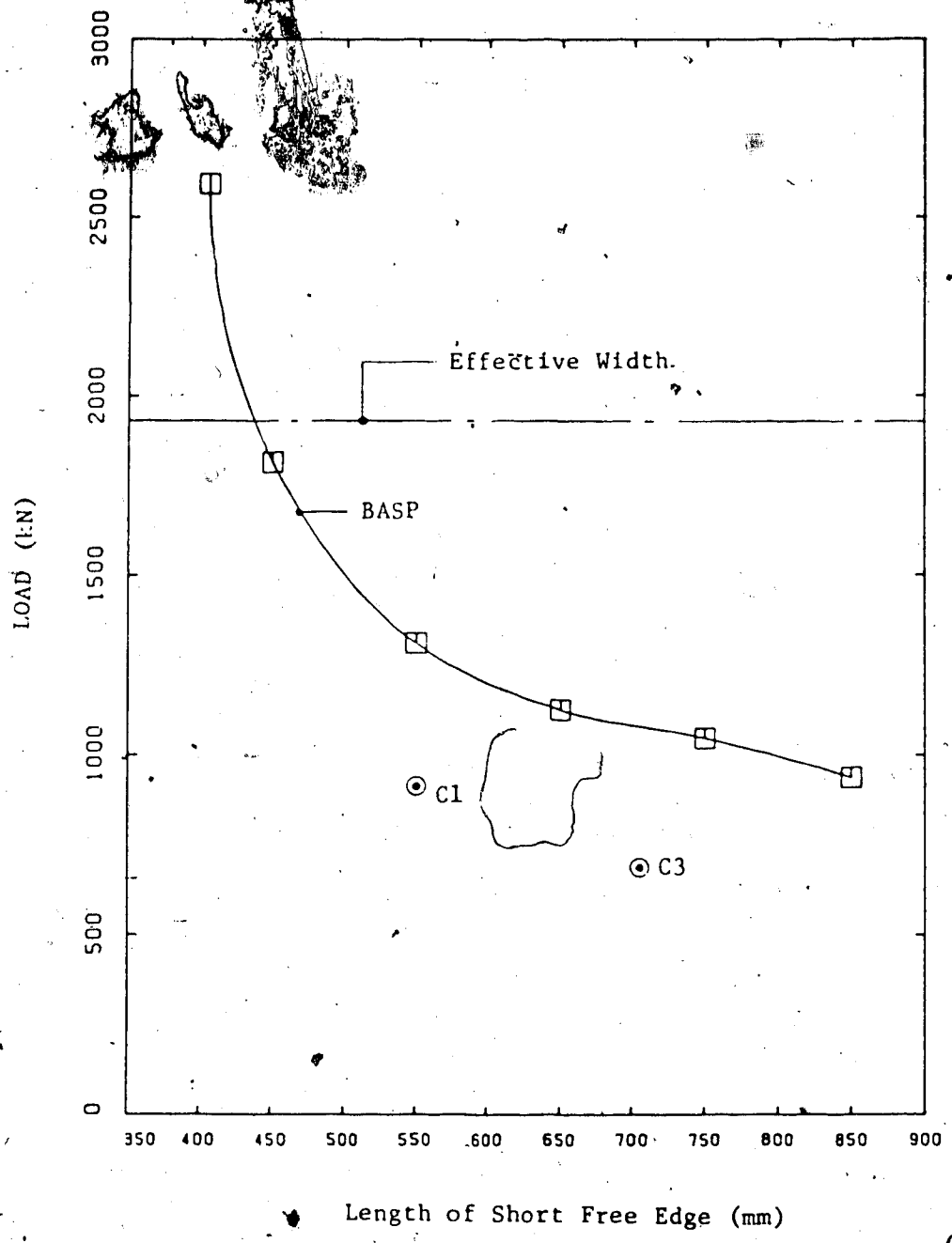

Figure 5.4 Comparison of Test Result for 6.7 mm Plates of Fixed Case

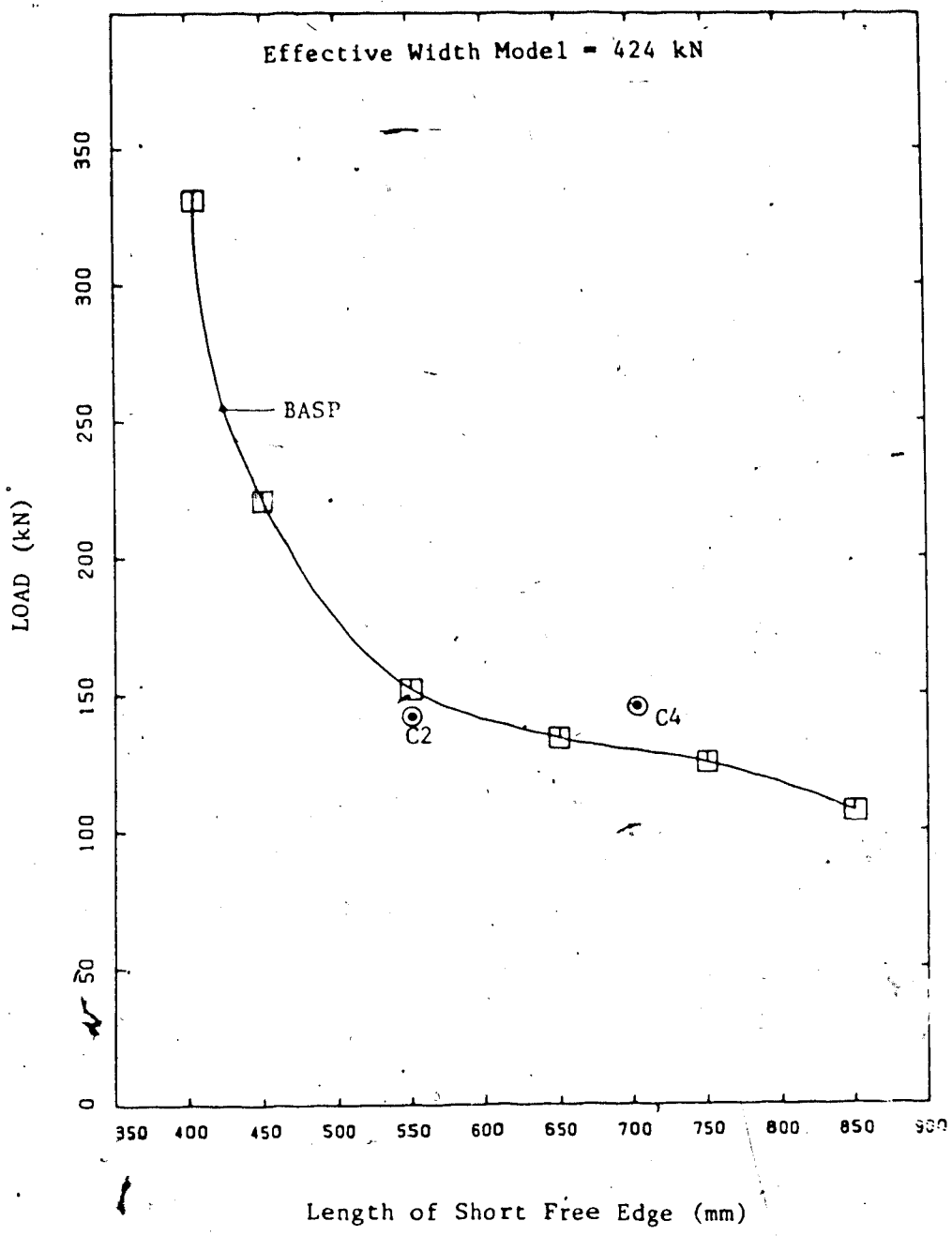

Figure 5.5 Comparison of Test Result for 3.11 mm Plates of Free Case

TEST RESULT Free Case - 23.1 MPa

Fixed Case - 23.3 MPa

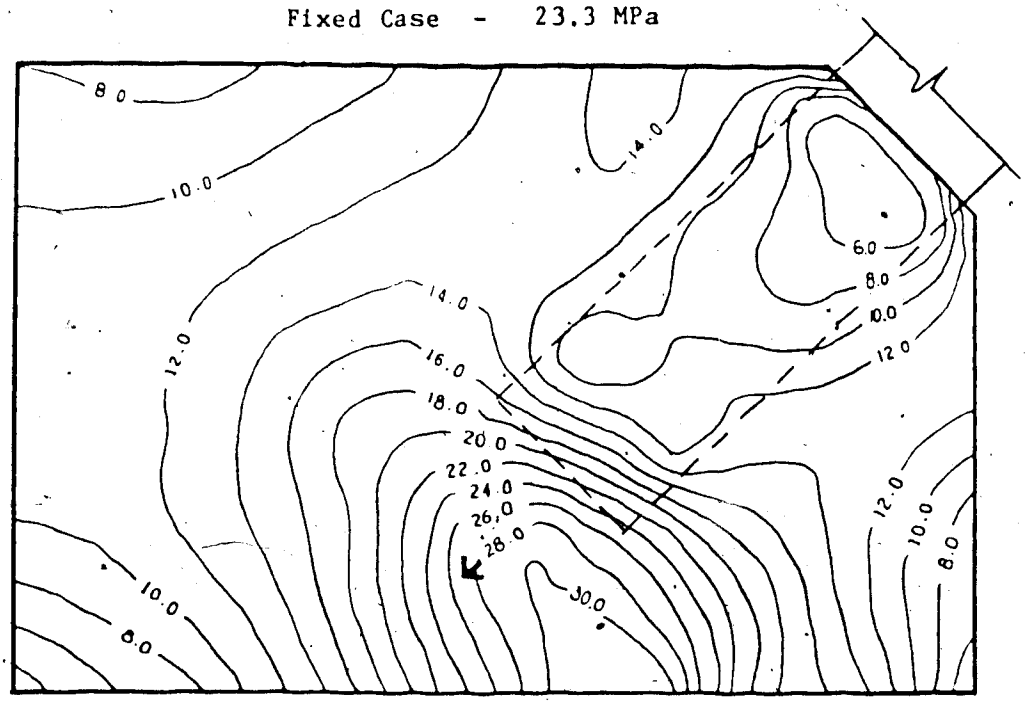

Corresponding Load 100 kN

↙ Rosette Gage

Figure 5.6 Contours of Maximum Compressive Stress (MPa) for 850 mm x 550 mm x 6.7 mm Plate

TEST RESULT Free Case - 24.9 MPa
Fixed Case - 24.6 MPa

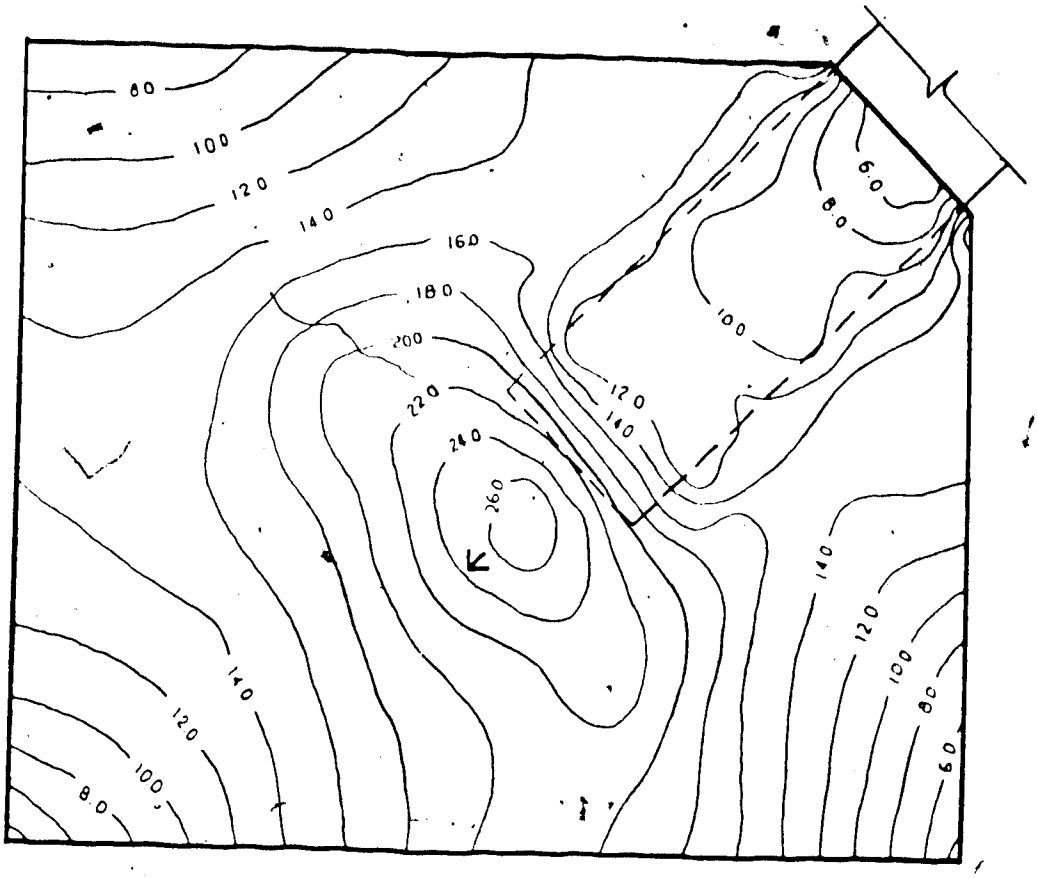

Corresponding Load 100 kN

Rosette Gage

Figure 5.7 Contours of Maximum Compressive Stress (MPa) for 850 mm x 700 mm x 6.7 mm Plate

TEST RESULT. Free Case - 33.9 MPa

Fixed Case - 36.2 MPa

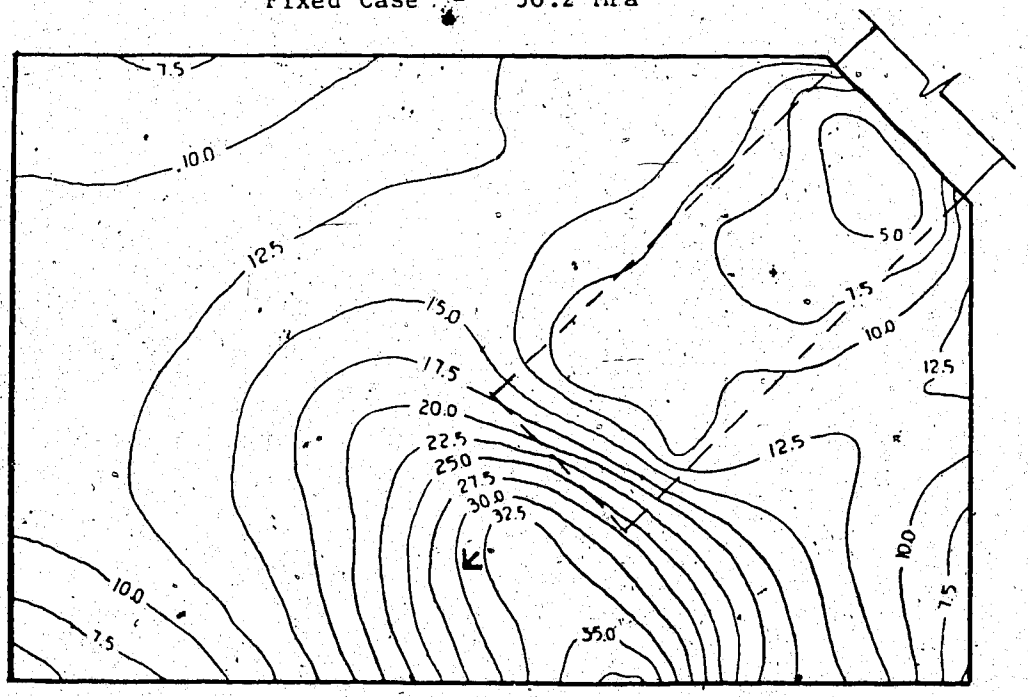

Corresponding Load 50 kN

↙ Rosette Gage

Figure 5.8 Contours of Maximum Compressive Stress (MPa) for 850 mm x 550 mm x 3.11 mm Plate

TEST RESULT Free Case - 12.6 MPa

Fixed Case - 29.9 MPa.

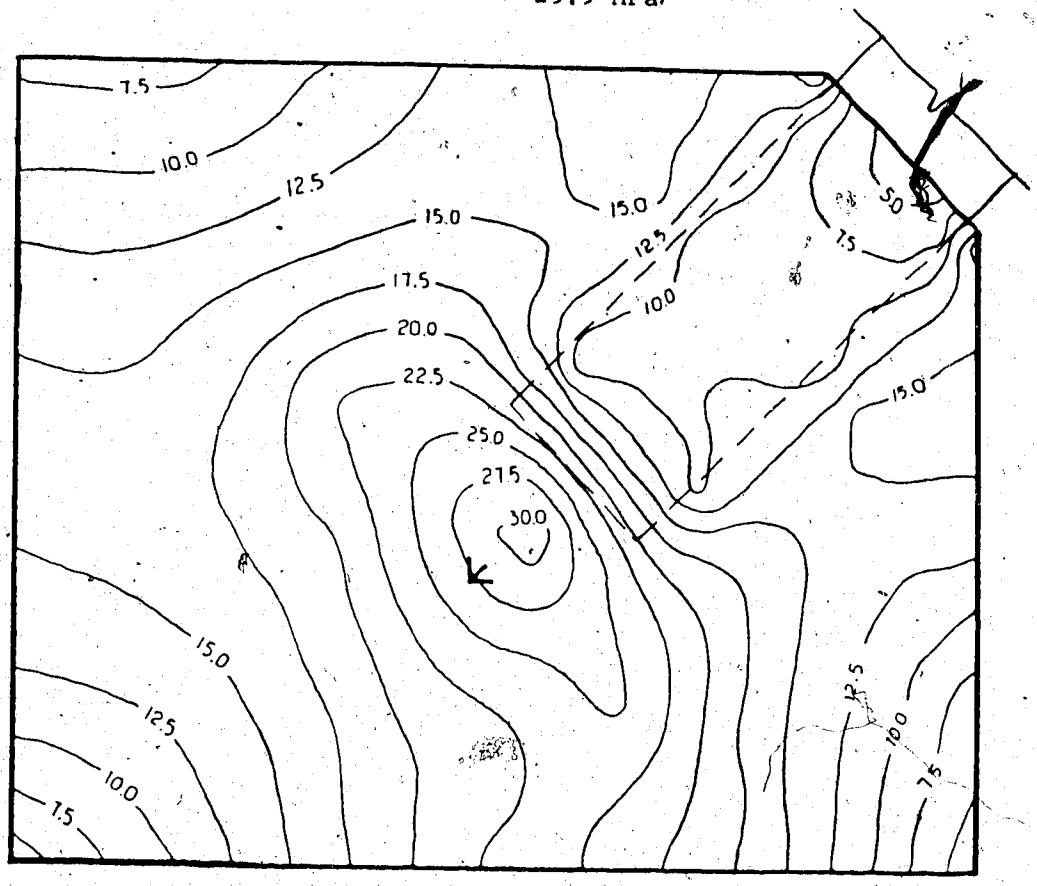

Corresponding Load 50 kN

Rosette Gage

Figure 5.9 Contours of Maximum Compressive Stress (MPa) for 850 mm x 700 mm x 3.11 mm Plate

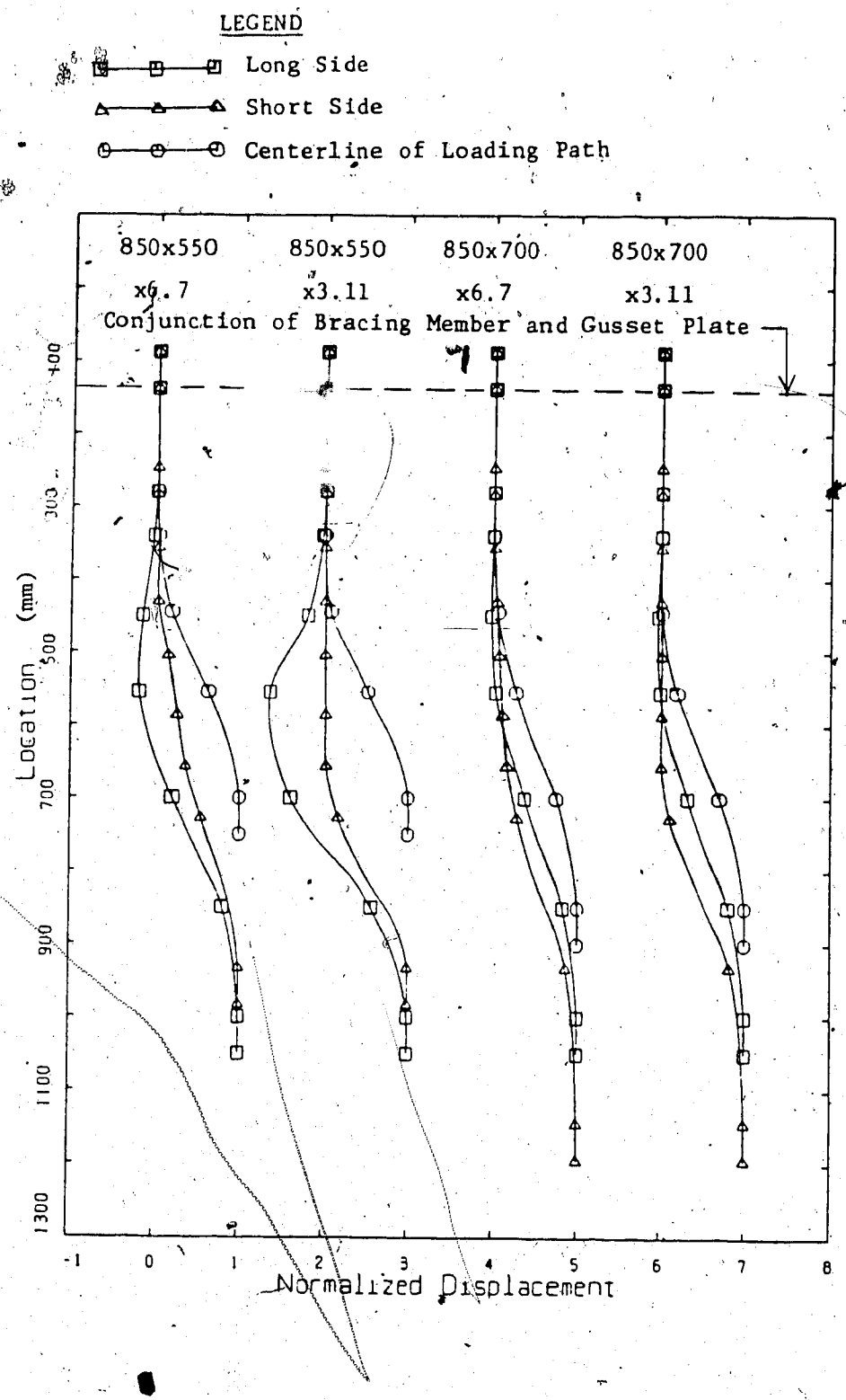

Figure 5.10 Buckling Shapes of Free Case using BASP

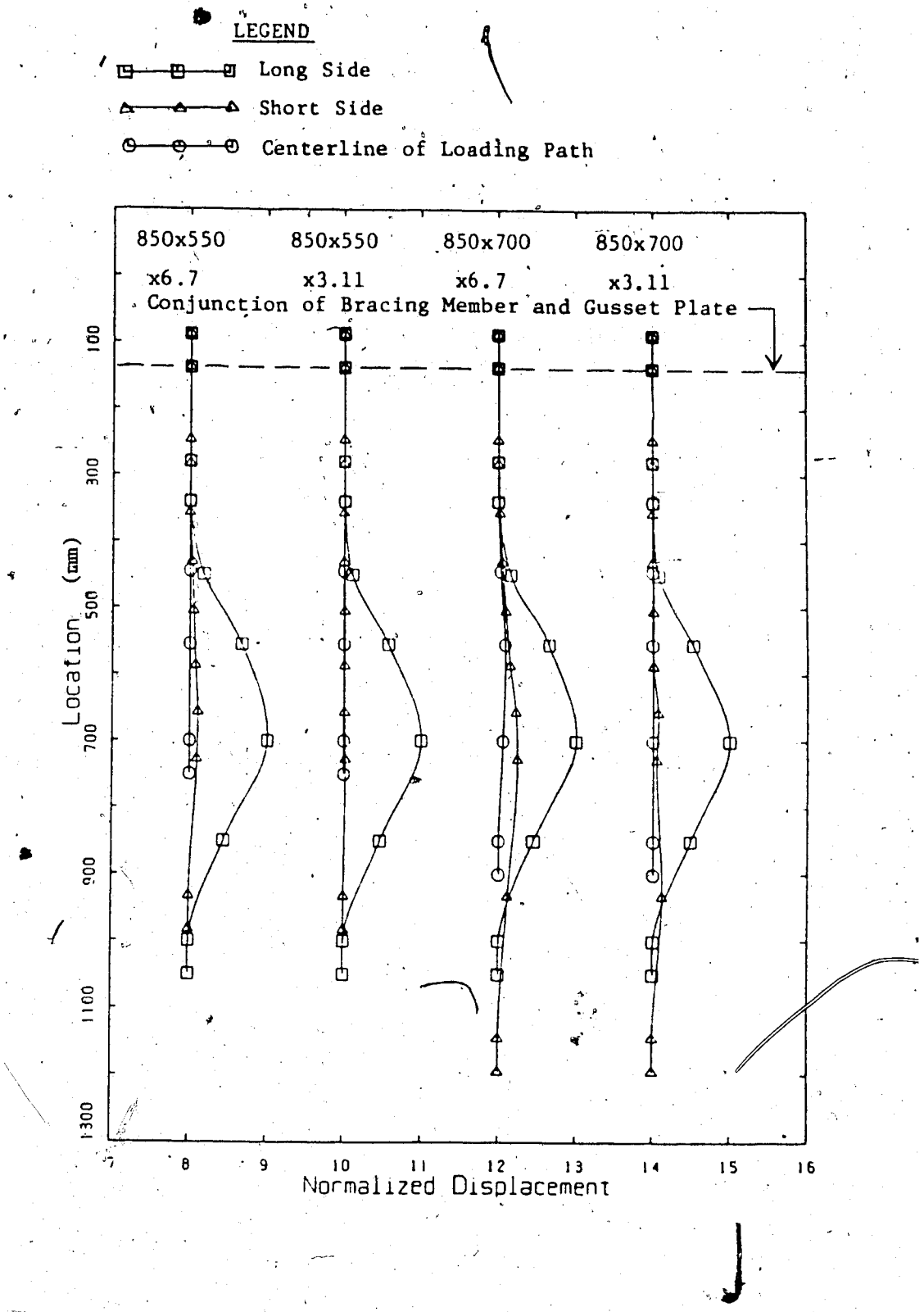

Figure 5.11 Buckling Shapes of Fixed Case using BASP

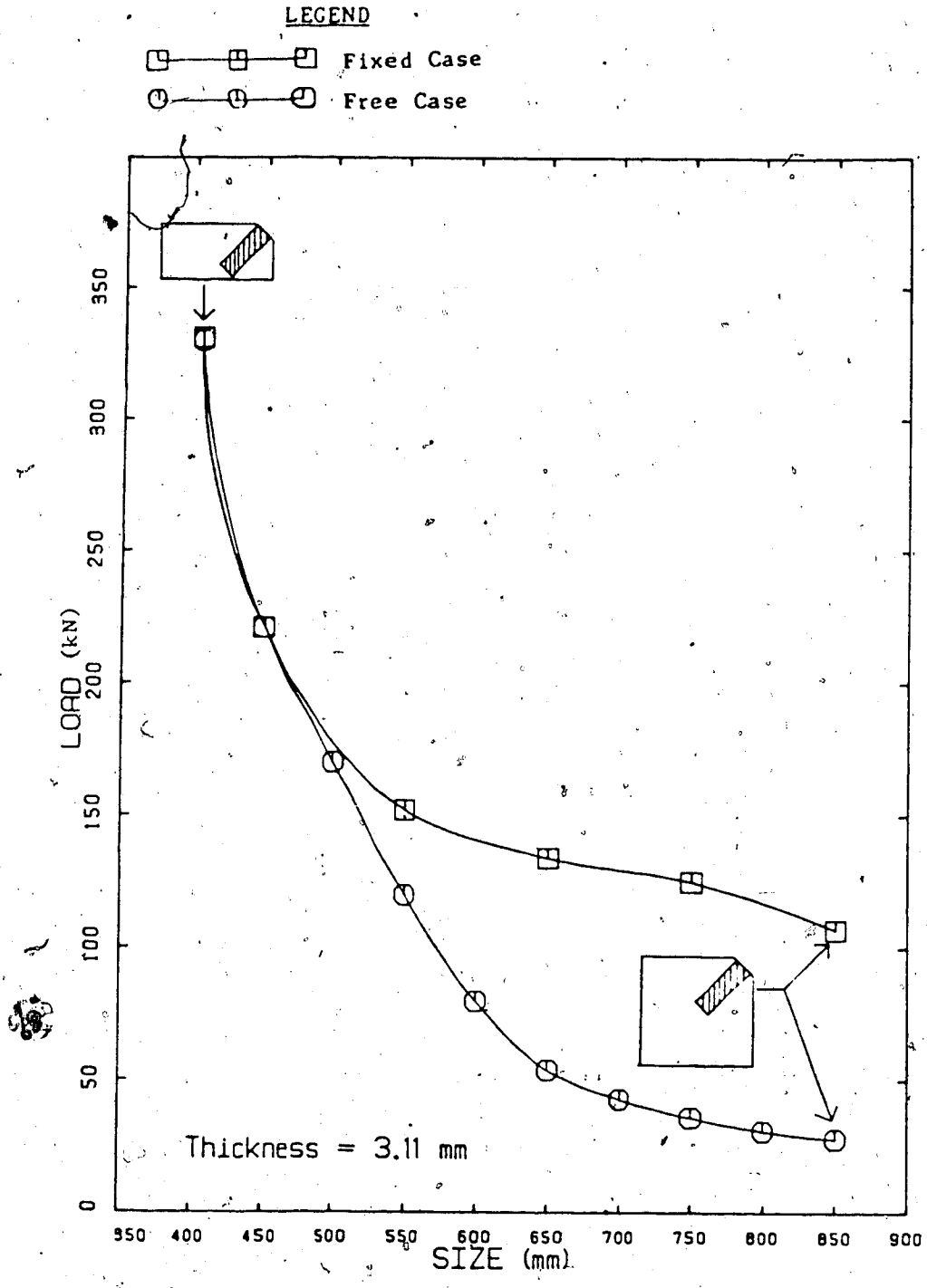

Figure 5.12 Effect of the Size of Gusset Plate for 3.11 mm Plates

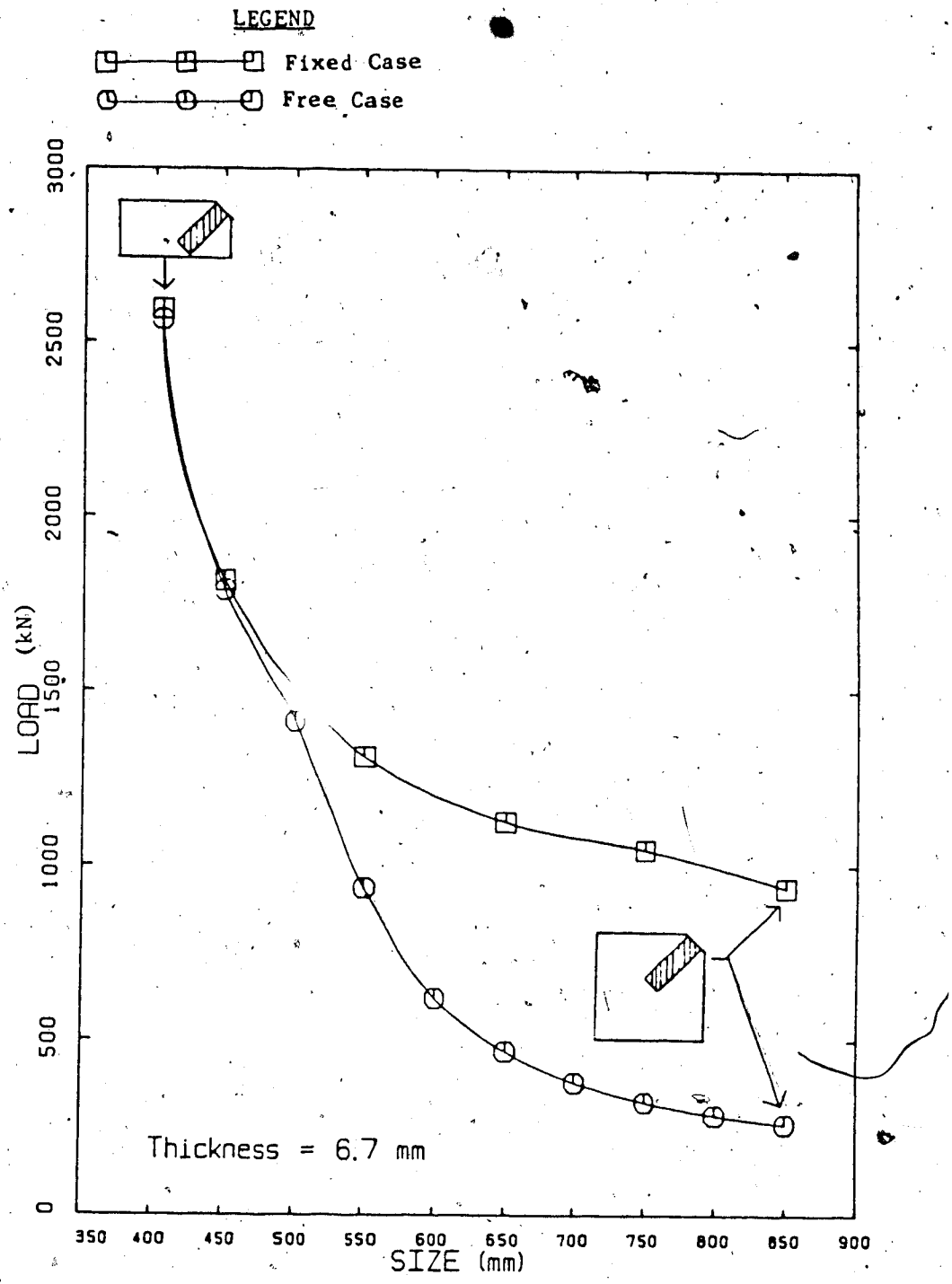

Figure 5.13 Effect of the Size of Gusset Plate for 6.7 mm Plates

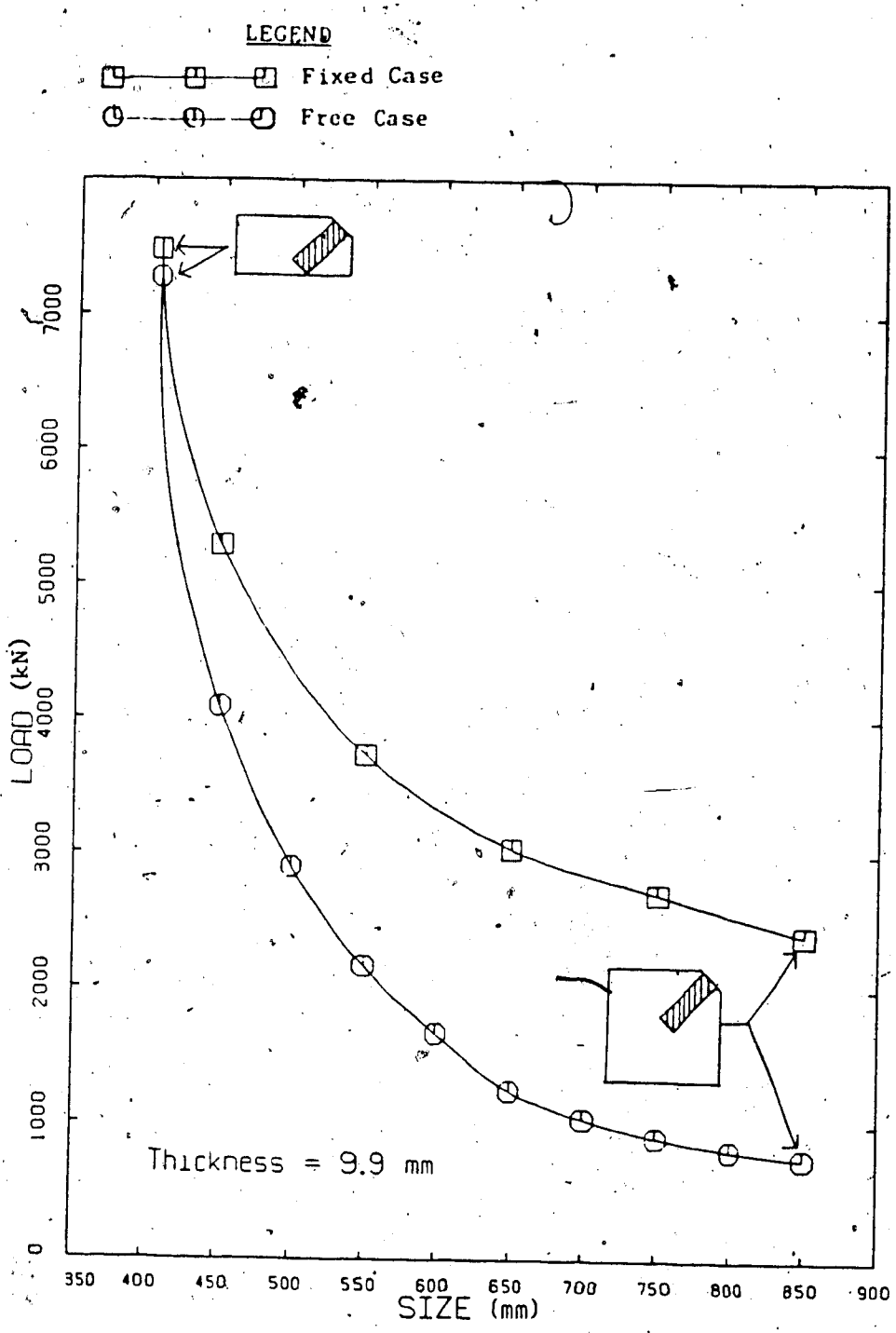

Figure 5.14 Effect of the Size of Gusset Plate for 9.9 mm Plates

6. SUMMARY AND DESIGN GUIDELINE

6.1 Summary

The compressive behavior and buckling strength of thin-walled gusset plate connections have been examined by an experimental investigation of full-scale diagonal bracing connections. The test parameters considered included plate thickness, plate size, boundary condition, eccentricity and reinforcement. A total of 14 tests were run on six connection specimens. Both current design practices and finite element solutions were used to compare the test results.

A parametric study was undertaken using the finite element program BASP to investigate the significance of each important variable. The following is a summary of the findings.

1. For the concentric loading cases that were examined, the primary failure mode for the free cases is overall buckling of the plate. The maximum deflection occurred at the roller locations. For the fixed cases, the failure is initiated at the free edges due to the local buckling of the plate. The maximum deflection occurred at the mid-point of the longer free edge.
2. Another type of failure may occur in the spliced plate due to the existence of the eccentricity. This has been shown in the cases of free case without stiffener of the plates E5 and E6. The reduction of the strength can be

significant.

3. The cases with stiffeners (plates E5 and E6) show that the reduction of the strength due to the eccentricity can be minimized by providing sufficient stiffeners at the splice plate locations.
4. The effective width concept which is currently used in designing gusset plates was found to be very unconservative if the primary failure mode is the plate buckling.
5. In the elastic region the maximum stresses obtained from both the tests and the computer solutions agree fairly well with the Whitmore concept of designing the gusset plate.
6. Despite the complexity of the problem, the finite element solutions are shown to be in reasonable agreement with the test results. The discrepancy between the tests and the analysis can be attributed to the uncertainty of the boundary restraints and the partial yielding observed in the splice plate.
7. The beam-column formula for a rectangular cross-section gives a reasonable predict[illegible]e carrying capacity of eccentrically loaded c[illegible]ates.
8. The rotational restraint [illegible] the boundary of a gusset plate is found to be a very imp[illegible]ant parameter in the buckling strength of the gusset plate.
9. The parametric study shows that increasing the bending stiffness of the splice plate and extending the splice

plate to the beam and/or column will increase the buckling strength of the gusset plate significantly. Actually, both free and fixed cases yield the same buckling load for the gusset plates with the relatively thick and continuous splice plates.

10. The buckling strength of the gusset plates with the same size and geometric configuration is found to be proportional to the cube of the thickness of the gusset plates if the splice plate provided is the same size and of infinite thickness.
11. The available design methods for compressive loaded gusset plates have been found to be inappropriate for determining the compressive behavior and failure of the gusset plates.

6.2 Design Guideline for Gusset Plates

Based on the test results and the parametric study, a design guideline for gusset plates loaded in compression is recommended as below. However, it should be noted that the effects of variables such as thickness, size, boundary condition, etc. on the compressive strength of a gusset plate which will be outlined in the next section should be further investigated for the improvement of the proposed design recommendation.

1. Avoid eccentricity, if possible, to prevent premature failure before buckling. If eccentricity can not be avoided, the beam-column formula (Eq.(5.1)) can be used

to calculate the bending strength of the gusset plate. Further improvement can be made by providing stiffeners at the weakest cross-section location to increase the carrying capacity of the gusset plate.

2. To increase the buckling strength of a gusset plate, thicker splice plates are preferred. An alternative is to extending the bracing member into (such as channel or angle sections back to back) the gusset plate and bolt it onto the gusset plate.

3. The distance between the end of splice plate or bracing member and the flange of the beam and/or column should be as small as possible.

4. The elastic buckling strength of a gusset plate can be calculated using an linear-elastic buckling analysis and the finite element model as shown in Fig. 5.1, provided that the thickness of the splice plate is relatively large compared to the thickness of the gusset plate. An alternative is to conduct a parametric study with various geometric configurations to find out the corresponding plate buckling coefficients k. Then, the elastic buckling strength of a gusset plate can be evaluated by the basic plate buckling formula as

$$P_x = \frac{k\pi^2 E_t t^3}{12(1-\nu^2)b} \qquad [6.3]$$

where b is the shorter free edge of the gusset plate.

5. Before further investigation is undertaken, it is

recommended that the Whitmore effective width method is used to evaluate the inelastic buckling strength of a gusset plate. However, the splice plate used in the connection should be free from yielding and have sufficient bending stiffness.

6.3 Recommendations for Future Research

Further research should be conducted on the compressive strength of gusset plate connections in the following areas:

1. A parametric study to determine the plate buckling coefficient k, as illustrated in the previous design guideline, in order to calculate the elastic buckling strength of a gusset plate.
2. Further studies on the influence of plate boundaries on the behavior and strength of the gusset plates.
3. The behavior and design of inelastic buckling of a gusset plate should be investigated by conducting a full scale gusset plate testing program and evaluating the results by using inelastic finite element analyses.
4. More tests should be conducted to evaluate the effects of variables such as plate thickness, size, boundary elements, loading angle, and so on.
5. The interaction of the buckling strength between gusset plates and bracing member should be examined.
6. The requirements for the splice plates and the stiffeners for the gusset plates loaded in compression should be investigated.

REFERENCES

Akay, H.U., Johnson, C.P. and Will, K.M., **Lateral and Local Buckling of Beams and Frames**, Journal of the Structural Division, ASCE, Vol. 103, No. ST9, September, 1977, pp.1821-1832.

American Society for Testing and Materials, **Metal Test Methods and Analytical Procedures**, Annual Book of ASTM Standards, Vol. 03.01, 1985.

Bjorhovde, R. and Chakrabarti, S.K., **Tests of Full-Size Gusset Plate Connection**, Research Report, Dept. of Civil Engineering, University of Arizona, Tucson, April 1983.

Canadian Standards Association (CSA), Design of Highway Bridges, CAN3-S6-M78, CSA, Rexdale, Ontario, 1978.

Canadian Standards Association (CSA), Steel Structures for Buildings---Limit State Design, CAN3-S16.1-M84, CSA, Rexdale, Ontario, 1984.

Davis, C.S., **Computer Analysis of the Stresses in a Gusset Plate**, thesis presented to the University of Washington, at Seattle, Wash., in 1967, in partial fulfillment of the requirements for the degree of Master of Science.

Gilmor, M.I., 1985, Private Communication.

Hardash, S.G. and Bjorhovde, R., **New Design Criteria for Gusset Plates in Tension**, Engineering Journal, AISC,

2nd. Quarter, 1985, pp.77-94.

Hardin, B.O., **Experimental Investigation of the Primary Stress Distribution in the Gusset Plates of a Double Plane Pratt Truss Joint with Chord Splice at the Joint**, Bulletin No.49, Engineering Experiment Station, University of Kentucky, Sept., 1958.

Irvan, W.G., **Experimental Study of Primary Stresses in Gusset Plates of a Double Plane Pratt Truss**, Bulletin No.46, Engineering Experiment Station, University of Kentucky, Dec., 1957.

Kulak, G.L., Fisher, J.W.,and Struik, J.H.A., Guide to Design Criteria for Bolted and Riveted Joints, Second Ed., Wiley-Interscience, New York, N.Y.,1987.

Richard, R.M., Rabern, D.A., Hormby, D.E. and Williams, G.C., **Analytical Models for Steel Connections**, Behavior of Metal Structure, Proceedings of the W.H. Mupse Symposium, ASCE, Edited by W.J. Hall and M.P. Gaus, May 17, 1983, pp.128-155.

Southwell, R.V., **On the Analysis of Experimental Observations in Problems of Elastic Stability**, Proc., Royal Soc. of London, Vol. 135A, 1932, pp. 601-616.

Structural Stability Research Council, Guide to Stability Design Criteria for Metal Structure, edited by B.G. Johnston, 3rd edition, John Wiley & Sons, Inc., New

York, N.Y., 1976.

Struik, J.H.A., **Applications of Finite Element Analysis to Non-Linear Plane Stress Problem**, Ph.D. Dissertation, Department of Civil Engineering, Lehigh University, Bethlehem, Pa., November 1972.

Vasarhelyi, D.D., **Tests of Gusset Plate Models**, Journal of the Structural Division, ASCE, Vol. 97, No. ST2, Feb.,1971.

Whitmore,R.E., **Experimental Investigation of Stresses in Gusset Plates**, Bulletin No. 16, Engineering Experiment Station, Univ. of Tennessee, May, 1952.

Yamamoto, K. and Akiyama, N., **Elastic Analysis of Gusseted Truss Joints**, Journal of the Structural Division, ASCE, Vol.111, No.12, Dec. 1985, pp. 2545-2564.

APPENDIX A. Load versus Displacement Curves for Eccentric Loading Case

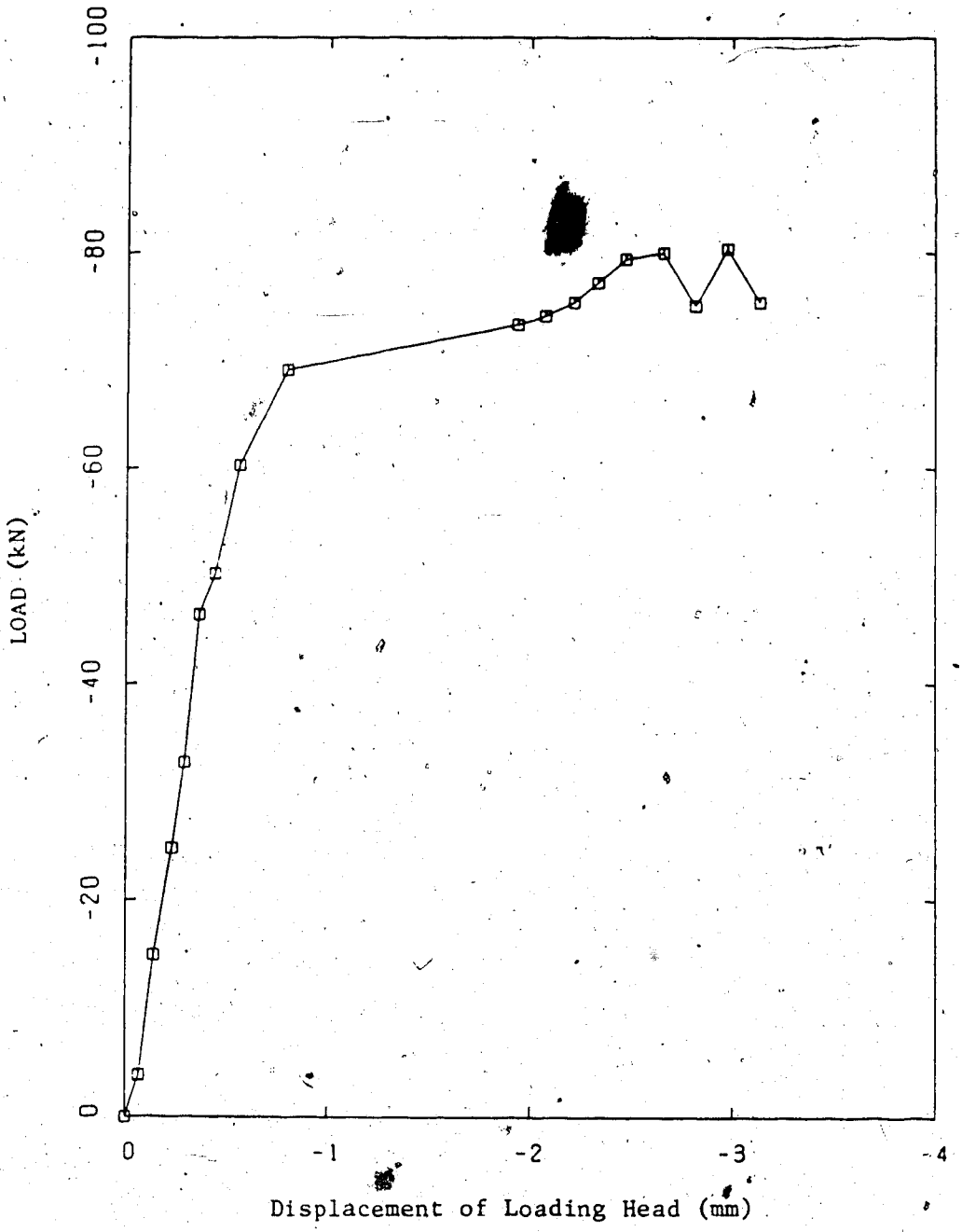

Figure A.1 Load versus Vertical Displacement Curve for Plate E5 of Free Case without Stiffener

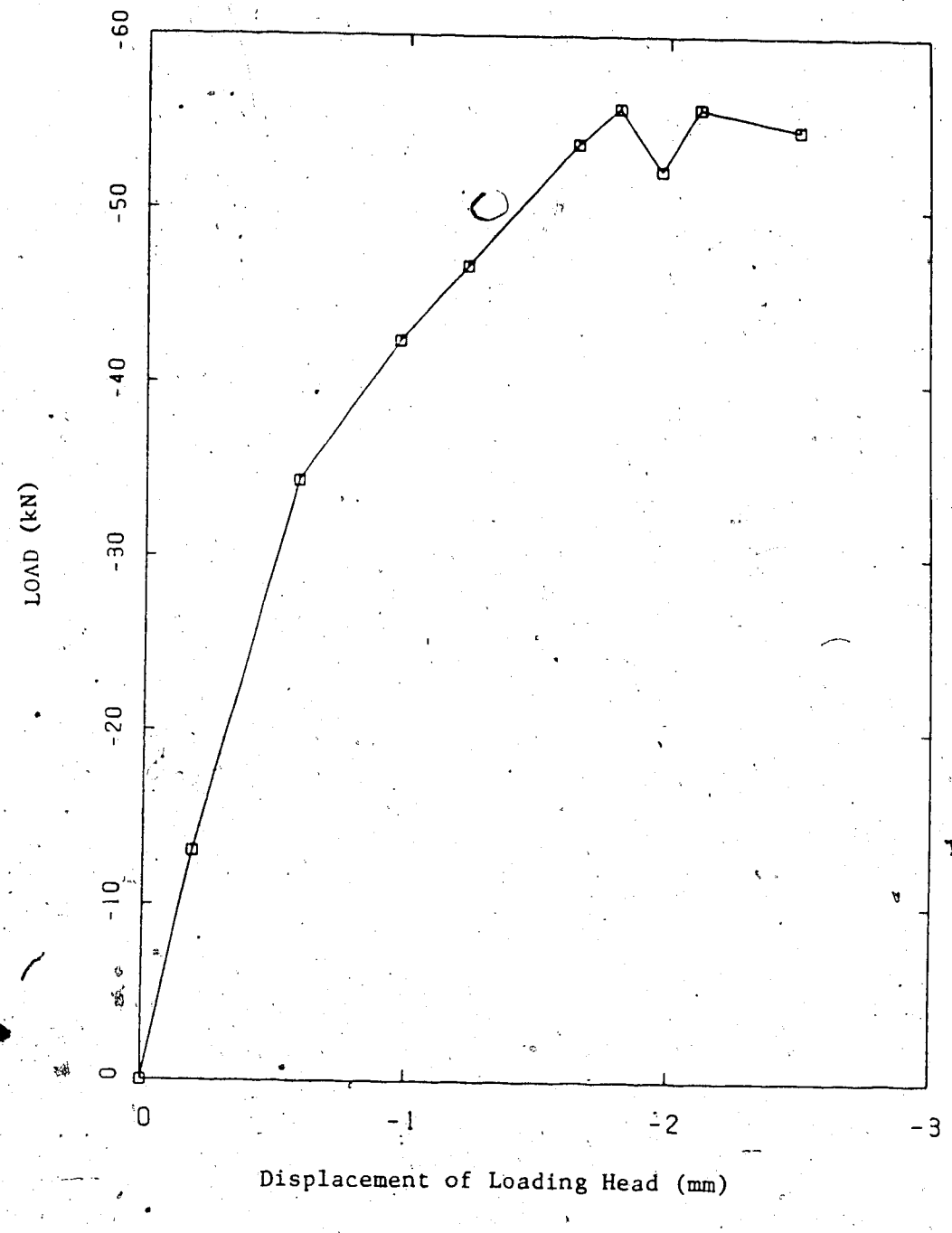

Figure A.2 Load versus Vertical Displacement Curve for Plate E6 of Free Case without Stiffener

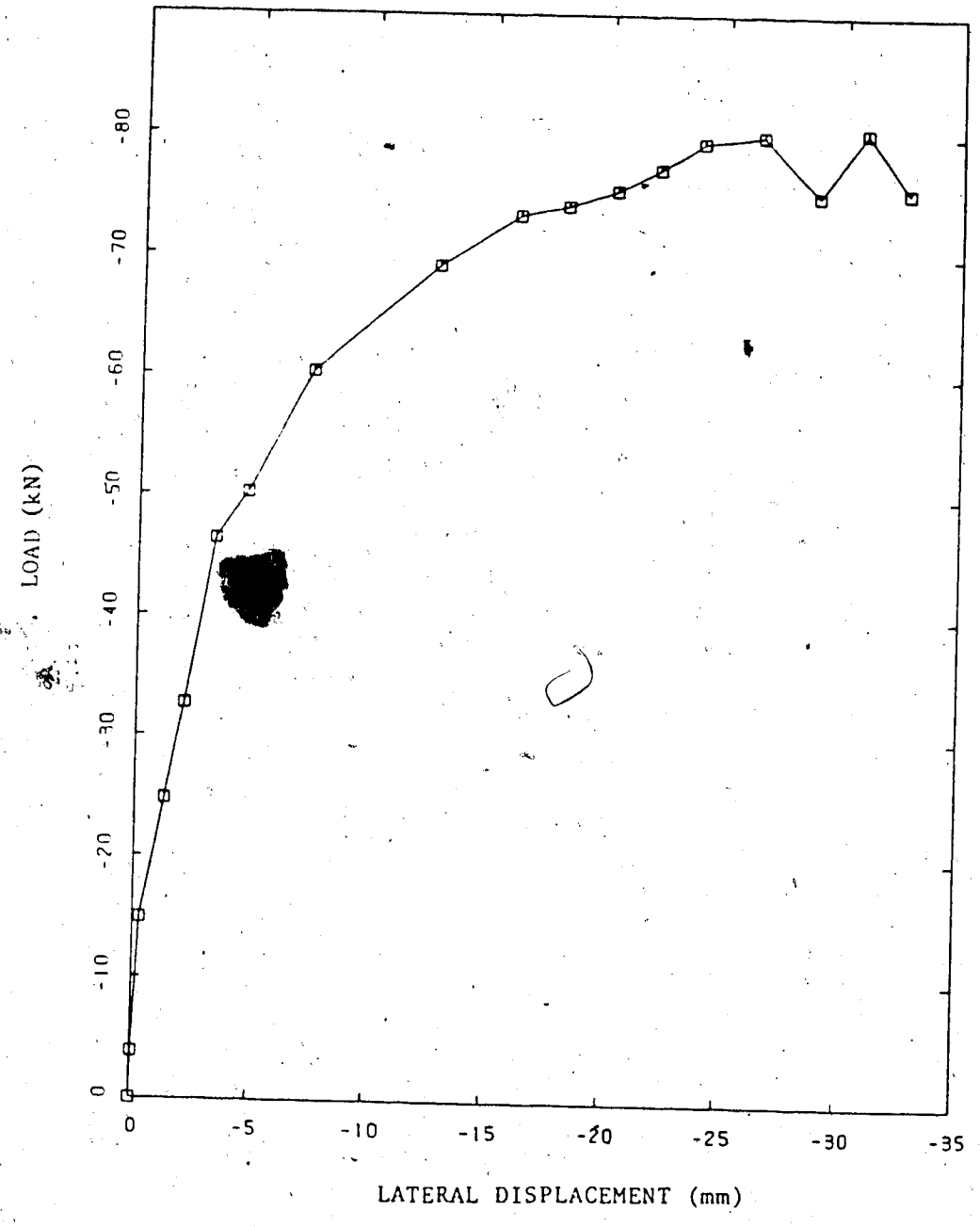

Figure A.3 Load versus Lateral Displacement Curve for Plate E5 of Free Case without Stiffener

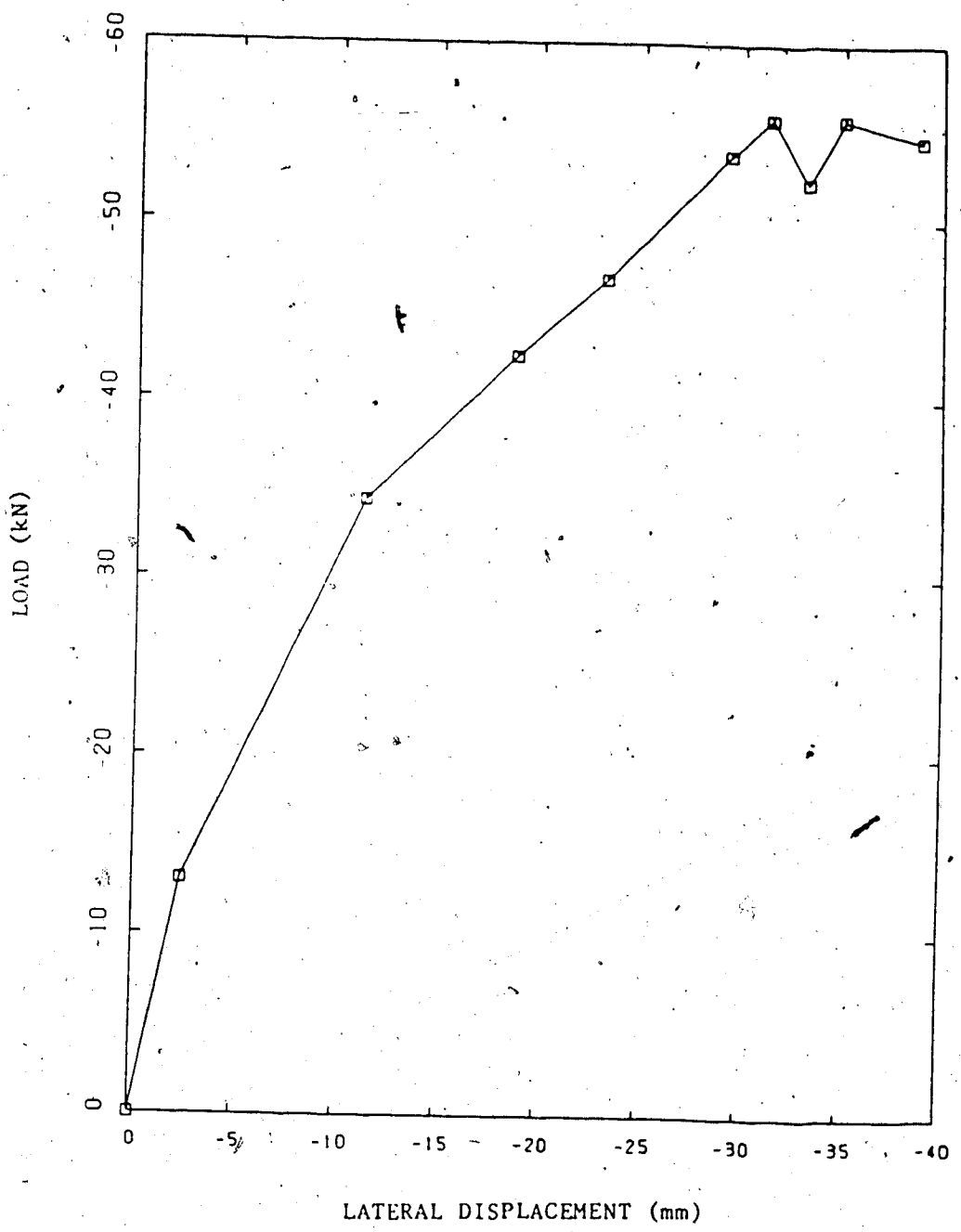

Figure A.4 Load versus Lateral Displacement Curve for Plate E6 of Free Case without Stiffener

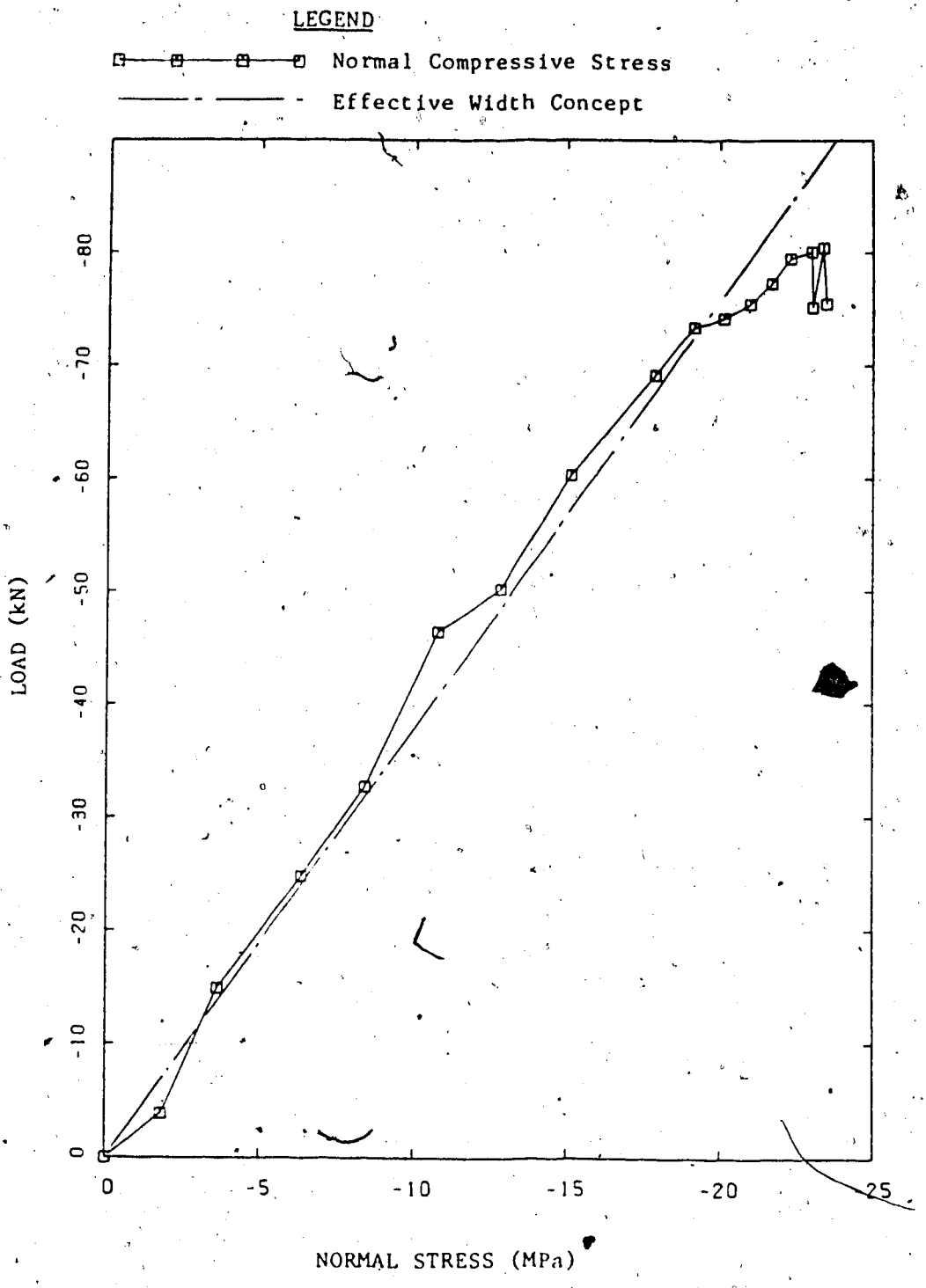

Figure A.5 Load versus Normal Compressive Stress Curve for Plate E5 of Free Case without Stiffener

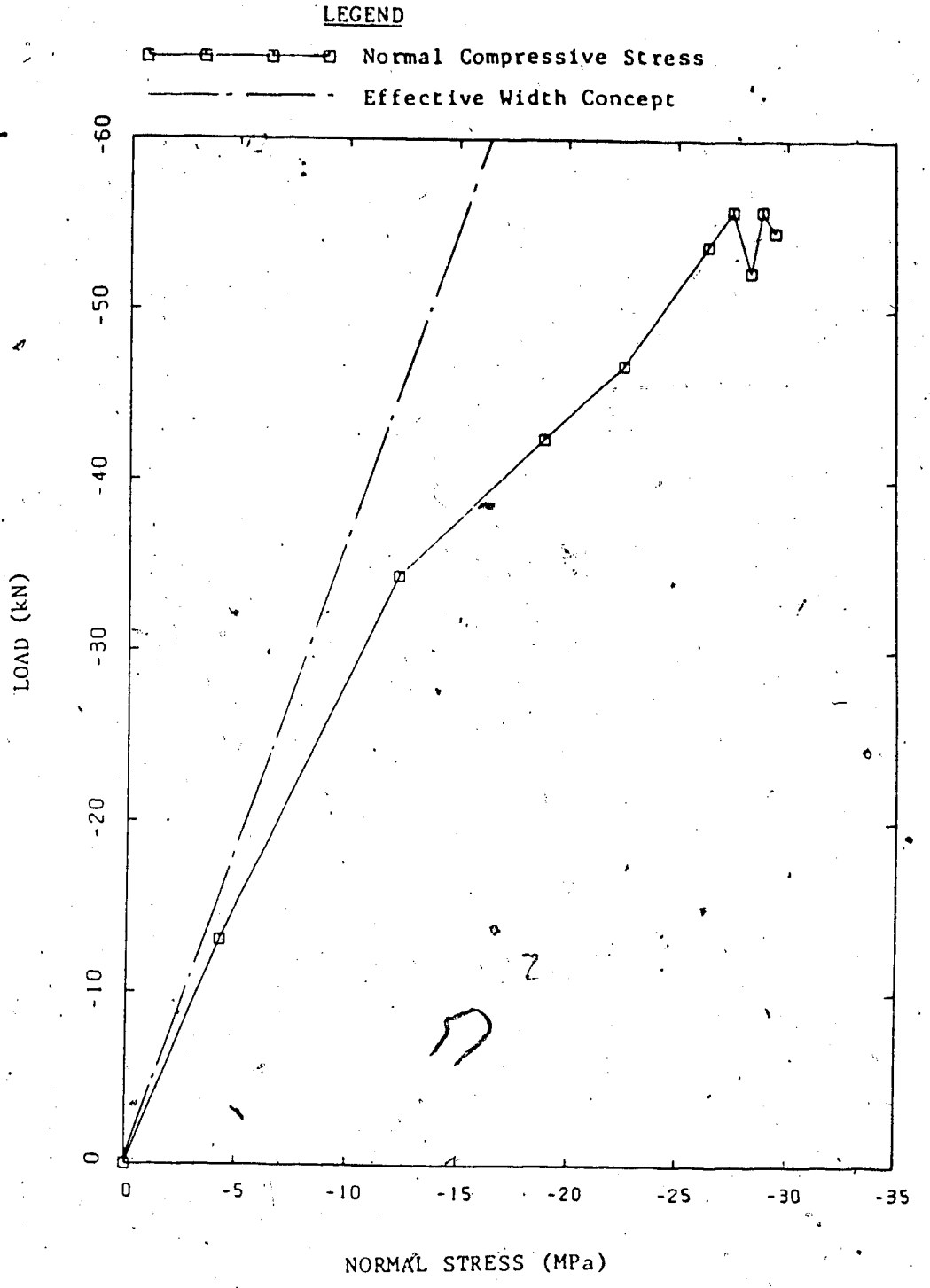

Figure A.6 Load versus Normal Compressive Stress Curve for Plate E6 of Free Case without Stiffener

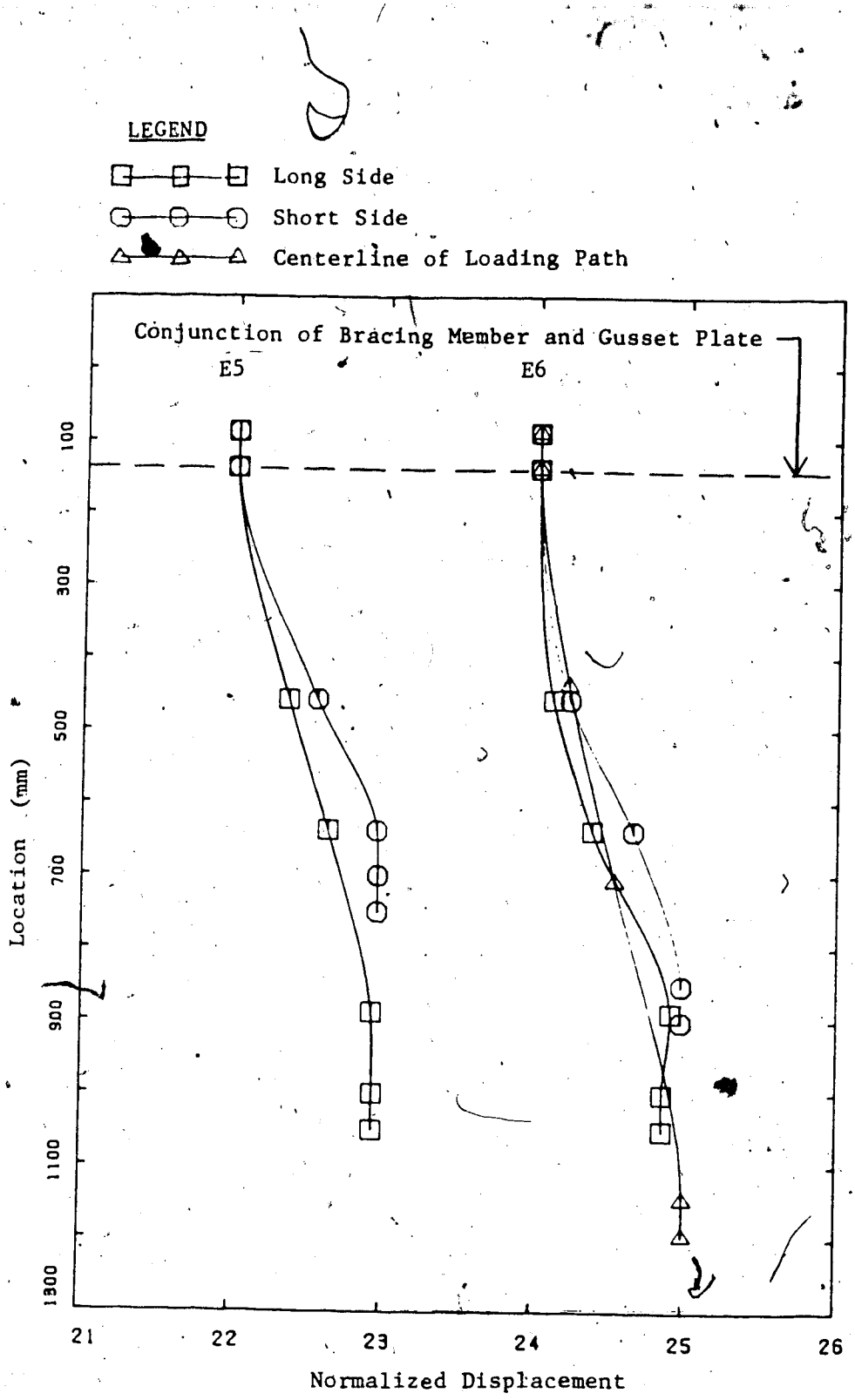

Figure A.7 Normalized Deflected Shapes of Free Case with Stiffener of Eccentric Loading Corresponding to the Maximum Load

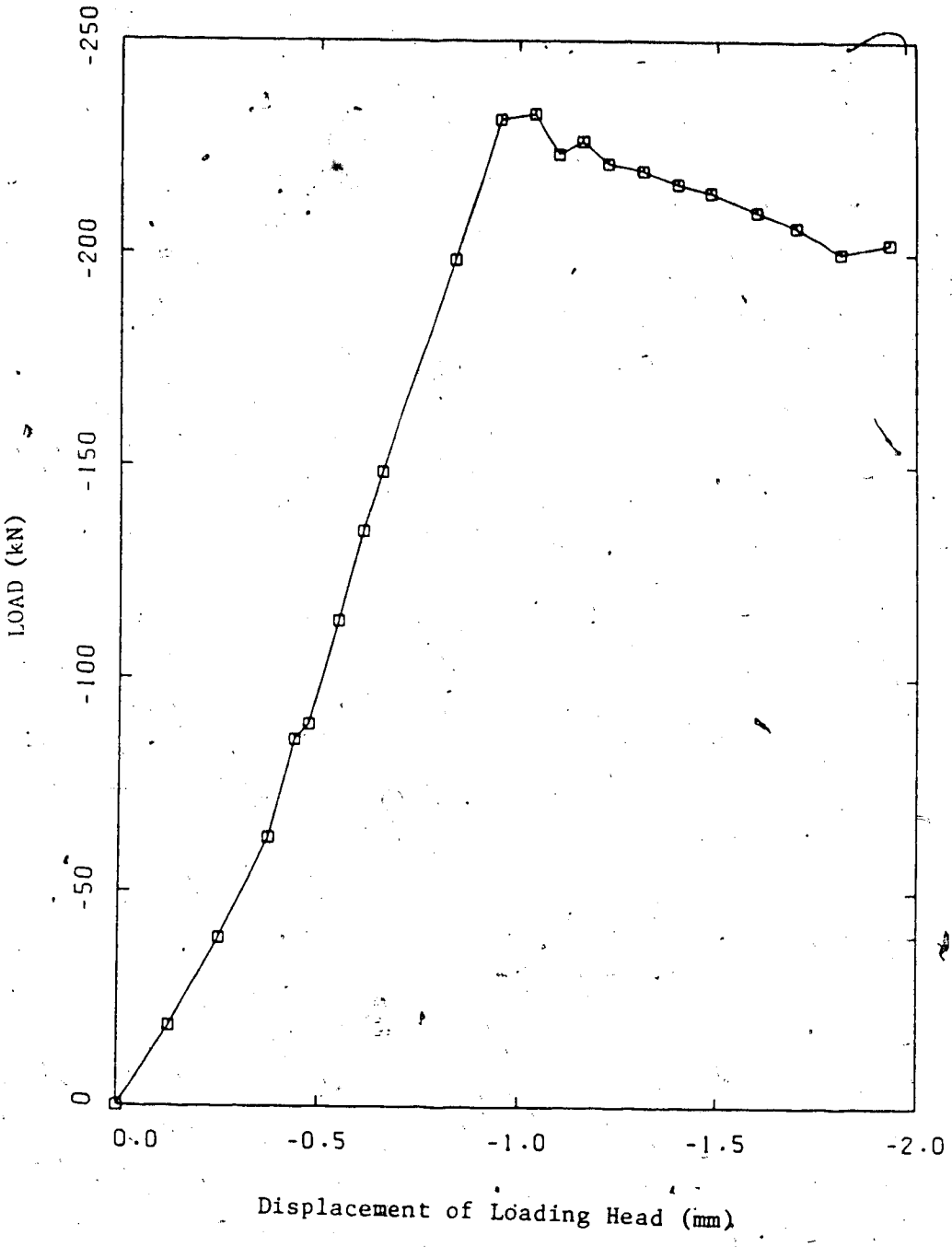

Figure A.8 Load versus Vertical Displacement Curve for Plate E5 of Free Case with Stiffener

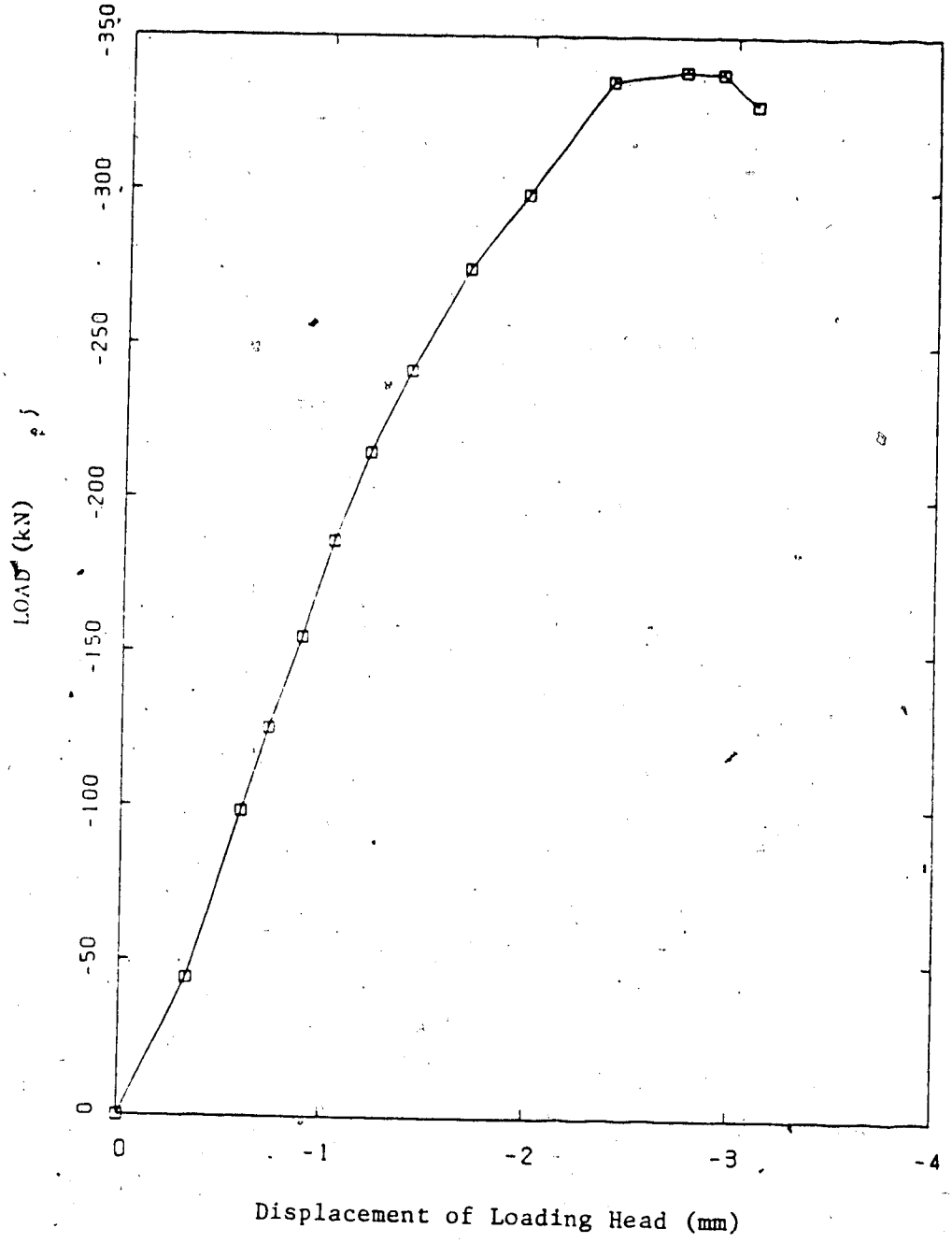

Figure A.9 Load versus Vertical Displacement Curve for Plate E6 of Free Case with Stiffener

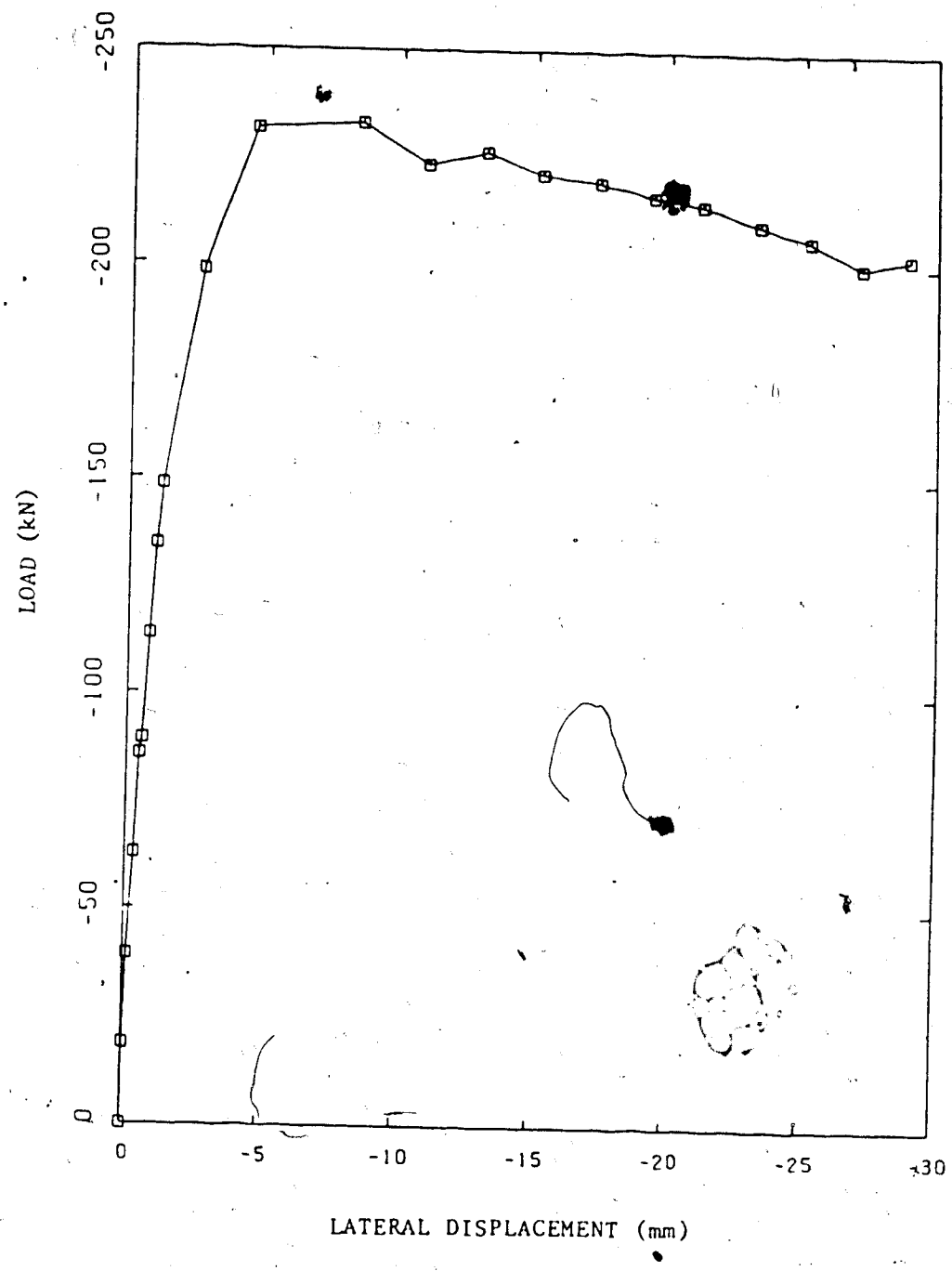

Figure A.10 Load versus Lateral Displacement Curve for Plate E5 of Free Case with Stiffener

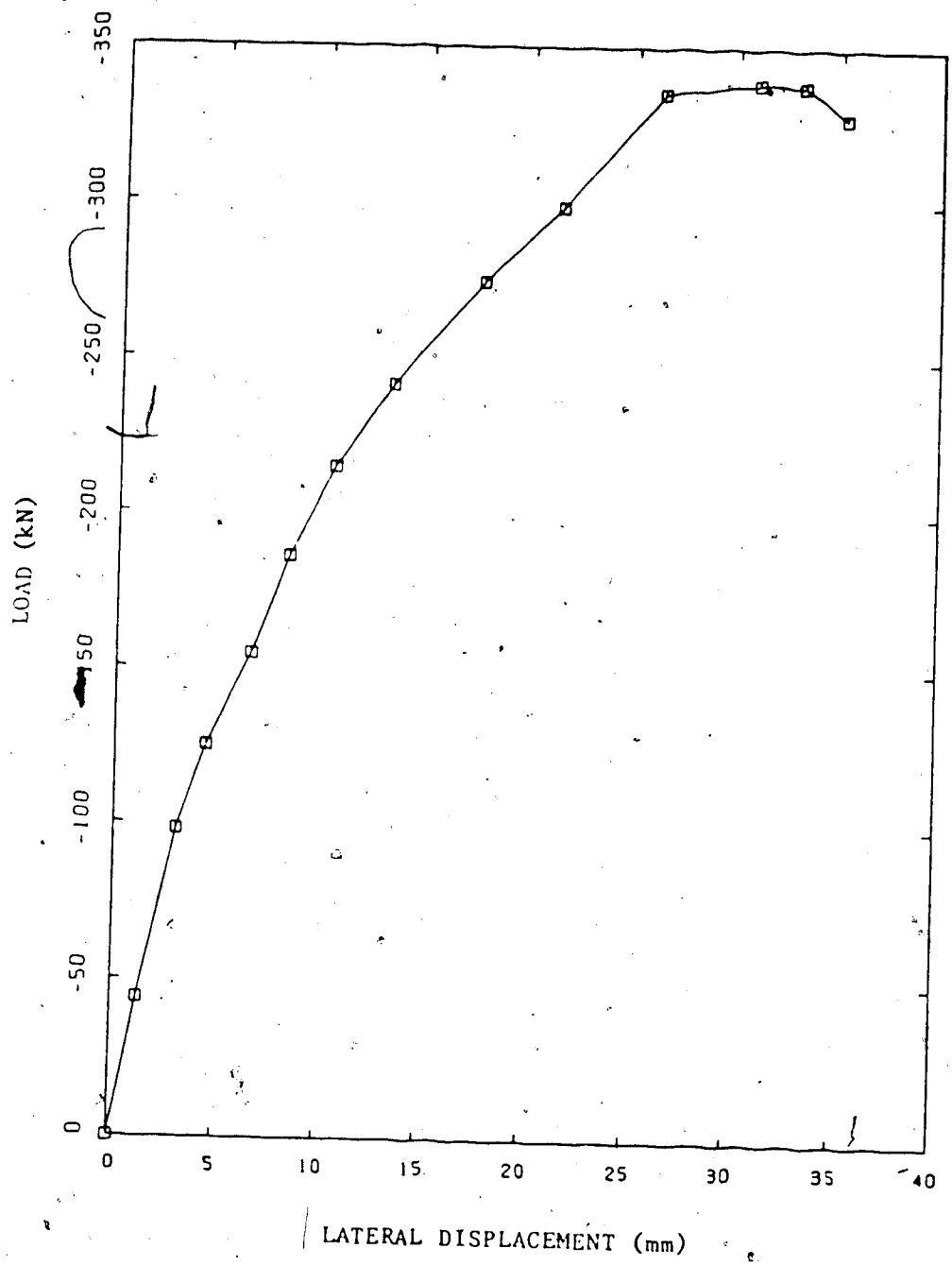

Figure A.11 Load versus Lateral Displacement Curve for Plate E6 of Free Case with Stiffener

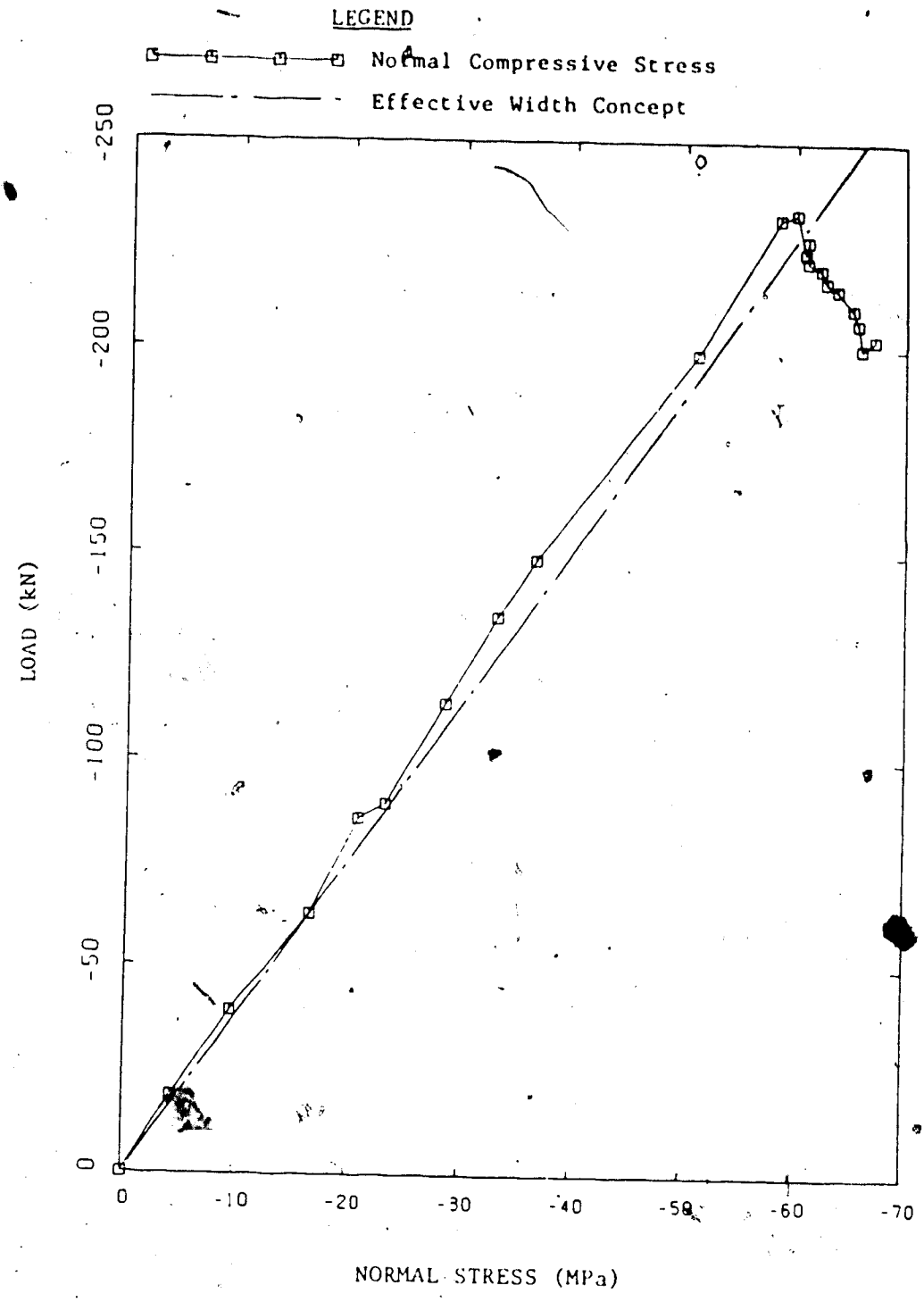

Figure A.12 Load versus Normal Compressive Stress Curve for Plate E5 of Free Case with Stiffener

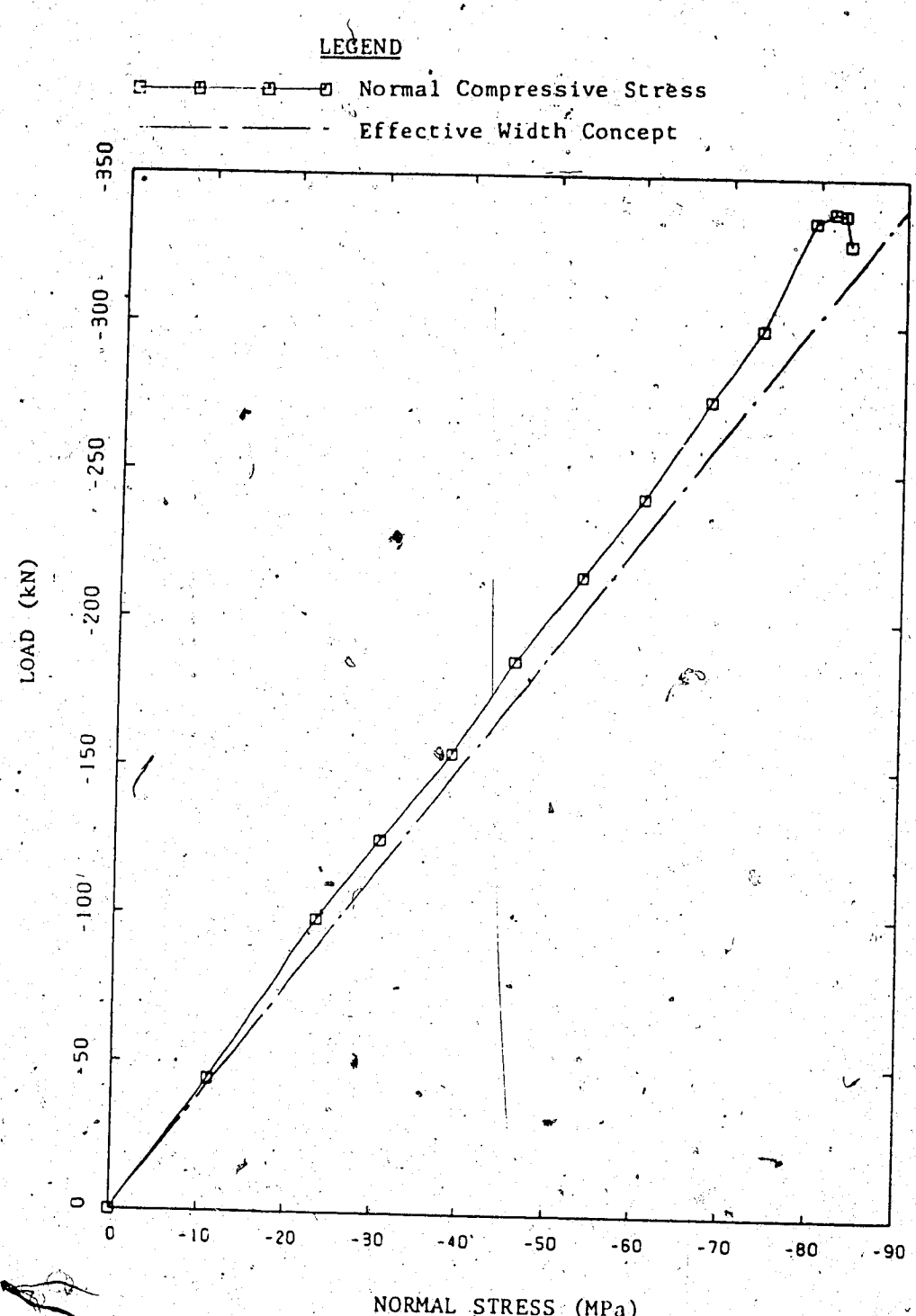

Figure A.13 Load versus Normal Compressive Stress Curve for Plate E6 of Free Case with Stiffener

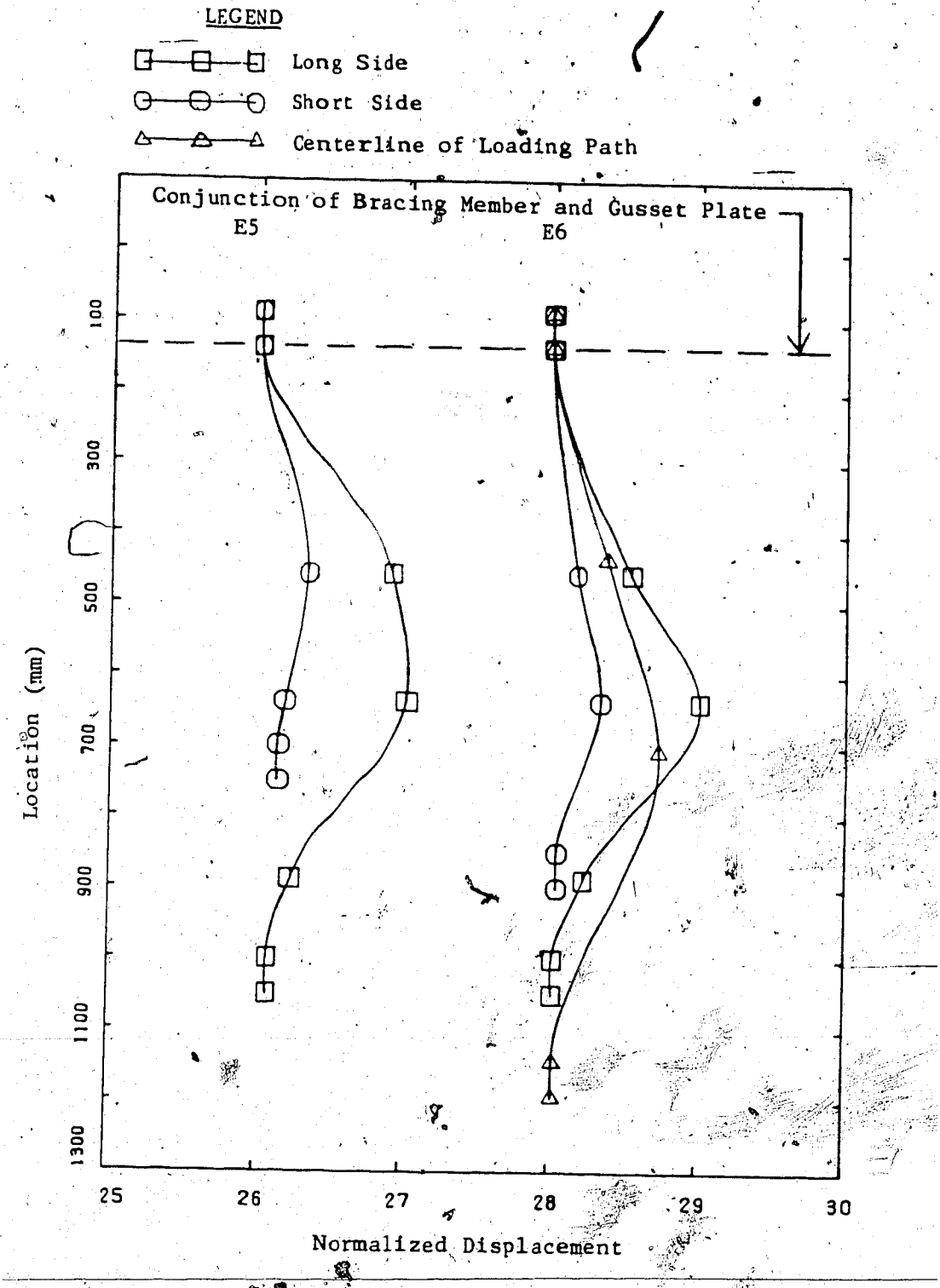

Figure A.14 Normalized Deflected Shapes of Fixed Case with Stiffener of Eccentric Loading Corresponding to the Maximum Load

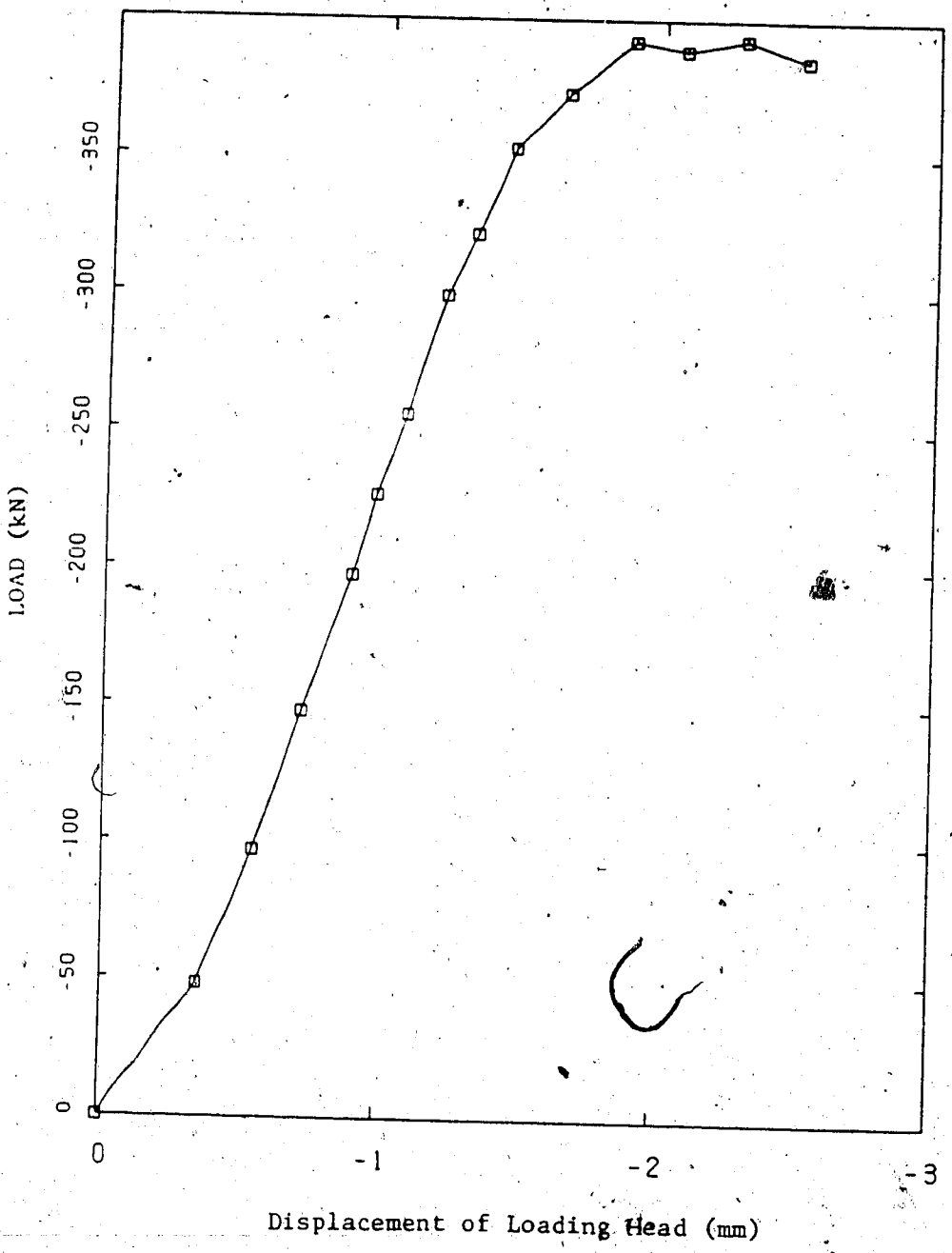

Figure A.15 Load versus Vertical Displacement Curve for Plate E5 of Fixed Case with Stiffener

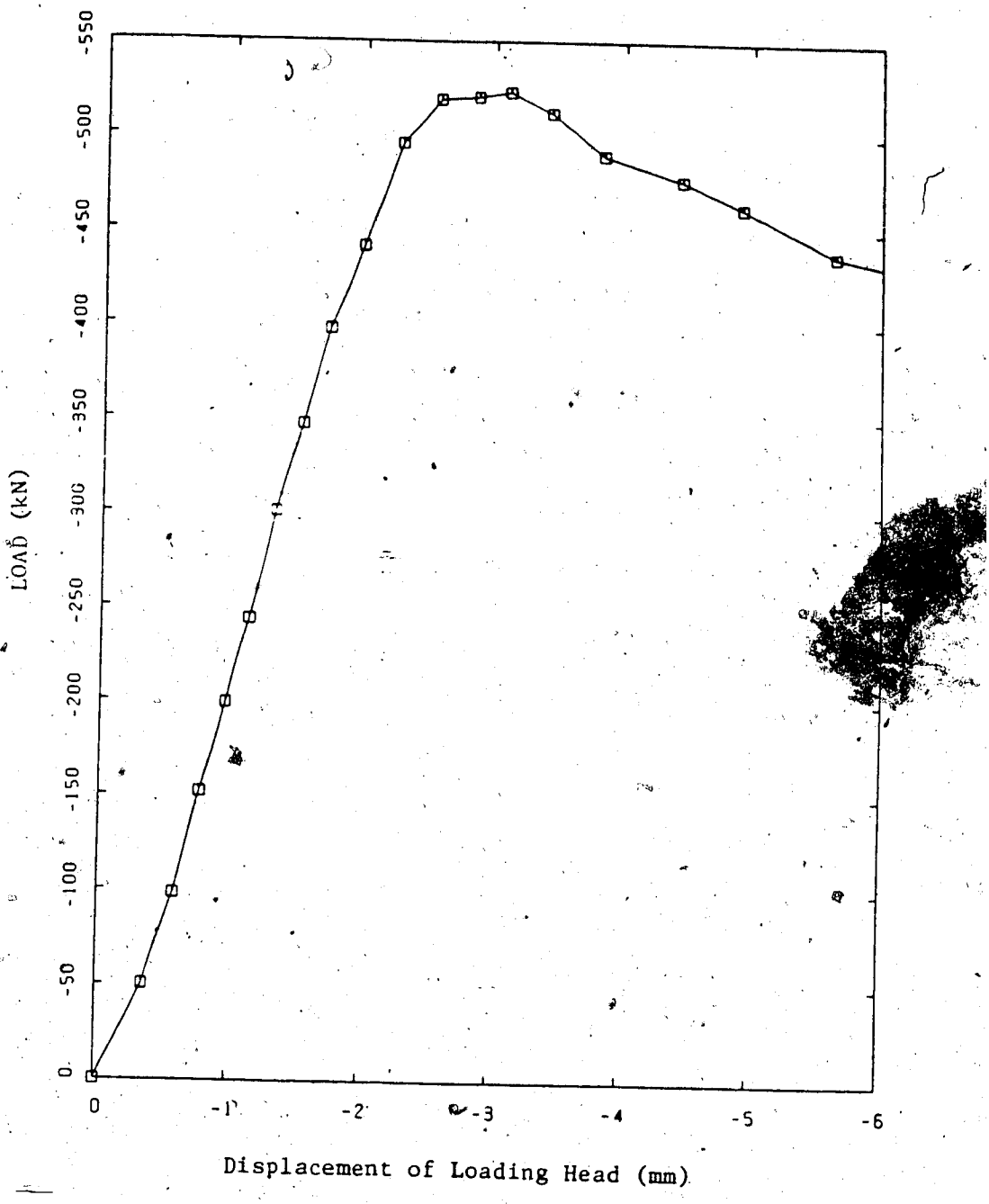

Figure A.16 Load versus Vertical Displacement Curve for Plate E6 of Fixed Case with Stiffener

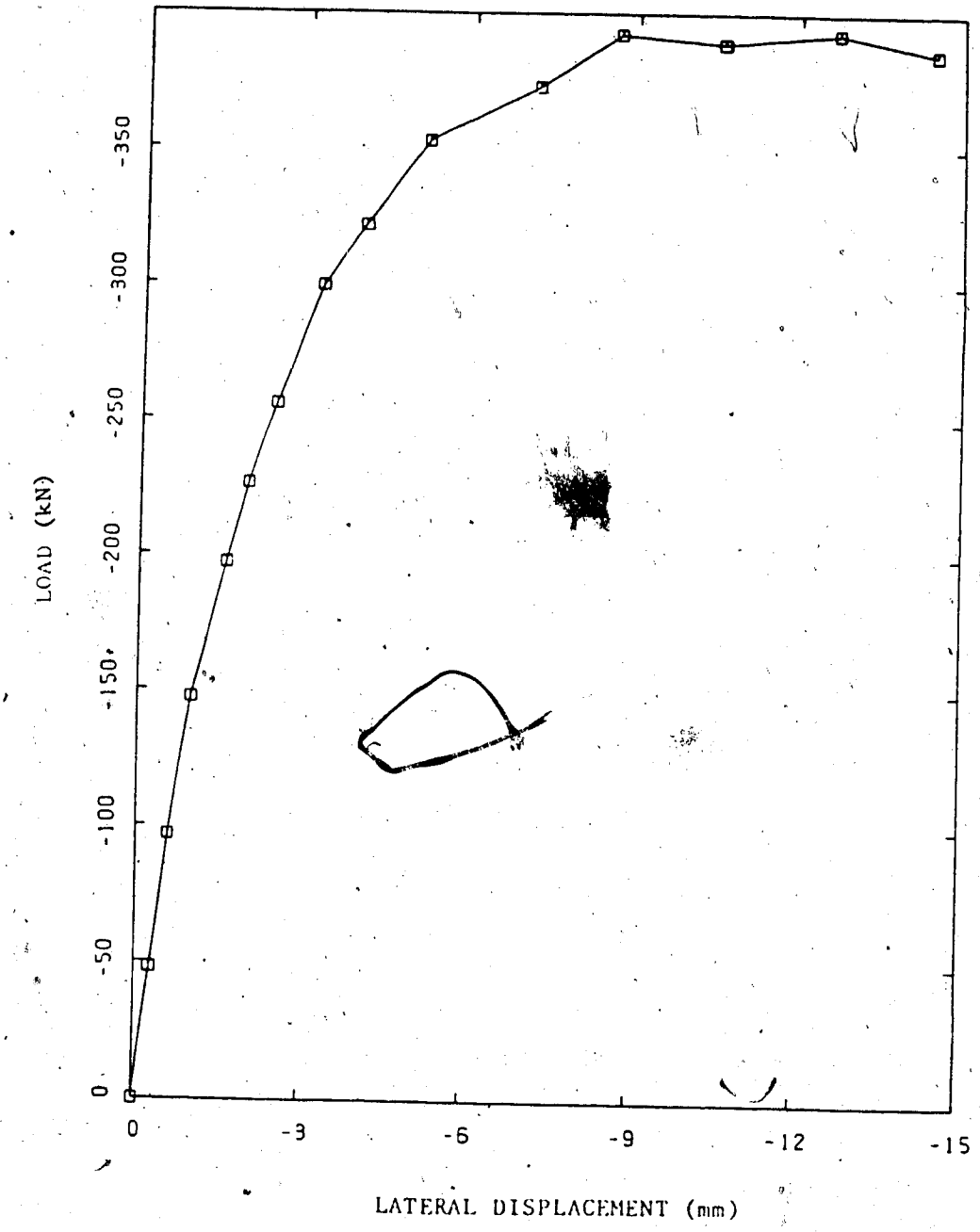

Figure A.17 Load versus Lateral Displacement Curve for Plate E5 of Fixed Case with Stiffener

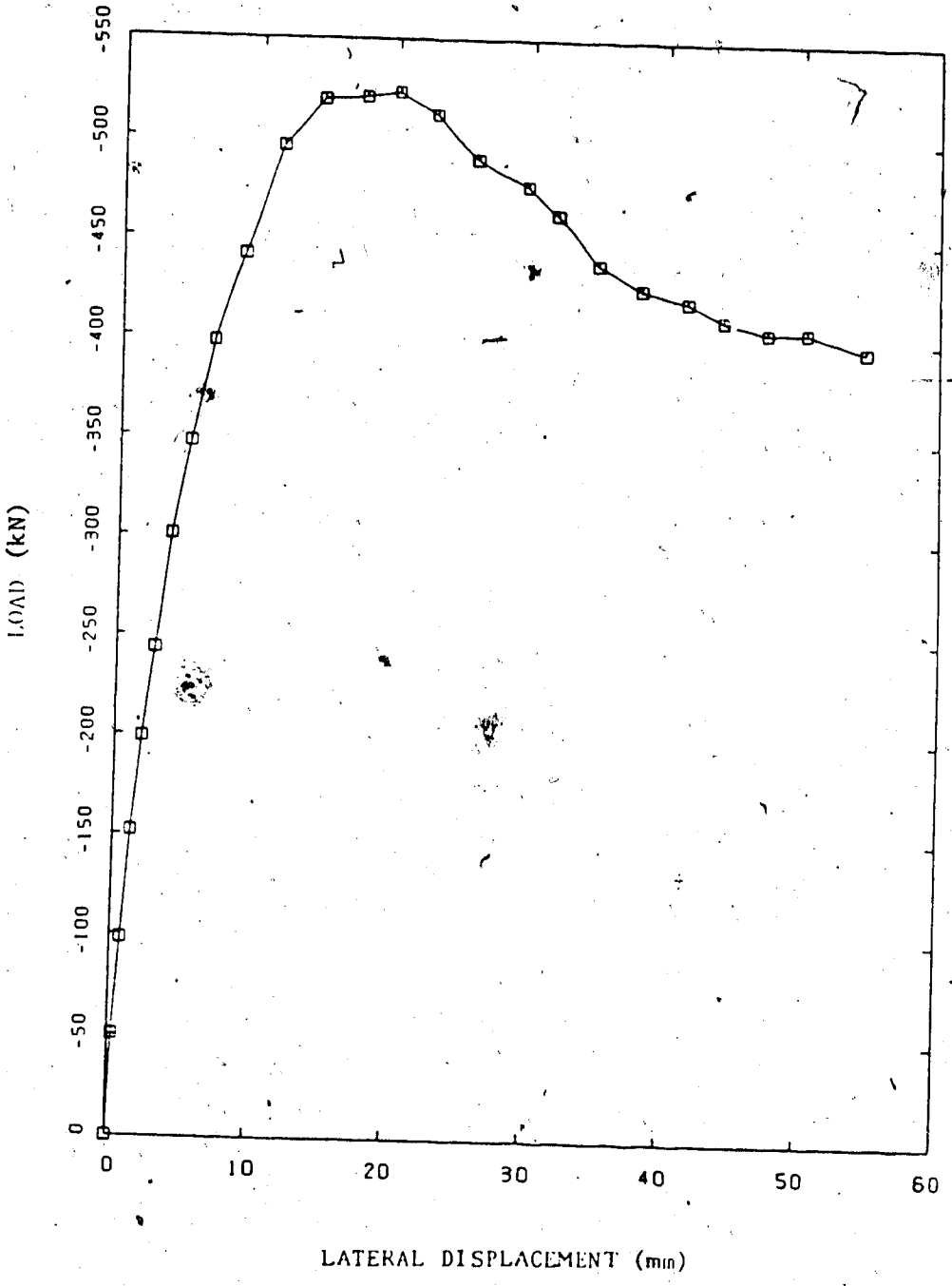

Figure A.18 Load versus Lateral Displacement Curve for Plate E6 of Fixed Case with Stiffener

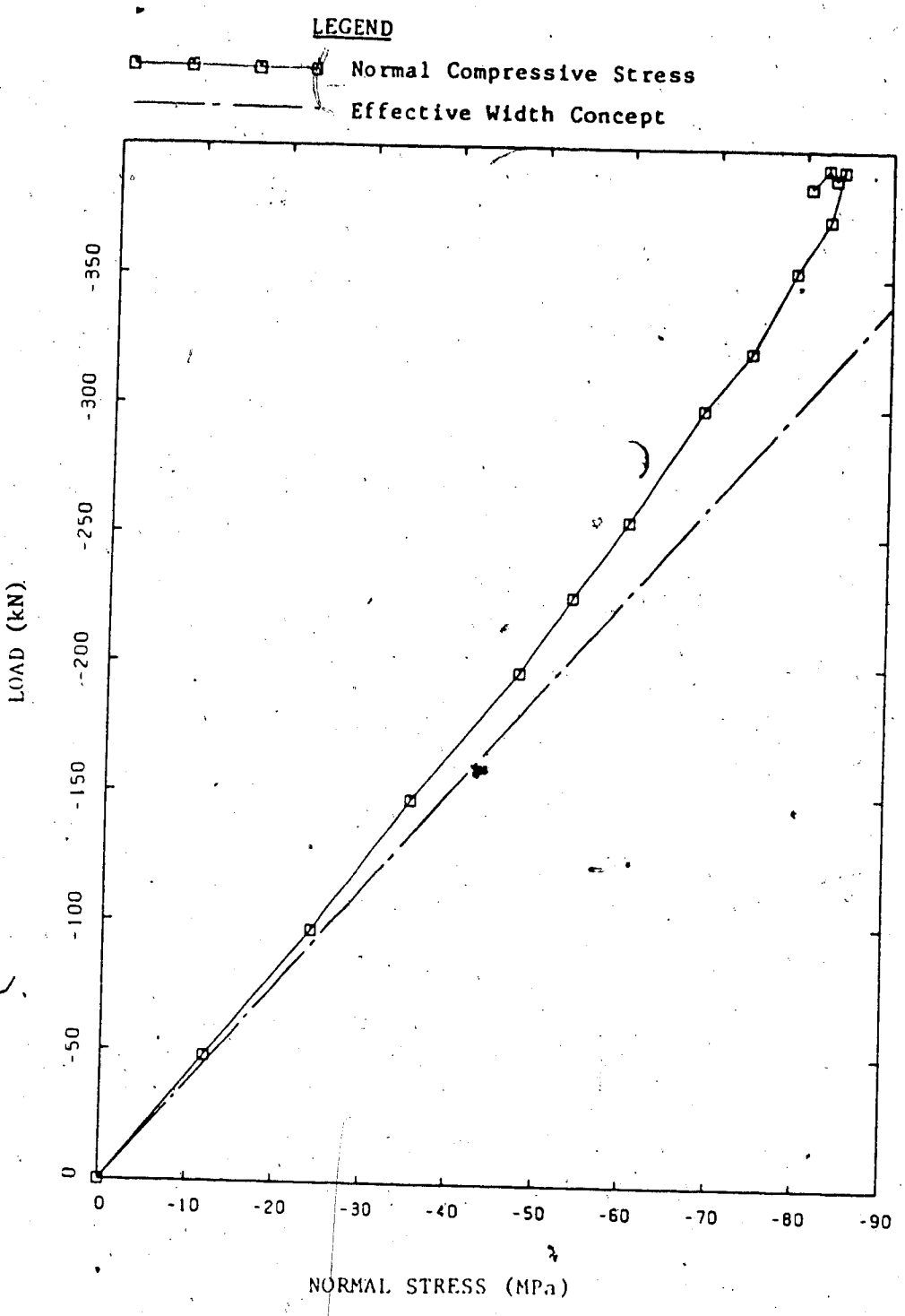

Figure A.19 Load versus Normal Compressive Stress Curve for Plate E5 of Fixed Case with Stiffener

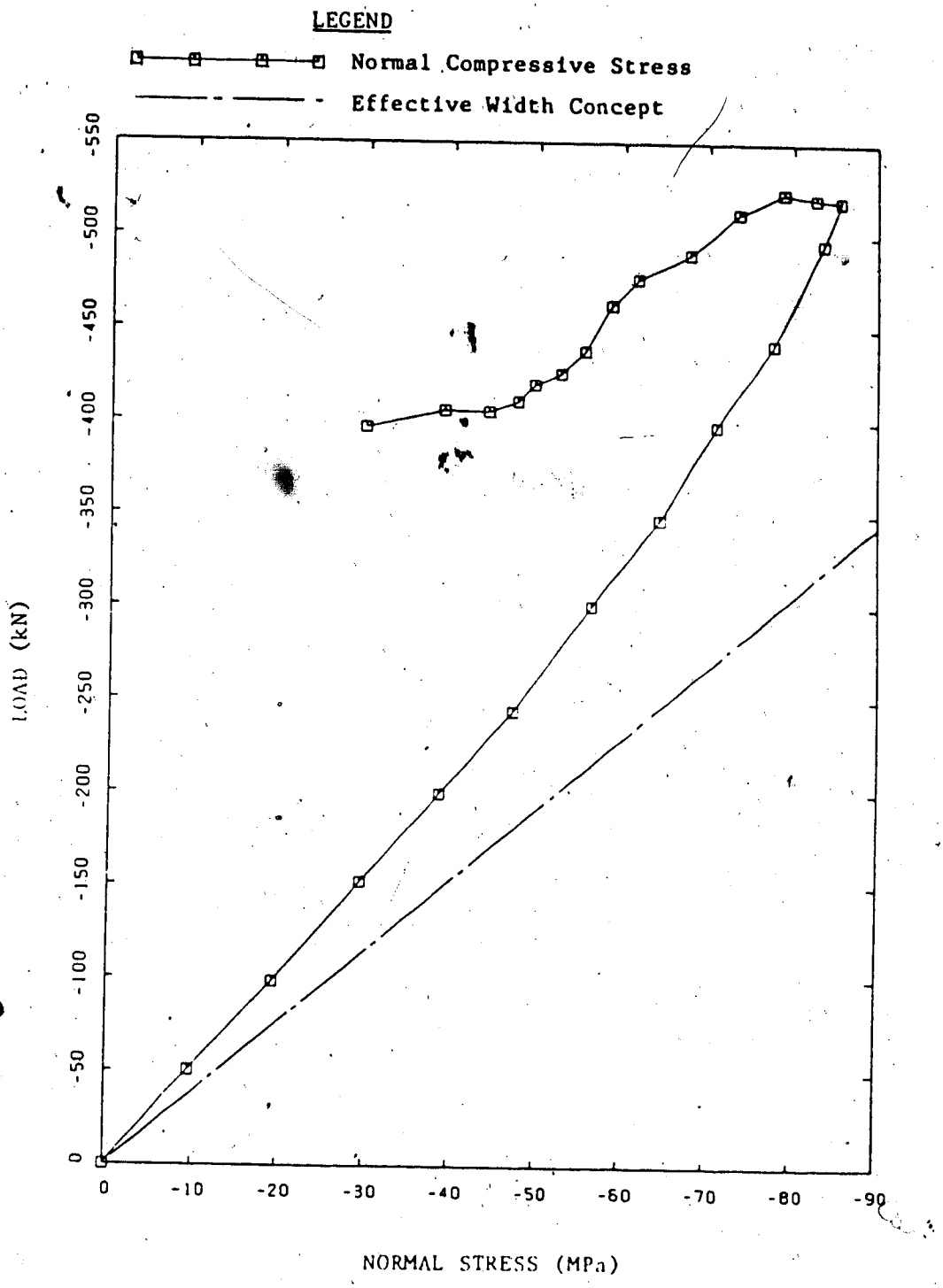

Figure A.20 Load versus Normal Compressive Stress Curve for Plate E6 of Fixed Case with Stiffener

APPENDIX B. Calculation Examples

A gusset plate with the configuration and loading arrangement similar to the test specimen E6, as shown in Fig. B1, is used to illustrate the calculation procedures using the effective width model and the beam-column formula (Eq.(5.1)) proposed in Chapter 5. The actual yield strengths of the splice plate and the gusset plate of 305 MPa and 505 MPa, respectively, are used in the calculation.

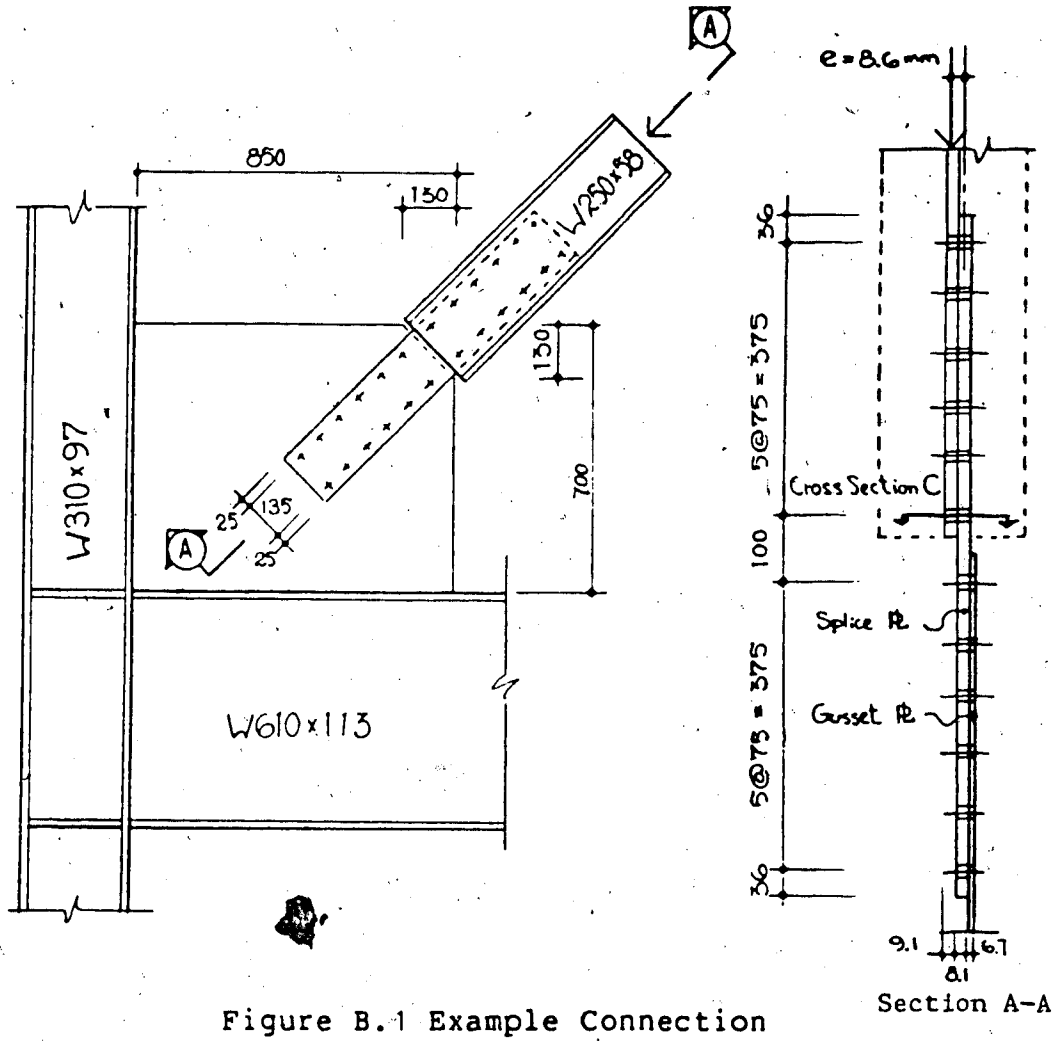

Figure B.1 Example Connection

Example 1 - Effective Width Concept:

Assume that the compressive stresses are uniformly distributed over an effective area at the end of the last row of the bolts on the splice plate using a spread-out angle of 30 degrees, as shown in Fig. B2. Then, check the cross-sectional strength at the effective area. The maximum load permitted by the effective width concept without reduction factor is

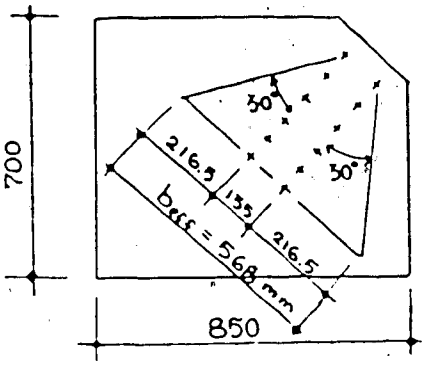

$$P_{max} = A F_y$$

$$= 568 \text{ mm} \times 6.7 \text{ mm} \times 505 \text{ MPa}$$

$$= 1922 \text{ kN}$$

Figure B.2 Effective Width Concept

Example 2 - Beam-Column Formula

Cross-section C in Fig. B1 gives the weakest section and the largest eccentricity. Thus, cross-section C is used to check against yielding by the beam-column formulus.

$P_y = b\ d\ \sigma_y = 146.9 \text{ mm} \times 8.1 \text{ mm} \times 305 \text{ MPa} = 363 \text{ kN}$

$$M_p = \frac{\sigma_y\ b\ d^2}{4} = \frac{305 \text{ MPa} \times 146.9 \text{ mm} \times (8.1 \text{ mm})^2}{4} = 735 \text{ kN-mm}$$

$M_{pc} = P \times e = 8.6 \text{ mm} \times P$

$$\left(\frac{P}{P_y}\right)^2 + \left(\frac{M_{pc}}{M_p}\right) = 1.0$$

$$\left(\frac{P}{363\ kN}\right)^2 + \frac{8.6\ mm \times P}{735\ kN\text{-}mm} = 1.0$$

$P = 81.2\ kN < 1922\ kN$; $P_{max} = 81.2\ kN$